The Dissertation Committee for Subhamoy Das Certifies that this is the approved version of the following dissertation:

Syndesomes for Enhanced Wound Healing and Therapeutic Angiogenesis in a Diabetic Diseased State

Committee:

Aaron B. Baker, Supervisor

Jeanne C. Stachowiak

Laura J. Suggs

David W. Terreson

Thomas M. Truskett

Syndesomes for Enhanced Wound Healing and Therapeutic Angiogenesis in a Diabetic Diseased State

by

Subhamoy Das, B.Tech. , M.S.E.

Dissertation

Presented to the Faculty of the Graduate School of

The University of Texas at Austin

in Partial Fulfillment

of the Requirements

for the Degree of

Doctor of Philosophy

The University of Texas at Austin

August 2014

Dedication

For Ma, Baba, and Dada

Acknowledgements

I would like to thank a lot of people who have contributed directly or indirectly towards my Ph.D. degree, my research, and my life. Please excuse me if I forget to mention your name explicitly. I really do appreciate your presence in my life.

First and foremost, I would like to recognize Ma, Baba, Dada, and now Boudi who have always supported me come what may. They are my source of strength, courage, and determination. Also, it will be my honor to become a doctor and join the league with my grandpa, dad, and brother. My life's journey to graduate school in Austin had a lot of roadblocks, but thanks to them, especially my mother, I am what and where I am today.

My path to graduate school has been a culmination of the discussions, teachings, and advice from many mentors, seniors, peers, and juniors. Particularly, I would like to recognize my school friends Dibya, Kaushik, Sandeep, Debapriya, and Rabi who not only provided me healthy competition but also useful advice and timely support. I had a truly memorable and enlightening time with my NIT Rourkela friends Rakesh, Avijit, Parth, Partha, and Sadangi. I would like to take this opportunity to express gratitude to my amazing teachers who set the foundation of my career viz. Lenka sir, Pradhan sir, Mishra sir, Ashok sir, Prajapati uncle, Debendra uncle, Sudha madam, Piyali madam, Parvathy madam, Pramod sir, and especially my father who has taught me since childhood.

The most indelible moments of my life was during the 4 years I spent in IIT Kharagpur (KGP) for my undergraduate education. Apart from taking courses, the KGP rituals like Illumination, Rangoli, Kshitij, Spring Fest, and Genesis will be ingrained in my mind forever. I had the most awesome time with my friends from freshmen year dormitory Jhalak, DD, Binoy, Golu, Asit, Pani, and Udit. Buddies from my Nehru hall at

KGP including Arindam, Vimmo, Sinhaji, Sonu, Vickyji, Sanky, Uma, Prerak, Chepa, etc. have made a huge impression on my life and have given shape to my personality during those impressionable years from sophomore to senior. Finally friends from biotechnology department Gotti, Meghs, Satty, DC, Sagar, Swetha, Sheetal, Tejas, and Shreyas have been really instrumental in my success. They were the worst critics and best friends. Internships have played a pivotal role in shaping my career even further. Specifically the summer of my sophomore year in 2008 spent in IGIB Delhi with Reema, Rhishi, Roshni, Liza, Kartik, Mahantesh, Jasmine, and Beena was an unforgettable learning experience. Winter of 2008 in JNCASR Bangalore with Nisha, Manju, Richie, Pankaj, Koustubh, Shantala, and Dr. Sharma provided an exhilarating introduction to new animal models and novel molecular biology techniques. Finally the experience at UC Berkeley in Dr. Jasper Rine's laboratory was the turning point in my career. That is when I decided that I wanted to pursue graduate school in USA. Notably I would like to thank Lenny, Nick, Meru, Erin, Oliver, Rachel, Laura, and obviously Jasper! That was one of the most productive as well as fun filled summer I had ever spent.

Graduate school in a foreign country was an exciting as well as scary idea for me at first. Rachit helped me get settled in Austin since day one when he picked me from the airport. I learnt dedication, hard work, and inquisitiveness from him. Tushar was the best workout buddy, teammate, and source of tremendous inspiration I could ever ask for. Vinay was the best running mentor, trainer, and now a great friend. Sucheta, Sid, and Garima - my hangout buddies are family to me now. Most importantly, I found my life partner Riddhi right here in Austin while training for Austin marathons. I am the most blessed to be in love and be loved by her.

My Ph.D. research would not have been possible without the significant contributions from the Baker laboratory members. I would specifically like to thank Peter

who has helped me innumerable times in the last 4 years. I would also like to acknowledge other members including Jason, Anthony, Collin, Shuang, Vicky, and Adrianne. I would not be able to finish my Ph.D. in time if it was not for my amazing undergraduate mentees. Gunjan stands out among them due to her mighty dedication and discipline. Matthew, Emmanuel, Alan, Selena, Smridhi, and Divya have also assisted a great deal with all the experiments whenever I needed. I would also like to take this opportunity to thank Lisa from Dr. Dunn's laboratory for her constant support in troubleshooting the laser speckle contrast imager. Friends from my class including Jardin, Kevin, Frank, Nishant, Gauri, Robin, and Maria were always supportive of my research and ideas.

Most importantly, I would like to sincerely thank Dr. Aaron Baker, who gave me the remarkable opportunity to work on one of his most innovative projects, which later won the NIH New Innovator Award too. He has always been there like a pole star guiding me through thick and thin of biomedical research. The conversations and discussions that we had have made much impact on my scientific thinking. He has always been immensely supportive of any idea that I pitched to him and I could rely on him to take the time to provide valuable feedback and constructive criticism. I am really fortunate to have him as my advisor.

Finally I would like to acknowledge my committee consisting of Dr. Stachowiak, Dr. Suggs, Dr. Terreson, and Dr. Truskett who found time out of their busy schedules to attend my dissertation proposal and defense. Dr. Suggs has helped me in every step of my graduate school and also provided valuable feedback from a biomaterials point of view. Dr. Stachowiak has helped me a lot in understanding the effects of lipid compositions and its biophysical characteristics. The feedback and advice of this committee has been instrumental in the progress of my thesis.

Syndesomes for Enhanced Wound Healing and Therapeutic Angiogenesis in a Diabetic Diseased State

Subhamoy Das, Ph.D.

The University of Texas at Austin, 2014

Supervisor: Aaron B. Baker

Peripheral vascular disease (PVD) affects more than 202 million people globally and about 20% of the population above 65 years of age in the United States alone. Type-2 diabetes afflicts around 347 million people worldwide and leads to the death of 4.6 million people. The rising prevalence of strong risk factors like smoking, hypertension, hypercholesterolemia, and obesity indicate that the affected population will continue to grow. Currently no long-term therapies exist in clinical practice for peripheral ischemia and non-healing chronic ulcers, both of which are common clinical consequences of PVD and type-2 diabetes. Current clinical treatments including exercise therapy, pharmaco-therapy, and surgical intervention can provide only relatively short-term relief from progressive vascular disease. Some attractive therapeutic strategies are to use growth factors, cytokines, viral delivery of growth factor genes, or the implantation of stem cells to revascularize ischemic tissue and heal chronic wounds. While these emerging therapies have been successfully applied in healthy animal models, they have achieved only limited success in humans with long-term disease. Thus, the overall goal of this thesis is to understand the reasons behind the failure of the clinical trials using growth factor therapy and to engineer therapeutics to circumvent the problems.

We observed a dramatic reduction in the protein levels of growth factor co-receptors, including syndecan-4, in the diabetic mouse model. We speculated that since co-receptors are critical for growth factor signaling cascade, this reduction in expression might lead to inefficient growth factor signaling. Our hypothesis was confirmed in the diseased ob/ob mice where we observed significant resistance to angiogenesis via growth factor therapy. Co-delivery of syndecan-4 along with fibroblast growth factor-2 (FGF-2) in an optimized liposomal formulation (syndesome) drastically improved the body's responsiveness to FGF-2. Treatment with syndesomes also enhanced revascularization in ischemic hind limbs and increased wound healing in full thickness cutaneous wounds in the diseased mouse model. The studies performed and described here are the first attempt, to our knowledge, for an effective understanding of the mechanisms involved in metabolic disorder in humans due to long-term disease and to explore steps for overcoming the associated clinical problems.

Table of Contents

List of Tables

List of Figures

Chapter 1: Introduction

1.1 MOTIVATION

Type-2 diabetes and peripheral vascular disease (PVD) have become more prevalent worldwide in the last few decades with the increase in average life expectancy leading to an older, diseased population [1]. PVD affects more than 202 million people worldwide and about 8.5 million people over 40 years of age in United States alone [1-6]. Type-2 diabetes affects around 347 million people and kills about 4.6 million people worldwide [7, 8]. Peripheral ischemia and non-healing wounds have emerged as clinically interdependent complications in both PVD and type-2 diabetes afflicted population. Statisticians predict that this affected population will continue to rise unless the risk factors are modified [1]. Presently, no long-term therapies exist in clinical practice to remedy ischemia and chronic wounds. Clinical standards only provide short-term relief from the symptoms [9]. An appealing therapeutic strategy is to deliver angiogenic factors to revive the diseased tissue to a relatively healthy state. This strategy has been highly successful in restoring perfusion in the ischemic tissues and healing wounds in healthy animal models. However, the delivery of growth factors [10, 11], cytokines [12], viral delivery of growth factor genes [13-16], and implantation of bone marrow cells [17] have achieved extremely limited success in clinical trials of diseased human patients [18, 19]. This thesis aims to understand why these growth factor based therapies have failed and seeks to create novel therapeutics to increase growth factor effectiveness in this context.

We hypothesized that the presence of co-morbid disease states inherently alters the ability of the body to respond to angiogenic therapies. To compare between the healthy and diseased state, we used a mouse model with diabetes and obesity called ob/ob (spontaneous mutation in the leptin gene leading to leptin deficiency) and wild type mice (C57BL/6J), which were healthy and age matched to the ob/ob mice. We examined alterations in the major components for the signaling pathways for FGF, VEGF, and PDGF. Both types of mice were fed with normal or high fat diet food to simulate the entire spectrum of diseased states i.e. from healthy mice on normal diet to obese mice on unhealthy high fat diet. In skeletal muscle of wild type healthy mice, a high fat diet increased protein levels of growth factor receptors and co-receptors including syndecan-1, syndecan-4, and PDGFR-α. These increases did not occur in ob/ob mice on a high fat diet. We found similar trends in myocardial tissue as well. To assess the responsiveness to growth factor therapy, we subcutaneously implanted alginate hydrogels encapsulating FGF-2, VEGF-A, or PDGF-CC. We found a drastic difference in therapeutic angiogenesis between the healthy and diseased groups. With the aim of increasing growth factor effectiveness in the context of disease, we examined whether co-delivery of FGF-2 with syndecan-4, which was depleted in the diseased tissue, could overcome the growth factor resistance in these mice. This syndesome (syndecan-4 protein embedded in a liposomal membrane) treatment enhanced the formation of new blood vessels in ob/ob mice by 6 fold in comparison to FGF-2 delivered alone. We tested the syndesomal therapy in clinically relevant mouse models of ischemia and wound healing. The syndesome with FGF-2 treatment significantly improved outcomes in a hind limb ischemia model in ob/ob mice compared to FGF-2 alone. We also demonstrated enhanced wound healing at day 14 with the syndesome and FGF-2 treatment. Our studies

support that diseased states cause a profound shift in growth factor signaling pathways and that co-receptor-based therapies have the potential to overcome growth factor resistance by restoring the tissue to a healthier phenotype.

1.2 DISSERTATION ROADMAP

The motivation behind this dissertation and the comprehensive summary of the thesis research are introduced in Chapter 1. A brief background and prior work are discussed in Chapter 2. Chapter 3 describes the extensive molecular study, specifically gene and protein expression experiments targeting various growth factors and their receptors and co-receptors. It includes the *in vivo* subcutaneous implantation study to assess the responsiveness to growth factors in healthy and diseased state. Chapter 4 discusses the syndesome therapy that was developed to overcome the disease-induced growth factor resistance. Chapters 5 and 6 represent the attempts to understand the clinically interdependent conditions of ischemia and chronic ulcers, and assess the effectiveness of the syndesomal therapy. Chapter 5 describes the experiments for efficacy of the syndesome treatment for peripheral ischemia in a clinically relevant diseased ob/ob mouse model. Chapter 6 describes the syndesomal therapeutics for enhancing wound healing in ob/ob mice. Finally, Chapter 7 concludes the dissertation and presents future research directions.

Chapter 2: Background

2.1 Peripheral Vascular Disease

Peripheral vascular disease (PVD) affects about 202 million people worldwide [1] and 8.5 million people in USA, which is 20% of the general population over 65 years of age[2, 20]. PVD is in fact the third most prevalent cause for mortality after stroke and coronary artery disease [1]. Lower and middle-income countries and low-income groups in high-income countries have an elevated risk of PVD and associated cardiovascular complications [1, 21]. PVD poses a significant burden on not only physical health but also mental health, work productivity, and greater usage of healthcare resources [22]. The increase in prevalence of strong risk factors for PVD, including smoking, diabetes, hypercholesterolemia, and obesity indicate that the affected population will continue to grow [1, 23]. A major sequela of PVD is the development of ischemia (reduction in blood flow) in the extremities. Severe PVD has serious clinical consequences for patients including the formation of chronic ulcers, pain from intermittent claudication and ultimately, increased risk for limb amputation [4, 24]. Although 50% of the patients are asymptomatic, their prognoses steadily worsens with time [4]. The 5-year mortality rate among patients with symptomatic PAD is about 20% [25]. Of those patients who develop critical limb ischemia, one out of four require amputation and 25% die due to other cardiovascular complications [26].

PVD manifests with other co-morbid cardiovascular problems like coronary artery disease, stroke, and other thromboembolic events. Therefore, managing PVD becomes a multifaceted problem. Abnormal muscle bioenergetics, ischemia due to

atherosclerosis, and endothelial dysfunction all contribute towards PVD. Interestingly, Fiotti et al showed that although PVD elevates haptoglobin, α1AT, TNF-α, IL-1β, and IL-6 soluble receptors, there were no significant increases in inflammatory cytokines [27]. These findings and others have warranted the search for novel biomarkers to detect PVD in its initial phases. D-dimer (two cross-linked D fragments of the fibrin protein formed after degradation of blood clot by fibrinolysis) has been demonstrated to be a marker for short-term outcomes [28] while circulating microRNAs have been shown to be correlative to disease progression [29]. Scientists have also developed a plethora of *in vivo* imaging techniques to diagnose PVD in early stages [30]. While these methods have shown promise, as of now, none of them have translated to the clinic.

For many years the most prevalent clinical treatment for PVD was composed either of pharmacological interventions aimed at treating the progress of vascular disease/co-morbidities or surgical revascularization through bypass grafting and endarterectomy [31]. More recently, there has been a rapid growth in the number of endovascular treatments such as angioplasty, stenting, and catheter-based atherectomy for PVD, although the overall benefit of these treatments versus surgery remains unclear [32]. For a significant portion of the clinical population, these methods are insufficient to restore blood flow over the long-term course of their disease [33]. Unfortunately, while each of these treatment modalities provides some benefit for some patients in the short-term, for many patients the disease is poorly managed by these therapies. A major limitation of these treatments is their reduced clinical durability due to restenosis and continuation of the atherosclerotic disease process.

An appealing and potentially revolutionary strategy for treating ischemia is the stimulation of angiogenesis within the ischemic tissue, harnessing the body's own

regenerative capacity to restore blood flow [34]. Previous studies have explored this strategy using exogenously-applied growth factors [10, 35, 36], viral vectors to express growth factor/angiogenic transcription factor genes [10, 15, 16, 37-43], or the implantation or mobilization of progenitors cells [38]. Unfortunately, while many of these strategies have shown promise in animal studies or small-scale clinical trials, none have found significant improvement in large randomized clinical trials [44]. Therefore, clinically effective angiogenic therapies remain elusive.

2.2 DIABETES MELLITUS

Type-2 diabetes, also known as diabetes mellitus, has been called the "epidemic of our generation" and it is estimated by the World Health Organization that 347 million people suffer from diabetes worldwide [45, 46]. In USA, there are around 29.1 million people with diabetes out of which 27.8% are still undiagnosed [47]. It is generally more common in men than women and most prevalent in people over the age of 65 years [48, 49]. The most troubling fact is that 1.7 million new cases of diabetes have been reported in a single year of 2012, which is 8 out of every 1000 people in USA [50]. Diabetes contributes for an immense financial burden on USA, accounting for a total of $245 billion every year, which includes $176 billion of direct medical costs and $69 billion of indirect costs [47].

Diabetic patients have abnormal pancreatic function which leads to glucose insensitivity and deficiency of insulin hormone. A host of other problems accompany diabetes including but not limited to heart disease, stroke, hypertension, hypercholesterolemia, neuropathy, nephropathy, chronic kidney disease, peripheral

vascular disease, non-alcoholic fatty liver, periodontal disease, erectile dysfunction, loss of hearing, depression, and pregnancy complications [47]. Neuropathy and microvascular angiopathy are common complications of diabetes and contribute to a 12-25% lifetime risk of developing diabetic ulcers [51]. Diabetic foot ulcers, specifically, are responsible for 25-50% of the total cost of diabetes treatment [52] and are the most common cause for limb amputations in the United States [53]. Diabetic ulcers are a complex clinical problem requiring a multifaceted treatment plan with standard therapeutic components including debridement of necrotic tissue, offloading, infection control, surgical revascularization, and limb elevation/compression [18, 19]. Unfortunately, these treatments routinely fail, leaving patients with chronic ulcers with an enhanced risk for limb amputation.

2.3 ANGIOGENESIS

Angiogenesis is an intricate physiological process requiring the complex coordination of endothelial cells, vascular smooth muscle cells, pericytes, and macrophages under the control of environmental cues from the extracellular matrix and a host of growth factors/cytokines [54]. Among these, members of the FGF family bind to cell surface heparan sulfate proteoglycans, interactions that are essential to stabilize the formation of active FGF-FGF receptor complexes [55]. Consequently, cell surface heparan sulfate proteoglycans, such as the syndecans, serve as essential co-receptors in this pathway. Vascular endothelial growth factor (VEGF) has also been recognized as a potent stimulator of endothelial proliferation/migration and plays an integral role in angiogenesis *in vivo* through interactions with its two primary receptors Flt-1 (VEGFR-1)

and KDR (VEGFR-2) [56]. Neuropilin-1 is a major co-receptor for VEGF acting to facilitate signaling with both Flt-1 and KDR [57]. In addition, syndecan-2 can bind VEGF and is essential for VEGF-mediated angiogenesis [58]. Platelet-derived growth factor-BB (PDGF-BB) is involved in pericyte recruitment around capillaries during angiogenesis and is consequently involved in blood vessel stabilization during angiogenesis and arteriogenesis [59]. The PDGF-β receptor has the high affinity for PDGF-BB, and this interaction has been linked to the control of cell migration and proliferation [60]. Both neuropilin-1 and the syndecans have been linked to regulation of PDGF activity [61-64]. In addition, PDGF-CC interacts with the PDGF-α and β receptors, inducing angiogenesis [65] and revascularization of ischemic tissues [66].

Given the intense study of the process of angiogenesis and the evidence for the potent induction of angiogenesis by growth factors in experimental models, we hypothesize that the reason for this therapeutic failure may lie in disease-mediated alterations in target tissue signaling. In animal models, ischemia is typically induced in a healthy animal by surgically ligating an artery either in the peripheral muscle or coronary arteries. Consequently, ischemia develops acutely in an animal that is often otherwise healthy. In human clinical use, the patient has developed ischemia most often through a long-term disease process. Thus, by the time patients have developed clinically-recognizable symptoms, they have had the disease for an extended period of time and the compensatory mechanisms of the human body may have been overwhelmed considerably. These mechanisms include, in all likelihood, the induction of the very angiogenic factors that we are attempting to use as therapeutic inducers of blood vessel growth. Accordingly, the presence of long-term ischemic disease in humans likely implies the presence of mechanisms to defeat growth factor therapy without modification.

Here, we explored this hypothesis by examining how the expression of signaling components of FGF-2, VEGF-A, and PDGF pathways change with diseased state caused by a high fat diet in the ob/ob mouse model. Our group has also recently shown that delivery of liposomally embedded co-receptors are effective in enhancing growth factor-induced signaling and trafficking in the cell as well as revascularization in healthy rats [67]. To examine if this strategy could overcome disease-induced growth factor resistance, we developed an alginate-based hydrogel system for the local delivery of syndecan-4 in combination with FGF-2.

2.4 SYNDECAN-4

A complex extracellular matrix (ECM) also called connective tissue, surrounds most mammalian cells. The ECM is composed of a variety of biomolecules including structural proteins (collagen, elastin), specialized proteins (fibrillin, fibronectin, and laminin), and proteoglycans. Proteoglycans are ubiquitous proteins with one or more GAG (glycosaminoglycan) chains attached to a core protein through a typical core protein region ending in a xylose residue linked to the hydroxyl group of a serine residue. They typically have a 90-95% carbohydrate content due to the GAG chains. Proteoglycans are different from glycoproteins, which are proteins with one or more glycans covalently attached to a polypeptide chain usually via N or O linkages with 2-30% carbohydrate content [68]. Proteoglycans are heavily glycosylated, generally with sulfate or uronic acid groups, which imparts a net negative charge to the protein. Proteoglycans are of four different kinds according to the glycosylations - chondroitin sulfate, dermatan sulfate, keratin sulfate, and heparan sulfate [68].

Heparan sulfate proteoglycans (HSPGs) are a specialized group of proteoglycans, which as the name suggests, contain heparan sulfate glycosylations. Among the four kinds of proteoglycans, HSPGs are perhaps the most versatile and hence most studied. They can be found as transmembrane or as extracellular matrix proteins. HSPGs have been implicated in diverse roles at cellular, tissue, and organismal levels. The HSPGs on the cell surface like glypicans and syndecans coordinate multiple cellular functions like binding to growth factors, receptors, ECM, and intracellular signaling [69, 70]. Overall, HSPGs contribute in cell proliferation, migration, adhesion, recognition, differentiation, matrix assembly, survival, hemostasis, defense mechanism, inflammation, and angiogenesis [71, 72]. Among the HSPGs, the syndecan family consists of four single-pass transmembrane proteins with a long extracellular domain with heparan sulfate and chondroitin sulfate chains and a relatively short intracellular domain. They interact with FGF, VEGF, TGF-β, PDGF, ECM proteins, and cytosolic proteins like FRS2, Ras, Akt, MAPK, Elk3, Erg1, and cFos [73, 74]. Syndecans generally dimerize or polymerize into complexes to exert its effects on other transmembrane protein. They regulate various physiological functions like wound repair [75-77], inflammation [78, 79], angiogenesis [80], migration [81, 82], body weight, and synaptic plasticity [83].

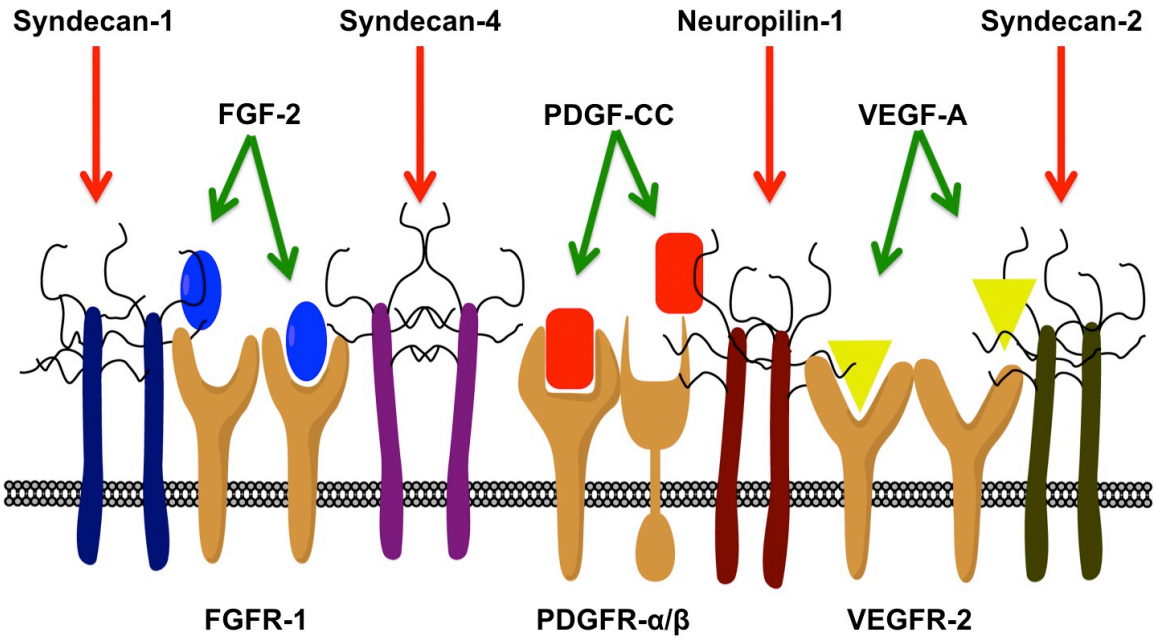

Figure 2.1 Schematic diagram showing the interactions on the cell membrane among the growth factors (FGF-2, VEGF-A, and PDGF-CC), the receptors (FGFR-1, PDGFR-α/β, and VEGFR-2), and the co-receptors (Syndecan-1, -2, -4, and Neuropilin-1).

We are interested in syndecan-4 in this study among the syndecan family. Syndecan-4 is ubiquitously found in the body in almost all cell types and exerts a crucial role in the microenvironment. It has only one isomer but can be converted into a soluble form by cleavage of the extracellular domain by proteases [84, 85]. These soluble forms have been shown to be a marker of acute myocardial infarction. Previous studies support a role for syndecan-4 in wound healing and have found that syndecan-4 gene expression promotes fibroblast migration and regulates integrin signaling and small GTPases during wound healing [77, 86]. Syndecan-4 also enhances keratinocyte migration [81] and is necessary for migration of fibroblasts in 3D gels [87]. In addition, syndecan-4 is induced

in the skin following wounding in both mice and neonatal humans [88]. Finally, mice with knockout of syndecan-4 gene have delayed wound healing and angiogenesis [75]. Syndecan-4 is one of the co-receptors for FGFR-1 that binds to FGF-2 (Figure 2.1). Our previous studies have shown that syndesomes improve the signaling response to FGF-2, proliferation, migration and the nuclear localization of FGF-2 in endothelial cells (Figure 2.2) [67]. In addition, we found that syndesomes improved the angiogenic response to FGF-2 in diabetic mice in a subcutaneous implantation model [89].

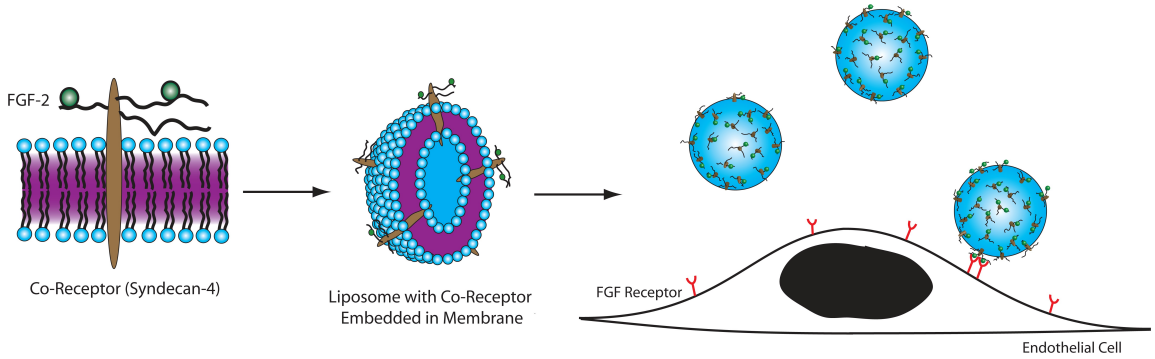

Figure 2.2 Schematic diagram showing formation of syndecan-4 loaded liposomes and treatment to endothelial cells.

2.5 Mouse Models

We have used two different mouse models in this thesis: C57BL/6J mouse (WT - normal healthy mice) and B6.Cg-*Lep* ^{ob}/J (ob/ob - diseased diabetic mice). The WT mice are the most widely used strain in the scientific studies and the first to have its genome sequenced. They have a permissive genetic background that allows scientists to induce spontaneous mutations in their genome to create various models of disease. The ob/ob mice are a result of one such spontaneous mutation in the leptin gene that results in the

inactivation of the gene. C57BL/6J mice are used in a wide variety of research areas including cardiovascular biology, developmental biology, diabetes, obesity, genetics, immunology, neurobiology, and sensorineural research. Overall, C57BL/6 mice breed well, are long-lived, and have a low susceptibility to tumors.

Figure 2.3 An ob/ob mouse model for diabetes and metabolic disease. A 10-week old male ob/ob mouse (left) that is fed for 10 weeks with a high fat diet (right) doubles its weight and becomes pre-diabetic with the symptoms of insulin resistance, hyperglycemia, and glucose insensitivity.

The ob/ob mice exhibit obesity, hyperphagia, diabetes-like syndrome of hyperglycemia, glucose intolerance, elevated plasma insulin, subfertility, impaired wound healing, and an increase in hormone production from both pituitary and adrenal glands. They are also hypometabolic and hypothermic. The obesity is characterized by an increase in both the number and the size of adipocytes. Although hyperphagia contributes to the obesity, homozygotes gain excess weight, and deposit excess fat even when restricted to a diet sufficient for normal weight maintenance in lean mice. Since the ob/ob mice have a C57BL/6J background strain, they are perfect match for our experiments with healthy WT mice.

Chapter 3: Disease-induced Growth Factor Resistance

3.1 Introduction

Growth factor based therapy is an interesting therapeutic strategy for revascularization, wound healing, and other clinical conditions. While these techniques have shown remarkable results in normal healthy animals, they have failed to show significant differences when compared with a placebo or clinical standard of care in human diseased patients. We hypothesize that resistance exists not only for insulin [90] but also for growth factors including FGF-2, VEGF-A, and PDGF-CC isoforms. Previous studies have indirectly supported this hypothesis by demonstrating reduced wound healing in diabetic animals [91], a reduced capacity for ischemic pre-conditioning in reperfusion injury in ob/ob mice [92], and a defective response to angiogenic gene therapy in db/db mice that are deficient of the leptin receptor [93]. A previous study examined the broad set of gene expression following ischemia in WT and db/db mice using microarray analysis [94], which supported the occurrence of reduced vascularization in these mice and alterations in angiogenic gene regulatory networks.

In this chapter we investigate the gene and protein expression levels of receptors and co-receptors of various growth factors in different phases of disease progression. We simulated the human disease and sequela with an ob/ob mouse model [95]. These mice are pre-diabetic, obese, and show many characteristics similar to patients with long-term metabolic disease. We postulated that there must be some dysregulation at the cellular level due to presence of long-term disease. To evaluate the degree of resistance to growth factor therapy in a diseased state, we used a subcutaneous implantation model in the ob/ob mouse.

3.2 MATERIALS AND METHODS

3.2.1 Animal Model

All animal studies were performed with the approval of the University of Texas at Austin's Institutional Animal Care and Use Committee (IACUC) and in accordance with NIH guidelines "Guide for Care and Use of Laboratory Animals" for animal care. Wild type mice - C57BL/6J (Jackson Labs) and ob/ob mice - B6.Cg-Lep^{ob}/J (Jackson Labs) were used in these studies. The ob/ob mice are deficient of the hormone leptin that is normally produced by the fat cells, signaling the brain to stop the hunger signal. Therefore, these mice are chronically hyperphagic leading to obesity, subfertility, impaired wound healing and pre-diabetes like symptoms of insulin resistance, glucose intolerance, and elevated plasma insulin. The animals were fed normal chow diet (LabDiet - Prolab RMH 1800) or high fat diet (Research Diets - D12331). Thus, we had 4 different groups henceforth referred as follows: **WT-NCD** (WT mice on normal chow diet), **WT-HFD** (WT mice on high fat diet), **ob/ob-NCD** (ob/ob mice on normal chow diet), and **ob/ob-HFD** (ob/ob mice on high fat diet). The mice were fed a particular diet for 10 weeks and then sacrificed to harvest the heart and quadriceps muscle for downstream processing, as described in section 3.2.6.

3.2.2 Gene Expression Analyses

Slices of the tissue were sectioned (10-20μm) with a Leica CM 1850 cryotome equipped with a steel knife. The tissue sections were dissolved in the RLT buffer (Qiagen) using a TissueLyzer with a stainless steel bead. RNA was isolated using the Qiagen RNeasy Midi kit and purity checked on an UV-Vis spectrophotometer (Nanodrop

2000c). Pure RNA was reverse transcribed into cDNA using the TaqMan Reverse Transcription reagents (Applied Biosystems). The cDNA was used with SYBR Green PCR master mix (Life Technologies) for real-time qPCR quantification using the Applied Biosystems ViiA™7 system. GAPDH was used as the reference gene. The cycling conditions used were 95°C for 10 minutes followed by 40 cycles of 95°C for 15 seconds and 60°C for 60 seconds. Primers for the PCR reactions are listed below in Table 3.1.

Table 3.1 Primers used for real time qPCR, adapted from [89].

Gene	*Forward Primer*	*Reverse Primer*
FGFR-1	ACCAAGAAGAGCGACTTCCA	AACCAGGAGAACCCCAGAGT
VEGFR-2	TTTGGTTTTGGAAGGTTTGC	AGGAGCAAGCTGCATCATTT
PDGFR-α	ACCACAATGGTGCTGTTGAA	AATCTCTGGGGCAAAGGTCT
PDGFR-β	CCGGAACAAACACACCTTCT	TATCCATGTAGCCACCGTCA
Syndecan-1	AGCCTTCCTCCCTCATGTTT	TCTAGCTGAGTGGCTGAGCA
Syndecan-2	ACATCTCCCCTTGCTGTGAC	TGAGGGGTTCTTTGGTCTTG
Syndecan-4	CTGATCCTGCTGCTGGTGTA	GGAGGAAGCTTCATGCGTAG
Neuropilin-1	GGAGCTACTGGGCTGTGAAG	CCTCCTGTGAGCTGGAAGTC
Heparanase	GGAGCAGGCAACTACCACTT	ACAGGAGCAAACTCCGAGTG
GAPDH	AACTTTGGCATTGTGGAAGG	GGATGCAGGGATGATGTTCT

Abbreviations used were as follows: FGFR-1 = Fibroblast Growth Factor-1; VEGFR-2 = Vascular Endothelial Growth Factor; PDGFR-α = Platelet Derived Growth Factor Alpha; PDGFR-β = Platelet Derived Growth Factor Beta; GAPDH = Glyceraldehyde 3-Phosphate Dehydrogenase.

3.2.3 Protein Expression Analyses

The tissues were cryosectioned and the slices lysed in a buffer containing the following: 20mM Tris at pH 8, 150mM NaCl, 1% Triton, 0.1% SDS, 2mM Sodium Orthovanadate, 2mM PMSF, 50mM NaF, and protease inhibitors (Roche). A Qiagen Tissuelyzer was used with stainless steel beads to facilitate tissue lysis. The lysates were

normalized to the amount of protein loaded into the wells by performing a Micro-BCA assay (Thermo-Scientific). The samples were then separated by gel electrophoresis (NuPAGE® Novex 10% Bis-Tris Midi Gel) and transferred onto a nitrocellulose membrane using the iBlot system (Life Technologies). The membranes were then blocked for 1h in 5% non-fat milk in PBS with 0.01% Tween-20 and exposed to primary antibodies (see Table 3.2 below for details) overnight at 4°C. The membranes were washed and incubated at room temperature for 2h at room temperature with a secondary antibody and were detected using a chemiluminescence substrate (Thermo Fisher Scientific). Imaging was performed using the FluorChem HD2 system (Protein Simple). Quantification of the blots was done by densitometric analysis using Metamorph.

Table 3.2 Antibodies used in the studies, adapted from [89].

Protein/Label	***Antibody***	***Type***	***Company***
GAPDH	Mouse monoclonal	Primary	Santa Cruz
Syndecan-1	Mouse monoclonal	Primary	ABCAM
Syndecan-2	Rabbit polyclonal	Primary	ABCAM
Syndecan-4	Rabbit polyclonal	Primary	ABCAM
Neuropilin-1	Rabbit monoclonal	Primary	ABCAM
Heparanase	Mouse monoclonal	Primary	Cell Sciences
PDGFR-α	Rabbit polyclonal	Primary	ABCAM
pPDGFR-α	Rabbit monoclonal	Primary	Cell Signaling
PDGFR-β	Rabbit monoclonal	Primary	Cell Signaling
FGFR-1	Rabbit polyclonal	Primary	ABCAM
PECAM	Goat polyclonal	Primary	Santa Cruz
VEGFR2/KDR	Rat monoclonal	Primary	Santa Cruz
AlexaFluor 594	Donkey polyclonal	Secondary	Life Tech
HRP	Donkey polyclonal	Secondary	Santa Cruz

3.2.4 Implant Preparation

Equal volumes of 4% sodium alginate solution and 0.85% NaCl solution were mixed, and then growth factors were added to the solution. The mixture solution was then extruded through a syringe with an 18G needle attached via luer lock into 1.1% $CaCl_2$ solution and cross-linked for 1h at 4°C. One bead was implanted in each of the subcutaneous pockets created (as described in the section 3.2.5 below). 10µg of the growth factors were encapsulated in a 400µl mixture solution that formed 12 alginate beads.

3.2.5 Subcutaneous Implantation Model

Prior to this subcutaneous implantation surgery, the animals were fed for 15 weeks on normal or high fat diet to replicate the long-term diseased state in humans. The aim of this study was to examine the resistance to therapeutic angiogenesis via exogenous addition of growth factors. There were two groups for the subcutaneous implantation surgeries - WT mice on normal chow diet and ob/ob mice on high fat diet - representing the two ends of the disease extent.

The dorsal surface of the mouse was clipped, depilated, and prepared with a swab of Betadine followed by a swab of 70% ethanol and repeating the swabs three times consecutively. A skin incision was made on the back with a scissors and blunt dissections (using hemostats) were used to create four subcutaneous pockets, two on each side of the midline. An alginate bead containing growth factors or a control solution was implanted in the subcutaneous space. The wound was closed using resorbable sutures (Ethicon 5-0 polydioxanone sutures). After 7 days, the animals were sacrificed. To perform en-face imaging of the gels, the full thickness skin of the entire dorsal surface was removed and

mounted on a dissection tray. The alginate gels were then imaged macroscopically and were flash frozen in liquid N_2-cooled isopentane along with the surrounding skin tissue for subsequent analysis.

3.2.6 Histological Analyses and Immunostaining

Eight-micron thick sections were obtained from frozen tissues using the Leica CM 1850 Cryotome equipped with steel knife. For H&E staining, the sections were fixed in 10% formalin for 10 minutes, washed in 1X PBS for 5 minutes and then air dried at 60°C for 1h. The standard H&E protocol [96] was then followed and imaged with an upright compound microscope. Briefly, after a wash in distilled water, the sections were stained in Harris Hematoxylin solution for 8 minutes. This was followed by a 5-minute wash in running tap water to get rid of excess hematoxylin. Then the slides were put in differentiation buffer for 30 seconds and quickly washed under running tap water for 1 minute. This was followed by staining in Bluing reagent for 1 minute, a wash in running tap water for 5 minutes, a rinse in 95% alcohol, a counterstain in Eosin solution for 1 minute, a dehydration step using 95% alcohol, and finally two changes of absolute alcohol, 5 minutes each. The stains were cleared in two changes of xylene, 5 minutes each, and mounted with xylene-based mounting medium and cover glasses.

The slides with the sections on them were also stained by standard Movat's Pentachrome staining procedure [97] to investigate the anatomical features. The slides were placed in a slide rack and mordanted with Bouin's fluid for 1 hour at 50°C. Traces of Picric acid were removed by washing in running water for 2 minutes. They were then stained in 1% Alcian Blue for 20 minutes and washed in distilled water by dipping 5 times in the bucket. Then the slides were placed in Alkaline alcohol for 10 minutes at

56°C. Slides were washed in running water for 2 minutes. Then they were stained in Orcein-Verheoff Hematoxylin solution for 15 minutes and washed in distilled water twice by dipping, and then running tap water rinses. This step is the crucial as it stains for collagen and elastin. This was followed by Woodstain Scarlet-Acid Fuchsin stain for 2.5 minutes, 0.5% Acetic acid for 30 seconds, 5% Phosphotungstic acid for 7.5 minutes, 0.5 Acetic acid for 30 seconds and ultimately, 3 ethanol washes of 1 minute each. The slides were then stained with Alcoholic Saffron for 8 minutes and 2 ethanol washes with three dips each. To clean the slides at the end, two 30-second dips in Xylene were used and then mounted with cover glass and Cytoseal™ .

For immunohistochemical staining, the sections were fixed in 4% paraformaldehyde for 5-10 minutes, blocked with 25% FBS for 45 minutes and then exposed to a 1:50 dilution of primary antibody (refer Table 3.2 for details) overnight at 4°C. The following day, samples were washed three times with PBS and treated with a 1:500 dilution of secondary antibody conjugated to a fluorescent marker (Table 3.2) for 2h at room temperature. The slides were rinsed with PBS and cover glass mounted using DAPI containing anti-fade mounting medium (Vector Labs). Imaging was performed with the Zeiss Axiovert or Leica SP2 AOBS, and images were analyzed using Photoshop and Metamorph.

3.2.7 Statistical Analysis

All results were shown as mean $\pm$ SEM. An ANOVA with Duncan post-hoc test was used to make comparisons between groups of continuous variables. When comparing between two groups only, Student's t-test was used. A two tailed probability with p-value, $p < 0.05$ was considered statistically significant.

3.3 RESULTS

3.3.1 Gene Expression in Diseased Skeletal Muscle Tissue

To better understand the potential mechanisms underlying growth factor resistance in pre-diabetic, hyperlipidemic ob/ob mice, we fed these mice with 10 weeks of a high fat or normal chow diet and examined gene expression in the heart and muscle tissue. We first examined the quadriceps muscle tissue for gene expression levels of receptors and co-receptors for the FGF-2, VEGF-A, and PDGF-CC pathways.

At the mRNA expression level, we did not notice any significant changes within the WT-NCD and WT-HFD groups for all of the genes except heparanase. However, we found a 5- to 28-fold increase in ob/ob-HFD group for the gene expression of growth factor receptors/co-receptors including syndecan-1 (sdc-1), syndecan-4 (sdc-4), neuropilin-1 (nrp-1), FGFR-1, and VEGFR-2 (Figure 3.1). For WT-HFD group, we found a significant increase in heparanase, an enzyme that degrades heparan sulfate proteoglycans and mediates the release of angiogenic factor from the extracellular matrix [98]. This trend was absent in the ob/ob mice groups. An overall summary of the gene expression is shown in Table 3.3.

Table 3.3 Summary of Gene Expression Relative to WT Mice on a Normal Chow Diet (NCD), adapted from [89].

Tissue	**Heart**			**Muscle**		
Strain	WT	Ob/Ob	Ob/Ob	WT	Ob/Ob	Ob/Ob
Diet	HFD	NCD	HFD	HFD	NCD	HFD
Syn-1	ND	+	**+**	ND	+	**+++**
Syn-2	ND	+	**+**	---	-	+
Syn-4	-	+	+	+	ND	**+++**
PDGFR-α	**+**	+	**---**	--	-	ND
PDGFR-β	ND	+	+	ND	-	+
FGFR-1	ND	ND	+	--	**+++**	**++++**
VEGFR-2	-	+	**+**	+	ND	**++**
NRP-1	**++**	**++**	**++**	+++	++	**++++**
HPA	-	+	ND	**++++**	+++	+

Labels: HFD = High Fat Diet, NCD = Normal Chow Diet, ND = No difference,
+ = 1.5-3 fold more, ++ = 3-5 fold more, +++ = 5-10 fold more, ++++ = 10+ fold more
- = 1.5-3 fold less, -- = 3+ fold less, --- = 5-10 fold less, ---- = 10+ fold less
Bold = Statistically significant difference

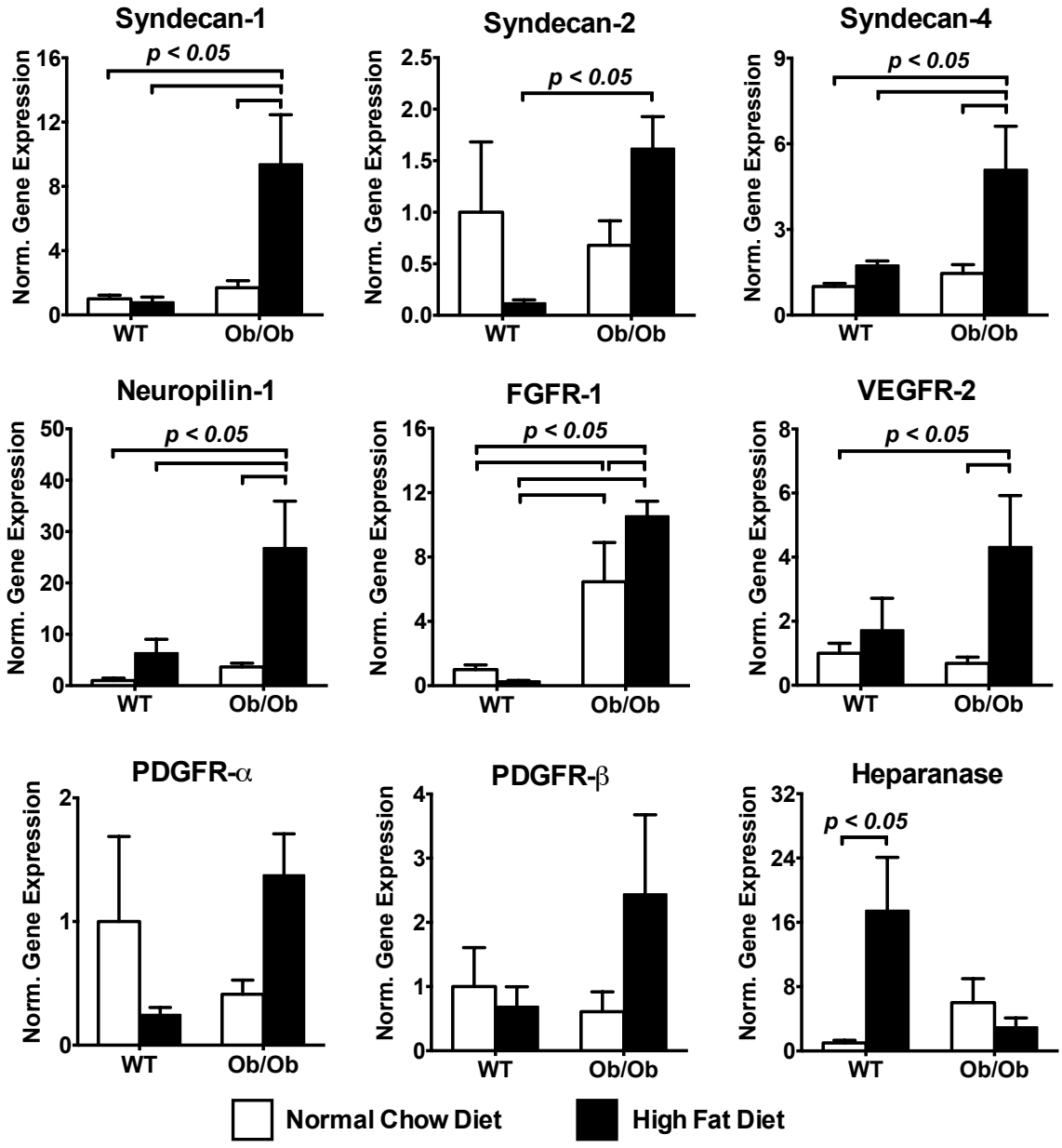

Figure 3.1 Gene expression in quadriceps muscle harvested from wild type (WT) and ob/ob mice after 10 weeks of normal chow diet (NCD) or high fat diet (HFD). Measurements were made using real time qPCR and are normalized to GAPDH expression and expressed relative to the mRNA levels of WT mice on NCD. n=10. Adapted from [89].

3.3.2 Protein Expression in Diseased Skeletal Muscle Tissue

We wanted to be certain about our findings and therefore, checked the protein expression levels of the receptors and co-receptors in the healthy and diseased tissues. Generally, it is expected that protein expression levels will be directly proportional to the gene expression levels in cells. Surprisingly, we observed a markedly different profile at the protein level compared to the gene expression levels in the muscle tissues.

For the co-receptors sdc-1, sdc-2, and sdc-4, and receptor PDGFR-α there was an increase in protein levels in WT-HFD group compared with WT-NCD (Figure 3.2). Interestingly, this increase was absent in the ob/ob mice. On the contrary, there was a significant reduction in the protein expression for the nrp-1 in ob/ob mice in comparison to the WT mice. All the protein levels were normalized by the protein mass in the tissue. We performed a GAPDH blot and found that the portion of GAPDH per unit protein was increased in the high fat diet group of the WT mice, and reduced in the ob/ob mice on high fat diet, suggesting a change in the number of cells per mg of protein in the tissue. The levels of heparanase protein corresponded well to the results for mRNA levels in the tissues, with an increase for the WT-HFD group and significant decrease in heparanase in the ob/ob-HFD group. An overall summary of the protein expression is shown in Table 3.4.

Table 3.4 Summary of Protein Expression Relative to WT Mice on a Normal Chow Diet, adapted from [89].

Tissue	**Heart**			**Muscle**		
Strain	WT	Ob/Ob	Ob/Ob	WT	Ob/Ob	Ob/Ob
Diet	HFD	NCD	HFD	HFD	NCD	HFD
Syn-1	**++**	ND	ND	**+**	ND	ND
Syn-2	+	-	-	+	-	-
Syn-4	**+**	ND	ND	**+**	ND	-
PDGFR-α	**+**	ND	ND	**++**	-	--
p-PDGFR-α/PDGFR-α	ND	ND	ND	-	**++**	-
PDGFR-β	**+**	ND	ND	ND	+	-
FGFR-1	**+**	ND	ND	ND	ND	-
VEGFR-2	ND	-	--	ND	ND	-
NRP-1	ND	ND	-	ND	**--**	**---**
HPA	**+++**	+	ND	**+++**	-	---

Labels: HFD = High Fat Diet, NCD = Normal Chow Diet, ND = No difference,
+ = 1.5-3 fold more, ++ = 3-5 fold more, +++ = 5-10 fold more, ++++ = 10+ fold more
- = 1.5-3 fold less, -- = 3+ fold less, --- = 5-10 fold less, ---- = 10+ fold less
Bold = Statistically significant difference

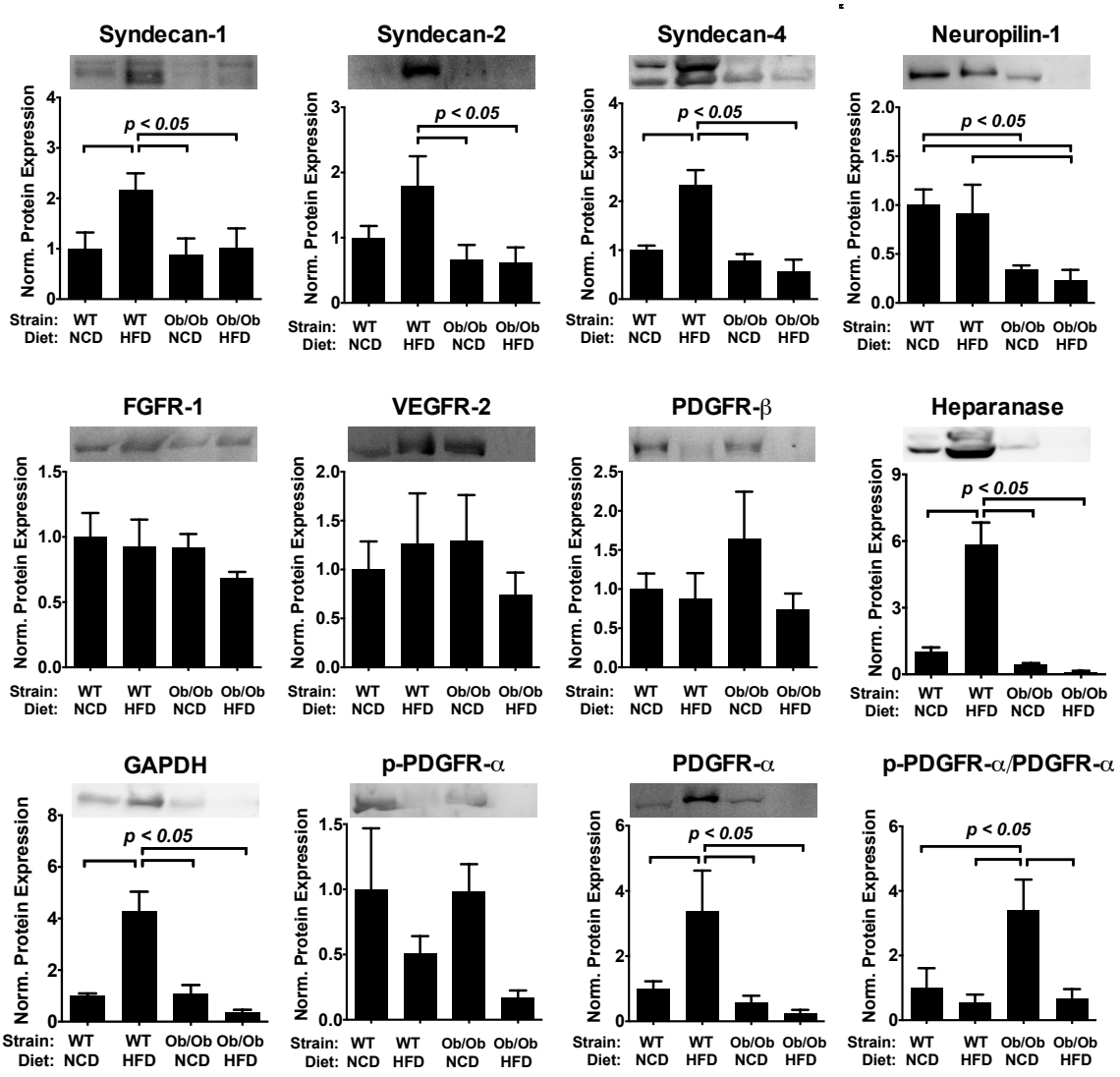

Figure 3.2 Protein expression of growth factor receptors and co-receptors in skeletal muscle harvested from wild type (WT) and ob/ob mice fed with normal chow diet (NCD) or high fat diet (HFD) for 10 weeks. Measurements are performed using densitometric analysis and expressed relative to the protein expression of WT mice on NCD. n=10. Adapted from [89].

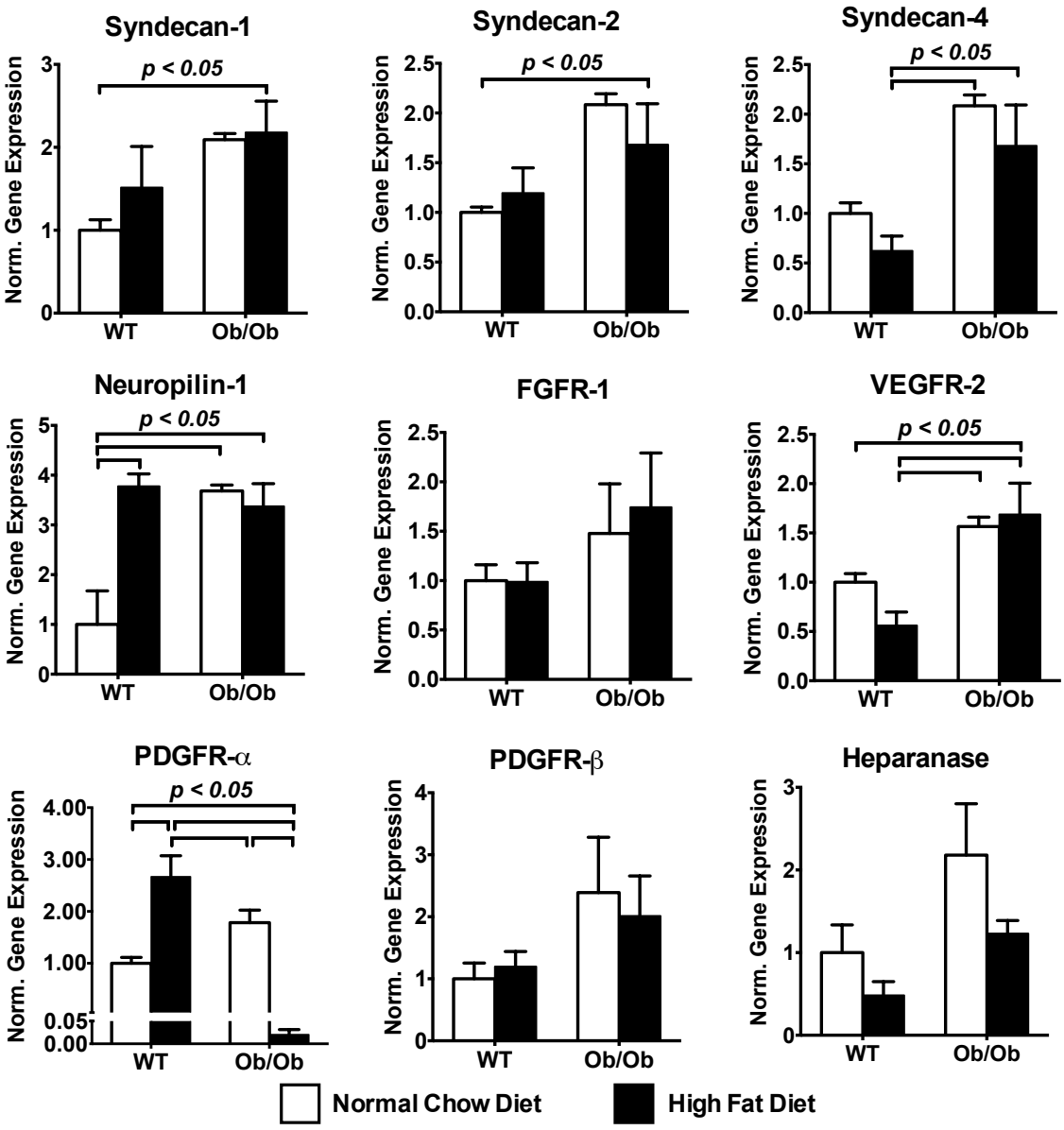

Figure 3.3 Gene expression in heart tissue harvested from wild type (WT) and ob/ob mice after 10 weeks of normal chow diet (NCD) or high fat diet (HFD). Measurements were made using real time qPCR and are normalized to GAPDH expression and expressed relative to the mRNA levels of WT mice on NCD. n=10. Adapted from [89].

3.3.3 Gene Expression in Diseased Myocardial Muscle Tissue

To examine if different mouse tissues were affected in a differential manner, we also analyzed the gene expression of growth factor receptors and co-receptors in myocardial tissue. We found that there were increased mRNA expressions for the syndecans and VEGFR-2 in ob/ob mice (both HFD and NCD groups), almost similar to the skeletal muscle results (Figure 3.3). For nrp-1, there was increased gene expression in the ob/ob groups and the WT-HFD group. The most striking result was a dramatic loss in gene expression for PDGFR-α (less than 3% of baseline WT levels) in the ob/ob-HFD group. We still have not figured out why this is happening but we speculate that it might be related to stem cell activity in the heart. A summary of these results can be found in Table 3.3.

3.3.4 Protein Expression in Diseased Myocardial Muscle Tissue

Similar to the results for skeletal muscle, we found a decrease in protein levels of receptors and co-receptors in contrast to gene expression levels, in the heart muscle. High fat diet induced an increase in the protein levels of sdc-1, -2, and -4 in WT mice, which was not observed in ob/ob mice (Figure 3.4). There was a similar trend for PDGFR-α with an over three-fold increase for WT-HFD group but a decrease in protein levels for the ob/ob-HFD group. Heparanase also increased in the WT-HFD but had WT baseline levels for both the groups of ob/ob mice. The overall summary of these results is shown in Table 3.4.

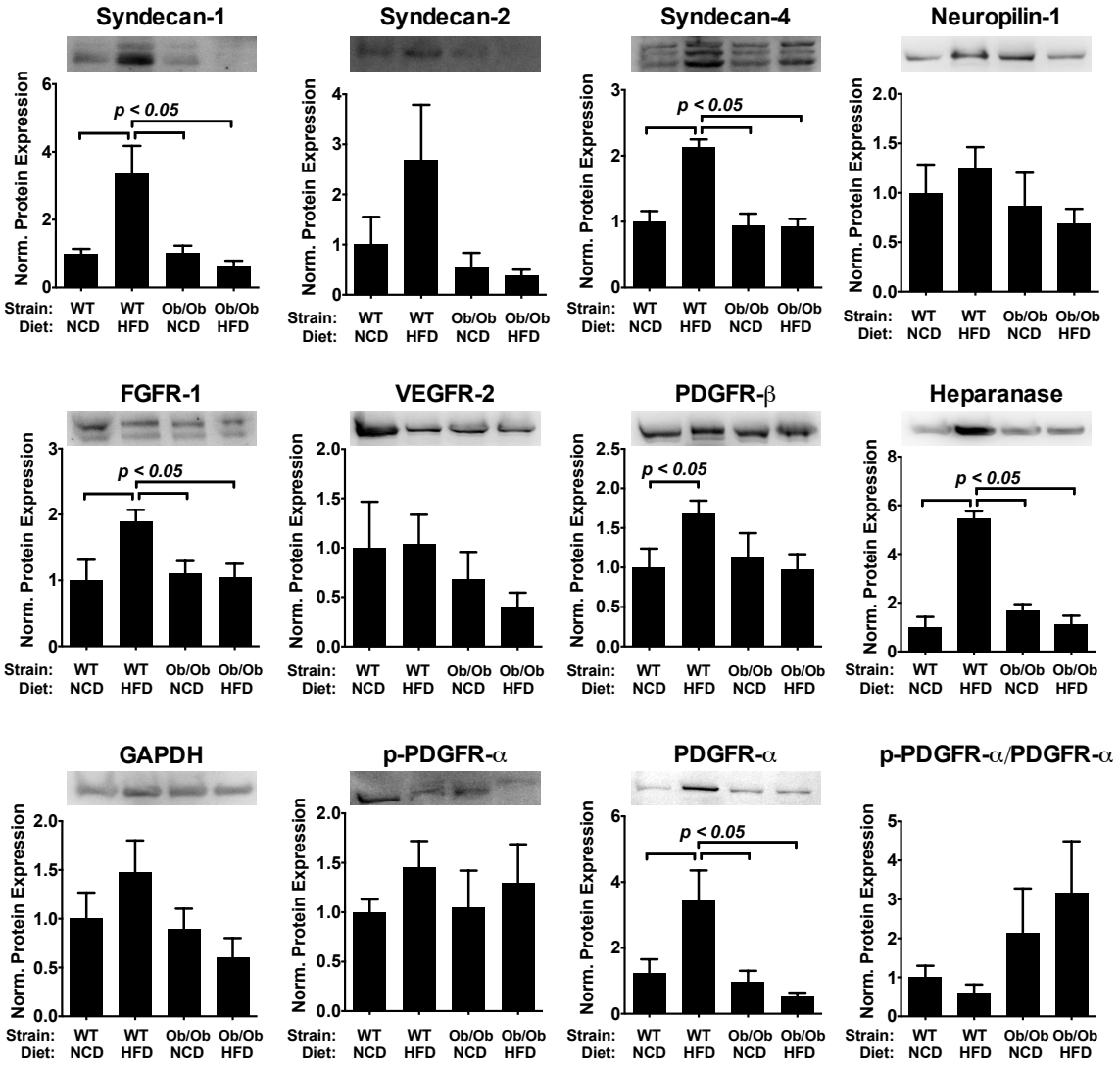

Figure 3.4 Protein expression of growth factor receptors and co-receptors in myocardial tissue harvested from wild type (WT) and ob/ob mice fed with normal chow diet (NCD) or high fat diet (HFD) for 10 weeks. Measurements are performed using densitometric analysis and expressed relative to the protein expression of WT mice on NCD. n=10. Adapted from [89].

3.3.5 Growth Factor Responsiveness in the Diabetic ob/ob Mouse Model

To examine whether ob/ob mice had growth factor resistance compared with WT mice, we implanted alginate gels that contained control (PBS), FGF-2, VEGF-A, or PDGF-CC, subcutaneously in the mice. We had two mouse groups - WT mice on normal chow diet and ob/ob mice on high fat diet. After 7 days, we found that there was little response to the control gel, both macroscopically (Figure 3.5A) and on histological analysis (Figure 3.6A). In WT mice, gels containing FGF-2 demonstrated increased vascularity (Figure 3.5B) as well as a thicker surrounding layer of vascularized tissue (Figure 3.6A,B, and Figure 3.7). In these mice, gels containing VEGF-A or PDGF-CC also had increased vascularity and moderately increased formation of a vascularized cellular layer. In ob/ob mice, vascularity and vascularized layer thickness was markedly decreased in the FGF-2 or PDGF-CC treated mice compared with the WT mice with the same treatments (Figure 3.5B). The decrease in cellular layer thickness (Figure 3.6B) was statistically significant in the FGF-2 and PDGF-CC groups. We also performed H&E and Movat's Pentachrome staining to the tissue micro-sections. The results showed that for both the mice, the surrounding layers were primarily cellular (Figure 3.6A, Figure 3.7). The cellular layer was confirmed to be composed of cells with high vascularity since they stained positively for CD31, also called PECAM-1, an endothelial cell marker (Figure 3.8). Histochemical staining confirmed the lack of fibrotic tissue (Figure 3.6A, Figure 3.7) and fluorescent immunostaining for CD45 (leukocyte common antigen) was negative for the surrounding tissue. Together these findings confirmed that WT mice had a more robust growth factor response compared with the ob/ob mice and supported the existence of growth factor resistance in this animal model.

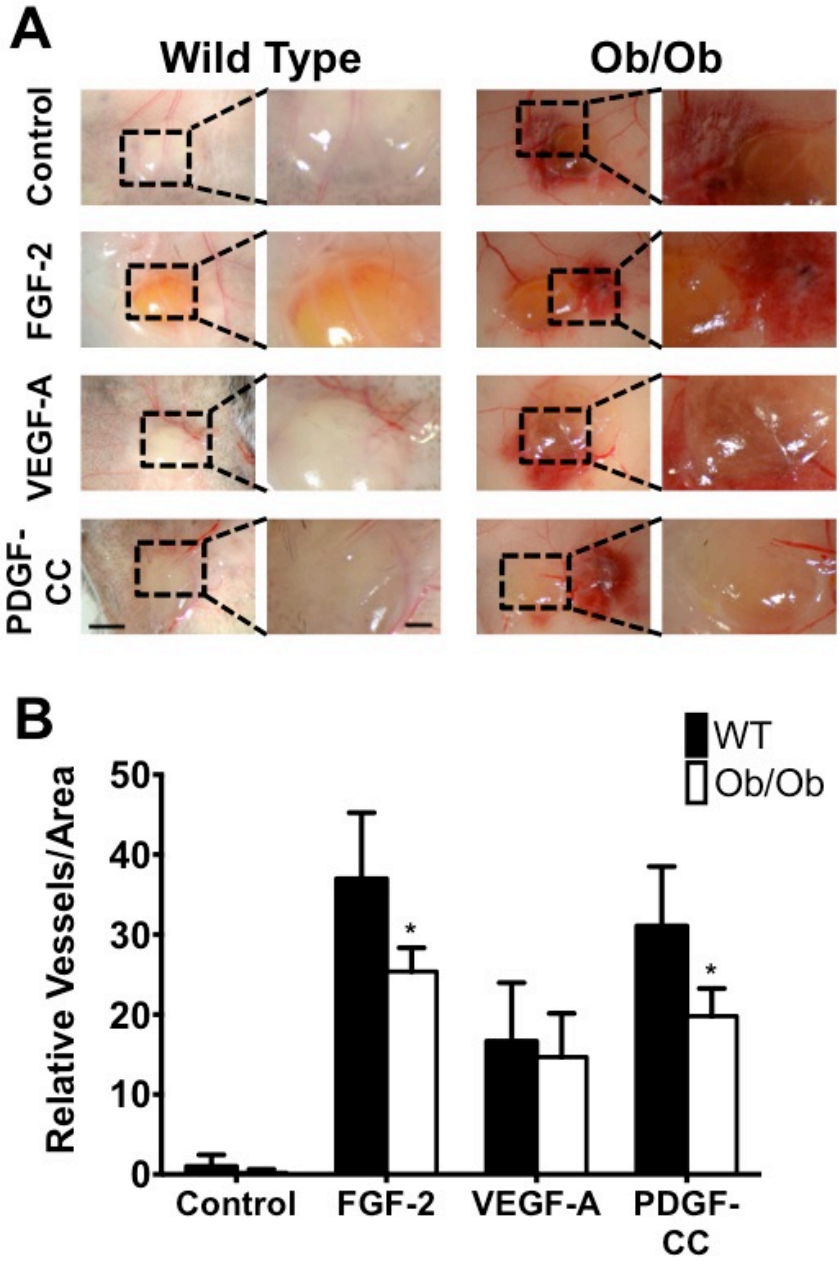

Figure 3.5 *In vivo* mouse model to test growth factor resistance by subcutaneously implanting alginate gels containing PBS, FGF-2, VEGF-A, or PDGF-CC on the back of mice. The gels were harvested after 7 days and macroscopically imaged (A). Vascularity on the gel was determined for the macroscopic images using Metamorph (B). Panel A - size bar = 3mm. Mag. size bar = 1mm. *Statistically different from WT group ($p < 0.05$). n=6. Adapted from [89].

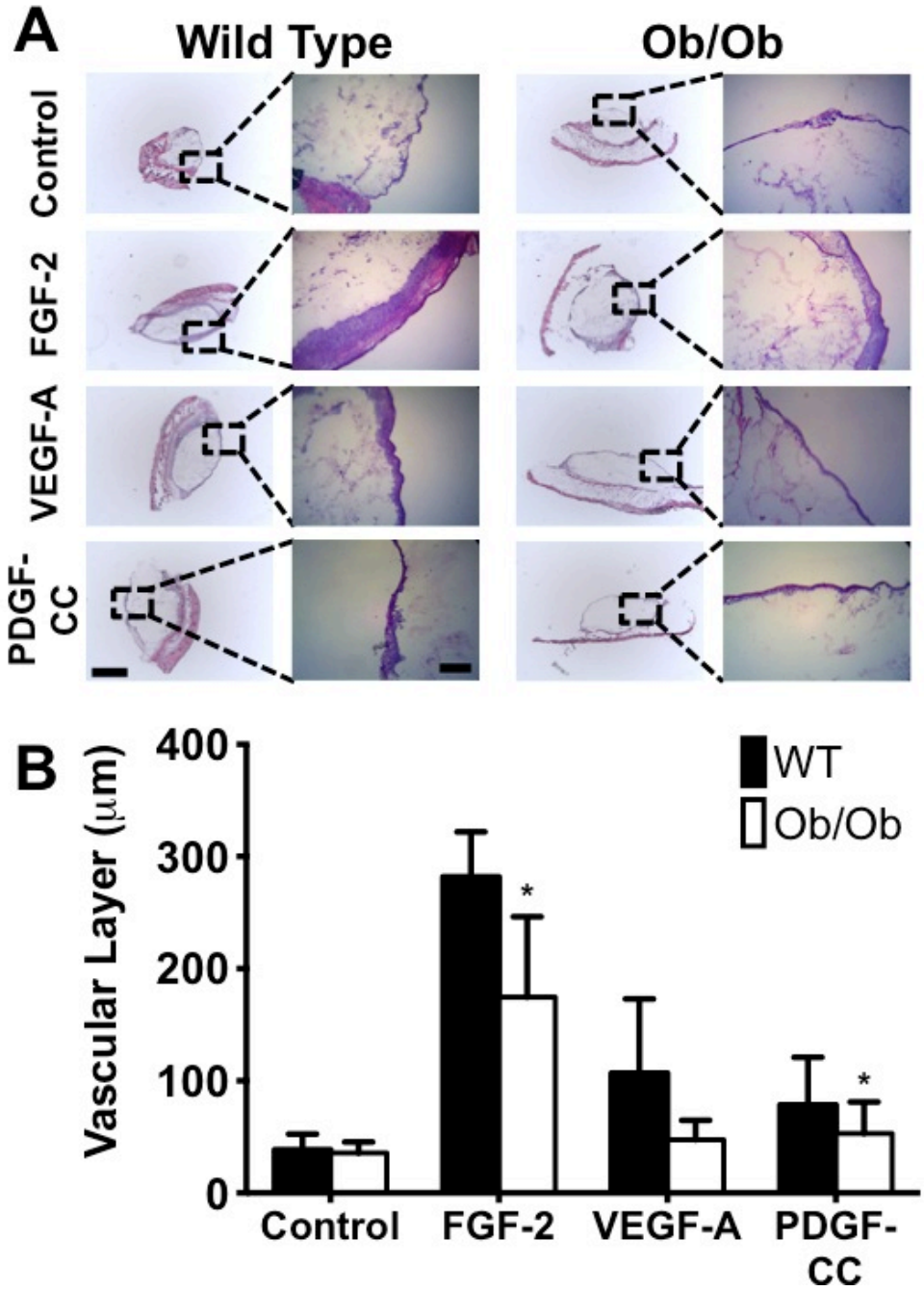

Figure 3.6 Gels harvested along with the native skin, frozen, sectioned, and H&E stained (A). The thickness of the vascular layer was quantified by analyzing the H&E stained images using Metamorph (B). *Statistically different from WT group ($p < 0.05$). n=6. Adapted from [89].

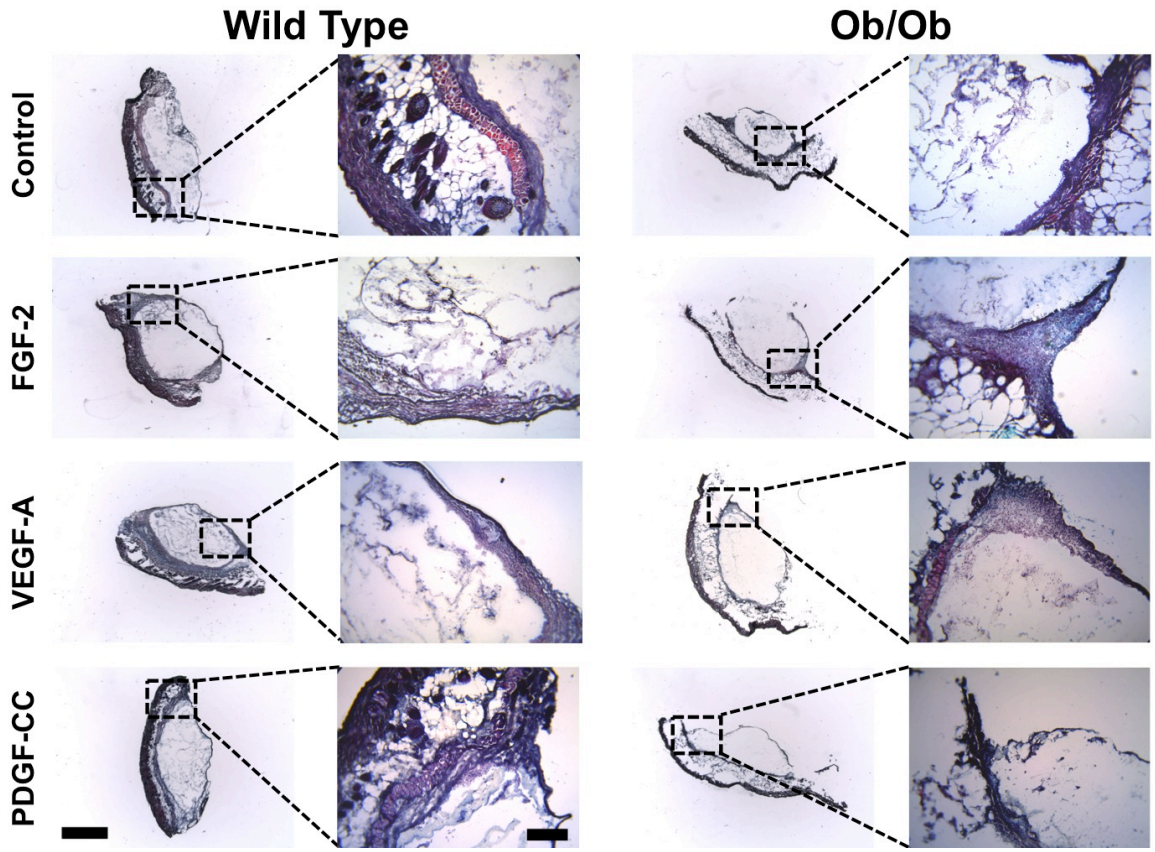

Figure 3.7 Movat's Pentachrome staining of the sections of alginate gels with PBS, FGF-2, VEGF-A, or PDGF-CC. The gels were harvested after 7 days frozen, sectioned, and stained as shown here. Size bar = 1mm. Mag. size bar = 250μm. n=6. Adapted from [89].

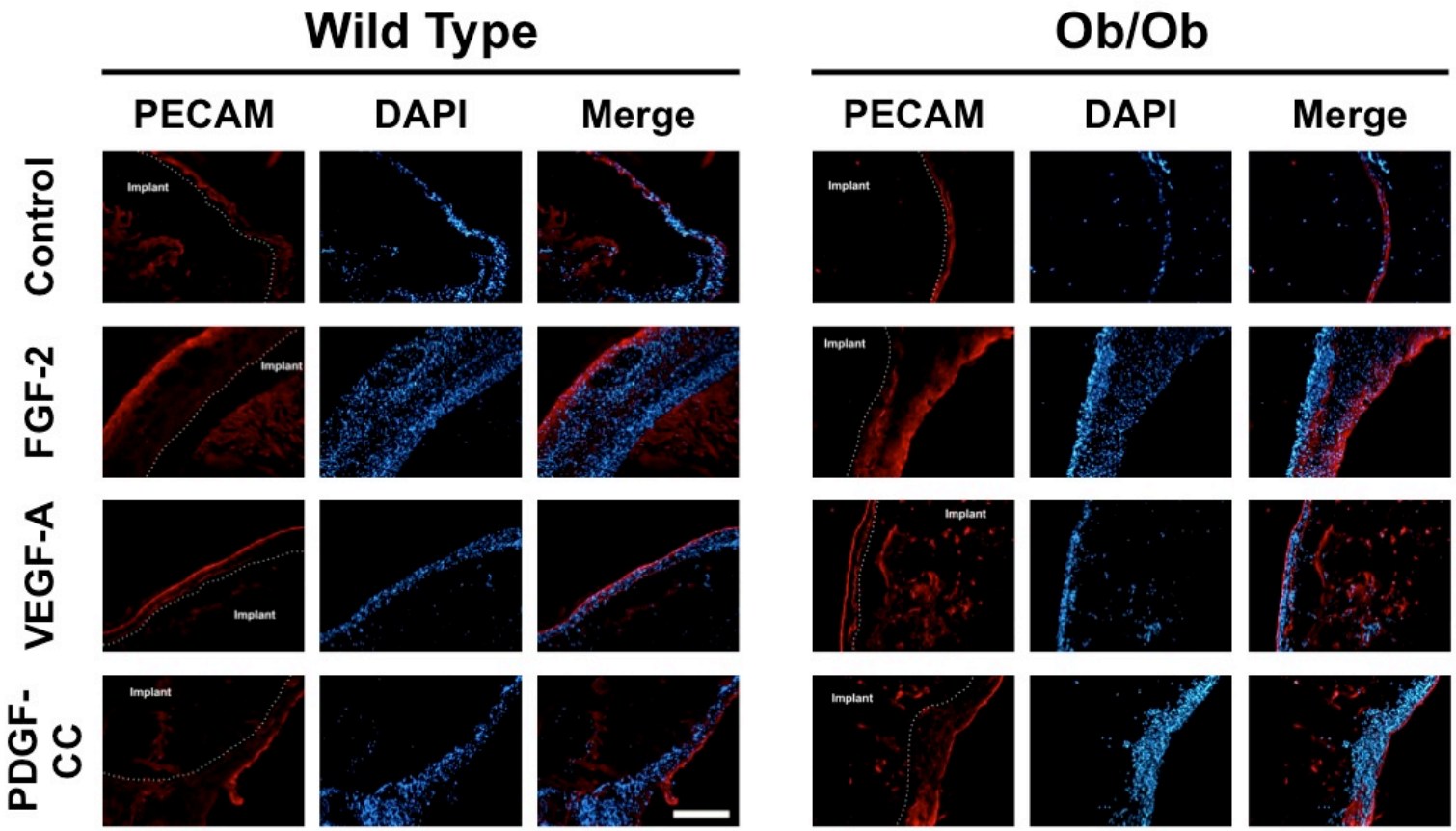

Figure 3.8 Sections immunostained with anti-PECAM1 antibody and imaged with an epifluorescence microscope. Size bar = 250μm. *Statistically different from ob/ob group ($p < 0.05$). n=6. Adapted from [89].

3.4 DISCUSSION

Diabetes and metabolic syndrome are major contributors to cardiovascular risk and mortality. Both diabetes and obesity have been associated with a loss of microvascular density and reduced formation of collateralization in ischemic tissues [99, 100]. Here, we show that the ob/ob mouse model has growth factor resistance in the context of therapeutic angiogenesis, to multiple growth factors including FGF-2, VEGF-A, and PDGF-CC. The results of this study also reveal a previously unrecognized loss in co-receptor levels in ob/ob mice and have broad implications in both understanding the mechanisms of growth factor resistance and designing new effective angiogenic therapies. One of the key findings of this study is the potential pitfall of drawing conclusions of growth factor pathway status through the use of gene expression analysis, particularly for receptors and co-receptors. In both the heart and muscle samples we found a paradoxical increase in mRNA levels in contrast to the protein levels of the receptors/co-receptors. Some potential implications of these findings include either post-transcriptional mechanisms of regulation for these proteins or increased degradation/shedding of these molecules resulting in removal of the protein from the cell surface. Syndecans, in particular, are known to be shed from the surface through the action of proteases [66]. In either case, it is clear from our studies that a proteomic rather than genomic approach to studying these pathways is required to capture the full complexity of the regulation of these processes due to diabetes and high fat diet.

The regulation of the growth factor receptors and co-receptors had a remarkably similar regulation for all the signaling pathways studied. The archetypal pattern was an increase in protein expression in the WT mice on a high fat diet, with no change in the

ob/ob mice on a high fat diet. A possible explanation for these findings is that with an unhealthy high fat diet that likely causes the initial stages of endothelial dysfunction and vascular disease, the WT mice being analogous to healthy people, up-regulate their angiogenic pathways. The ob/ob mice that are compromised by their additional metabolic defects could not compensate by increasing their receptor levels. This finding is consistent with the finding of previous studies that show an increase in neuropilin-1 (nrp-1) in WT mice following ischemia and no change in nrp-1 in db/db mice after induction of ischemia [94]. Thus, ob/ob mice have an altered compensation to disease that may in part recapitulate the long-term diseased state in human patients. In our studies, heparanase was found to increase with high fat diet in the WT mice. This finding is consistent with a previous study that demonstrated up-regulation of heparanase by fatty acids [101]. Our group has recently linked heparanase to restenosis and thrombosis following stenting [102, 103] and in the pathogenesis of atherosclerosis [104]. Heparanase is also linked to angiogenesis and is found to release angiogenic growth factors from sequestration in heparan sulfate proteoglycans [98]. Interestingly, elevated heparanase levels were not observed in ob/ob mice fed with high fat diet in our studies. This would suggest that the elevation of heparanase levels is critical for compensatory revascularization under the high fat diet in WT mice; however, this mechanism does not occur with the additional defects in the ob/ob mice.

3.5 CONCLUSIONS

Angiogenic therapies have generated great interest both in animal studies and in clinical trials. However, despite these many promising animal studies, no therapies have shown clinically meaningful benefits in controlled clinical trials. Our findings here suggest that this may be due to the development of growth factor resistance in patients with long-term disease that is absent when using healthy animal models. In this work, we have identified multiple defects in growth factor signaling pathways that involve loss of receptors and co-receptors at the protein level.

Chapter 4: Syndesome Therapy Characterization and Overcoming the Disease-Induced Growth Factor Resistance in ob/ob mice

4.1 Introduction

Our laboratory recently showed that syndesomes with fibroblast growth factor-2 (FGF-2) enhance migration, proliferation, and tube formation in human endothelial cells [67]. *In vivo* studies showed markedly improved neovascularization following femoral artery ligation in normal healthy rats treated with syndesomes (Figure 4.1). Ischemic limbs completely recovered in 7 days when treated with FGF-2 and syndesomes, compared with only partial recovery when treated with FGF-2 only. This trend continued beyond 16 days. The syndecans are a family of single-pass transmembrane proteins that can serve as co-receptors for FGF [105, 106]. Syndecans have sites for post-translational glycosylation with heparan sulfate chains that lend them this remarkable repertoire of physiological functions.

Therefore, we hypothesize that a major contributing factor in the failure of therapeutic revascularization therapies is the presence of long-term disease, which fundamentally alters the biology of angiogenesis in patients with PVD that leads to "growth factor resistance." We attribute this resistance to exhausted compensatory mechanisms in the diseased tissue. In this chapter, we demonstrate the optimization of the syndesome therapy. We use the therapy to reinstate the levels of syndecan-4 in the diseased tissue. We envision that by doing so, the diseased tissue will be revived to its native healthy phenotype and will respond to the growth factor treatment.

4.2 Materials and Methods

4.2.1 Protein Production

A constitutive expression vector containing the full-length syndecan-4 gene (Genecopoeia) was transduced into HEK-293Ta cells (Genecopoeia) using the Lenti-Pac transduction kit (Genecopoeia). Two days post-transduction, cell lysis was performed with a buffer containing the following: 20mM Tris (pH 8.0), 150mM NaCl, 1% Triton X-100, 0.1% SDS, 2mM sodium orthovanadate, 2mM PMSF, 50mM NaF, and protease inhibitors (Roche). The lysates were clarified by centrifugation for 15 minutes at 15,000 × g, and the supernatant was collected. The pooled lysates were desalted and separated sequentially using ion exchange and affinity chromatography. The separations were performed with an AKTA FPLC (GE Healthcare) using a Q anion exchange column. The samples were then concentrated using a Centriprep (Millipore). SDS-PAGE and silver staining were used to analyze the purity of the final concentrated samples.

4.2.2 Syndesome Fabrication

Syndesomes are liposomal nanoparticles with the syndecan-4 transmembrane proteins embedded on the membrane. Standard lipid stock solutions were prepared at 10mg/ml concentration in chloroform. The following lipids were used: 1,2-dioleoyl-sn-glycero-3-phosphocholine (DOPC), 1,2-dioleoyl-sn-glycero-3-phosphoethanolamine (DOPE), cholesterol, and sphingomyelin (Avanti Polar Lipids) mixed in a ratio of 40:20:20:20 by volume, respectively. The solution mixture was prepared in a round-bottom flask, and the solvent was removed first using a rotatory evaporator (Heidolph Collegiate) for 1h and then under a stream of argon gas for 15 minutes. The lipid film

was then resuspended in a HEPES-buffered salt solution (10.0mM HEPES and 150mM NaCl in PBS, pH 7.4) by mixing, sonicating, and freeze-thawing to achieve a final solution of 13.2mM total lipid. The final lipid solution was then extruded through a 400nm polycarbonate membrane (Avestin). A detergent, 1% n-octyl-β-D-glucopyranoside (OG), was added to both the 13.2mM lipid and the 25μg/ml syndecan-4 protein solutions. The concentration of the solution was reduced to 40% of the original in 10% increments every 30 minutes through dilution with PBS. The detergent and free protein was removed by extensive dialysis in PBS at 4°C. Residual OG was removed by repeated BioBead treatments (SM-2; Bio-Rad). The resulting syndesome solution was stored at 4°C with gentle shaking to reduce aggregation.

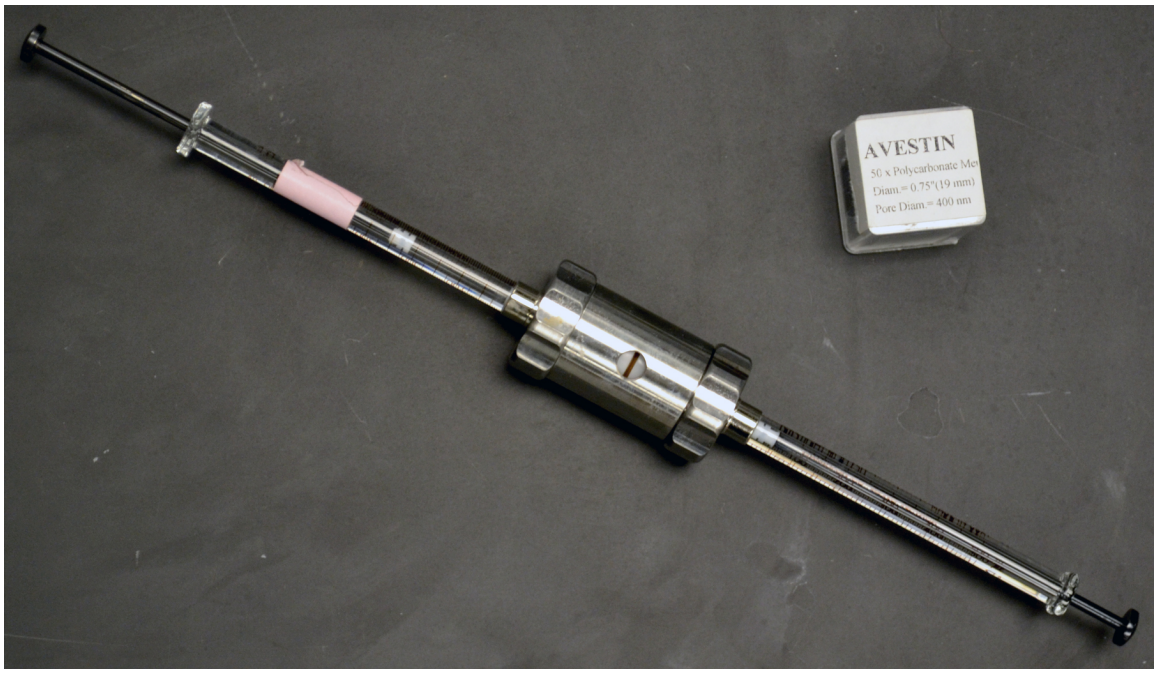

Figure 4.1 Extrusion apparatus used for fabricating liposomes.

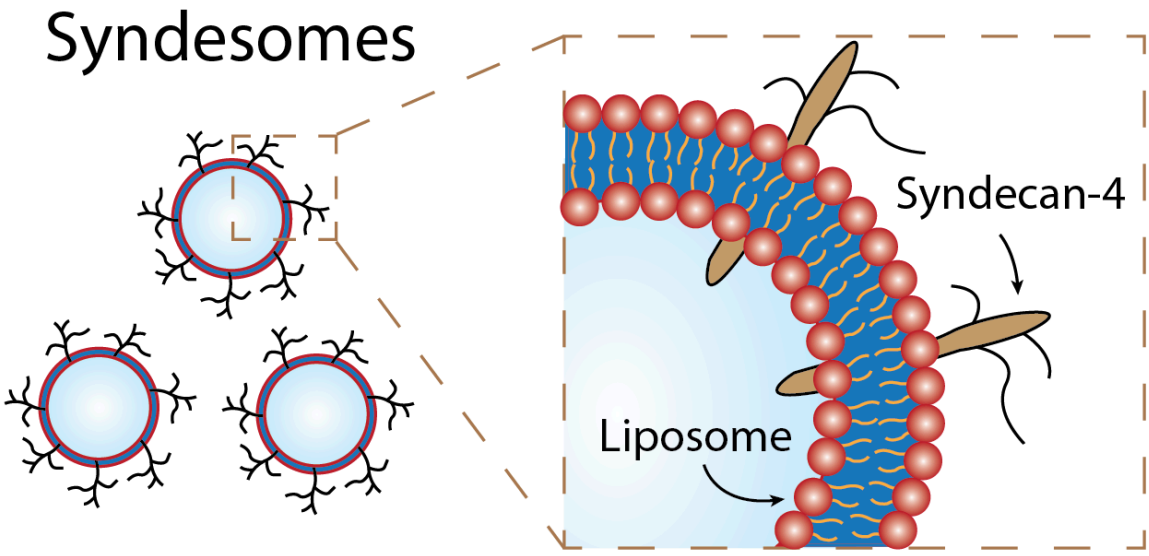

Figure 4.2 Schematic diagram showing syndesomes that have syndecan-4 protein embedded on the membrane.

4.2.3 Syndesome Characterization

The size and dispersion of the syndesomes were characterized by dynamic light scattering (Malvern Zetasizer Nano ZS). The instrument was calibrated using 54 nm polystyrene particles. The syndesomes were diluted 1:1000 to fit the detection region of the instrument and then aliquoted into a polystyrene cuvette to run in the machine. The results were averaged over 50 size measurements. For TEM, the syndesomes were infused with cryo-protectant for at least one hour. The samples were mounted onto cryo pins and frozen rapidly under liquid N_2. The cryo pins were stored in cryo vials in liquid N_2 Dewar flask until they were sectioned. The 50-80 nm sections were imaged on the cryo TEM (FEI Technai Spirit Transmission Electron Microscope)

4.2.4 Implant Preparation

Alginate hydrogels in the form of tiny spherical beads were used, similar to those used in the last study to probe growth factor resistance. Equal volumes of 4% sodium alginate (Sigma™) solution and 0.85% NaCl (Sigma™) solution were mixed and the syndesomes and/or growth factors were added to it. The solution was extruded through a syringe with an 18G needle into a 1.1% $CaCl_2$ solution and cross-linked for 1 hour at 4°C. For growth factor delivery, 10µg of the growth factors were encapsulated in 400µl solution to form 12 beads. For S4PL+FGF-2, 5µg of syndesomes and 10µg of FGF were added to 400µl of the solution to form 14 beads.

4.2.5 Animal Model

The ob/ob also called B6.Cg-Lep^{ob}/J (Jackson Labs) diseased mouse model was used for these studies. Since disease resistance was observed in this model, it made sense to test whether the co-delivery of growth factors with co-receptors might increase the potency of the growth factor activity. All animal studies were performed with the approval of the University of Texas at Austin's Institutional Animal Care and Use Committee (IACUC) and in accordance with NIH guidelines "Guide for Care and Use of Laboratory Animals" for animal care. Wild type mice C57BL/6J (Jackson Labs) were used as control healthy animals. The WT mice were fed normal chow diet (LabDiet - Prolab RMH 1800) and ob/ob mice were fed the high fat diet (Research Diets - D12331). The animals were fed for 15 weeks to simulate healthy, and long-term diseased state in humans before performing the subcutaneous implantation surgery.

4.2.6 Subcutaneous Implantation

The mice were fed for 15 weeks to simulate the normal and long-term diseased states in humans before examining the resistance to therapeutic angiogenesis via exogenous addition of growth factors. There were two groups for the subcutaneous implantation surgeries - WT mice on normal chow diet and ob/ob mice on high fat diet, representing two ends of the disease spectrum.

The dorsal surface of the mouse was clipped, depilated, and prepared with a swab of Betadine followed by a swab of 70% ethanol and repeating the swabs three times consecutively. A skin incision was made on the back with a scissor and blunt dissections (using hemostats) were used to create 4 subcutaneous pockets, two on each side of the midline. An alginate bead containing growth factors or a control solution was implanted in the subcutaneous space. The wound was closed using resorbable sutures (Ethicon 5-0 polydioxanone sutures). After 7 days, the animals were sacrificed. To perform en-face imaging of the gels, the full thickness skin of the entire dorsal surface was removed and mounted on a dissection tray. The alginate gels were then imaged macroscopically and gels along with the surrounding skin tissue were flash frozen in liquid N_2-cooled isopentane for subsequent analysis.

4.2.7 Histology and Staining

Eight-micron thick sections were obtained from frozen tissues using the Leica CM 1850 Cryotome equipped with steel knife. For H&E staining, the sections were fixed in 10% formalin for 10 minutes, washed in 1X PBS for 5 minutes and then air dried at 60°C for 1h. The standard H&E protocol [96] was then followed and sections imaged with an upright compound microscope. Briefly, after a wash in distilled water, the

sections were stained in Harris Hematoxylin solution for 8 minutes. This was followed by a 5-minute wash in running tap water to get rid of excess hematoxylin. Then the slides were put in differentiation buffer for 30 seconds and quickly washed under running tap water for 1 minute. This was followed by staining in Bluing reagent for 1 minute, a wash in running tap water for 5 minutes, a rinse in 95% alcohol, a counterstain in Eosin solution for 1 minute, dehydration through 95% alcohol, and finally two changes of absolute alcohol, 5 minutes each. The stains were cleared in two changes of xylene, 5 minutes each, and mounted with xylene-based mounting medium and cover glasses.

The slides with the sections on them were also stained by standard Movat's Pentachrome staining procedure [97] to investigate the anatomical features. The slides were placed in a slide rack and mordanted with Bouin's fluid for 1 hour at 50°C. Traces of Picric acid were removed by washing in running water for 2 minutes. They were then stained in 1% Alcian Blue for 20 minutes and washed in distilled water by dipping 5 times in the bucket. Then the slides were placed in Alkaline alcohol for 10 minutes at 56°C. Slides were washed in running water for 2 minutes. Then they were stained in Orcein-Verheoff Hematoxylin solution for 15 minutes and washed in distilled water twice by dipping and then running tap water rinses. This step is crucial as it stains for collagen and elastin. This was followed by staining in the Woodstain Scarlet-Acid Fuchsin for 2.5 minutes, 0.5% Acetic acid for 30 seconds, 5% Phosphotungstic acid for 7.5 minutes, 0.5 Acetic acid for 30 seconds and ultimately, 3 washes of ethanol 1 minute each. The slides were then stained with Alcoholic Saffron for 8 minutes and 2 washes of ethanol with three dips each. To clean the slides at the end, two 30-second dips in Xylene were used, and then mounted with cover glass and Cytoseal™ .

For immunohistochemical staining, the sections were fixed in 4% paraformaldehyde for 5-10 minutes, blocked with 25% FBS for 45 minutes and then exposed to a 1:50 dilution of primary antibody (refer Table 3.2 for details) overnight at 4°C. The following day, samples were washed three times with PBS and treated with a 1:500 dilution of secondary antibody conjugated to a fluorescent marker (refer Table 3.2 for details) for 2h at room temperature. The slides were rinsed with PBS and cover glass mounted using DAPI containing anti-fade mounting medium (Vector Labs). Imaging was performed with the Zeiss Axiovert or Leica SP2 AOBS, and images were analyzed using Photoshop and Metamorph.

4.2.8 Statistical Analysis

All results were shown as mean $\pm$ SEM. When comparing only two groups, Student's t-test was used. A two tailed probability with p-value, $p < 0.05$ was considered statistically significant.

4.3 RESULTS

4.3.1 Characterization of Syndesomes

We created syndesomes by isolating the recombinant protein (Figure 4.3) and combining it with liposomes using the detergent extraction method. We confirmed the integrity of the liposomes by performing a TEM analysis of ultrathin sections of the syndesomes (Figure 4.5). In addition, we measured the size distribution of the isolated recombinant protein and the syndesomes following liposomal embedding and dialysis. This analysis demonstrated that the recombinant protein in isolation had significant self-

association and separated into three distinct peaks, likely representing three oligimerization states (Figure 4.4A). The syndesomes exhibited a single peak corresponding to the liposome diameter of ~400 nm. (Figure 4.4B) To obtain a slow and sustained release of FGF-2 and syndesomes, we encapsulated them in an alginate gel. Measurements of the release of growth factor and lipid from the gel revealed that it is dependent on the crosslinking density and shape of the hydrogel. While a 4% alginate bead released all the contents by 8 days, the 2% alginate disk needed only 5 days to disintegrate. The release profiles of FGF-2 were similar for both the FGF-2 alone and FGF-2 with syndesomes.

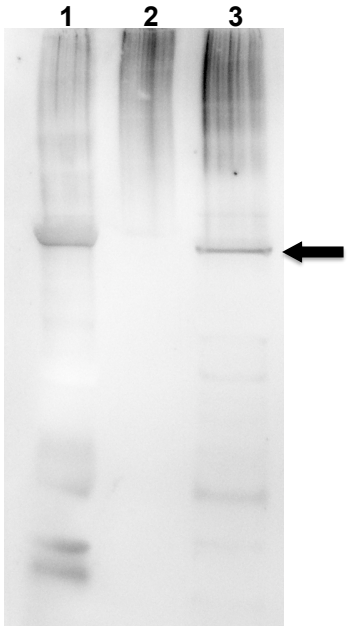

Figure 4.3 Western blot after SDS PAGE gel run showing three lanes - Ladder (**1**), negative un-transfected control (**2**), and cell lysate of transduced cells (**3**). The nitrocellulose membrane was incubated in syndecan-4 antibody. Purified syndecan-4 protein (**black arrow**) and some degraded or extracellular domain of syndecan-4 (lower band) show up on the developed blot.

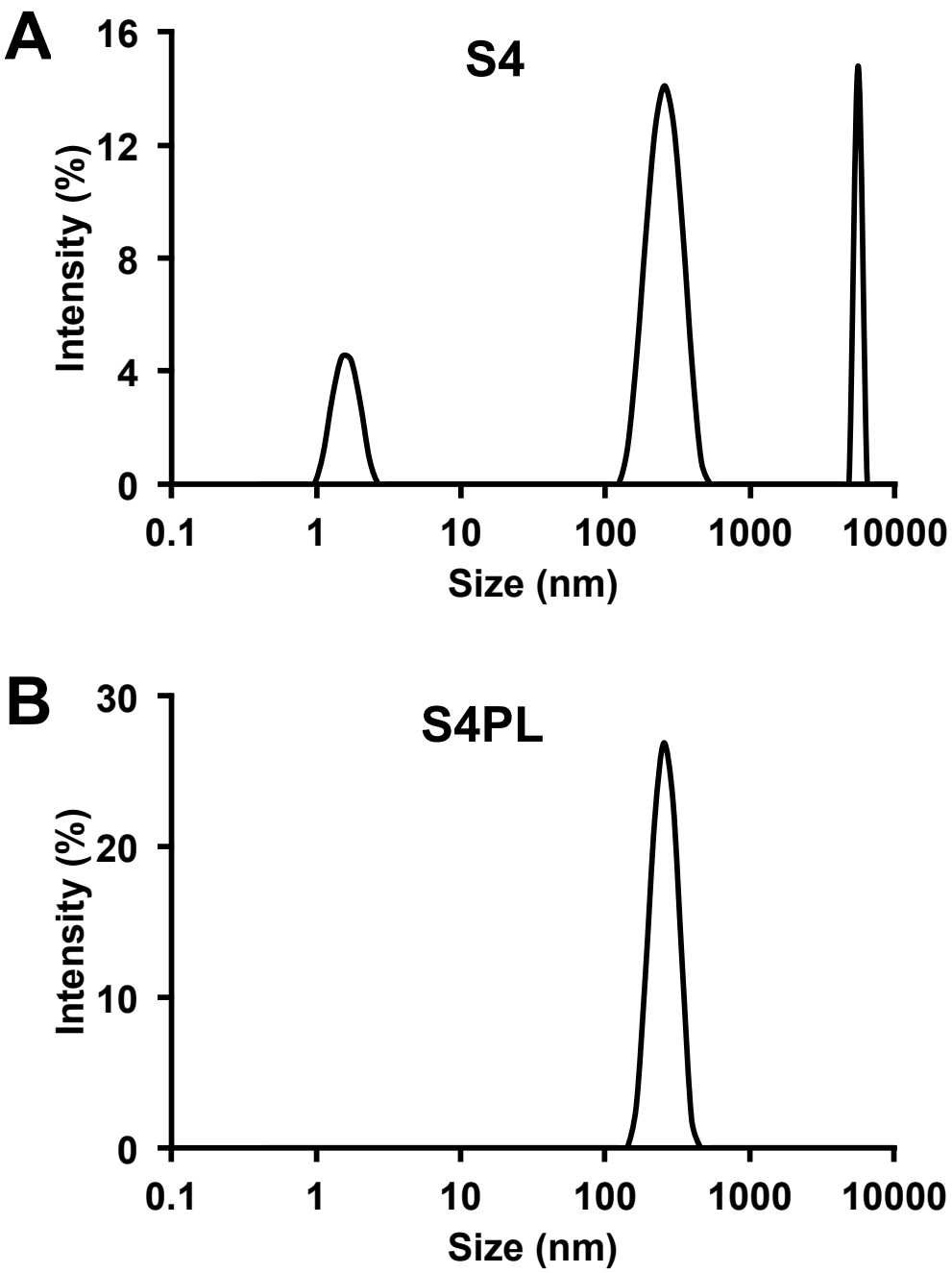

Figure 4.4 Dynamic light scattering results for syndecan-4 protein in solution (A) and syndesomes (S4PL) in solution (B).

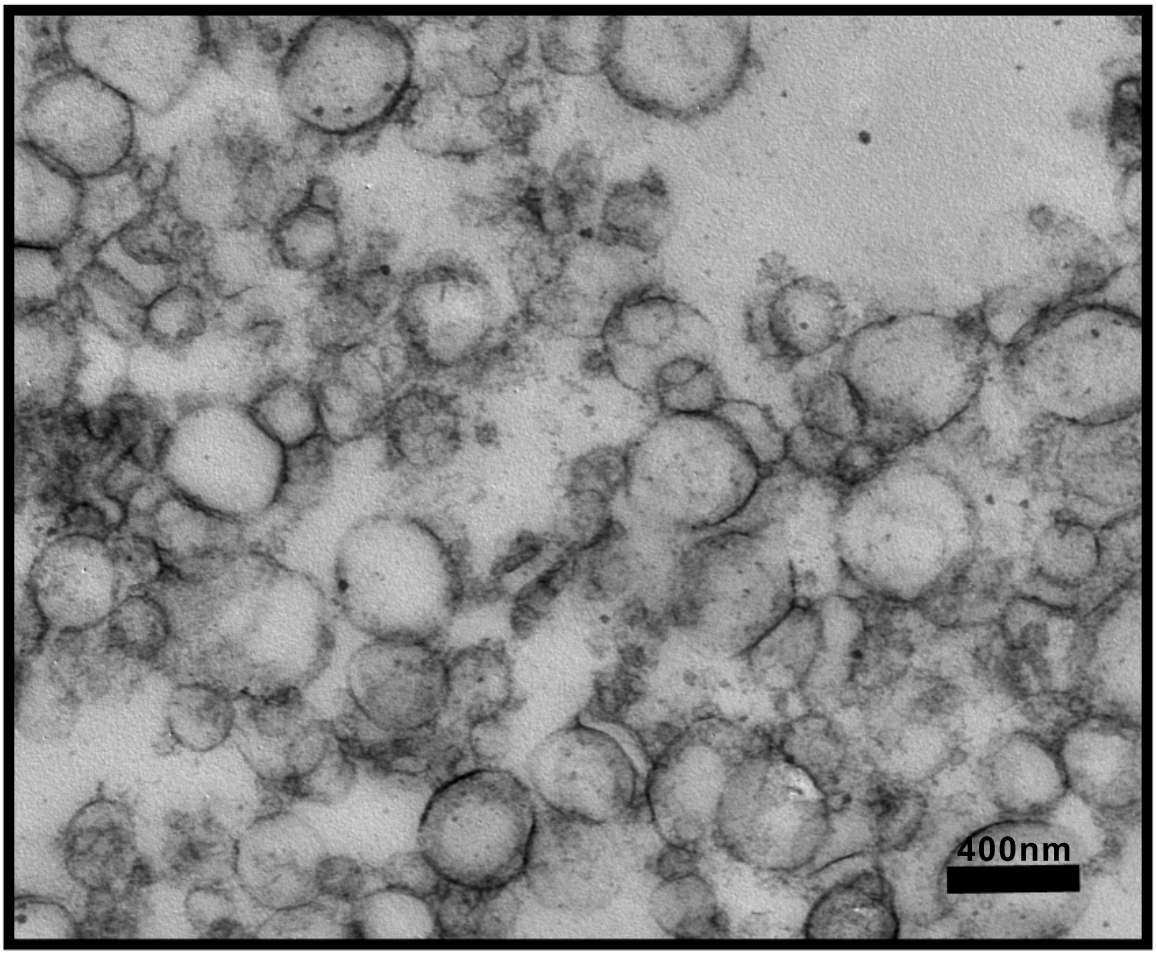

Figure 4.5 Cryo-TEM image showing the syndesomes in a cross sectional view.

4.3.2 Overcoming Growth Factor Resistance in ob/ob Mouse Model

The failure of many human trials for growth factor therapies has highlighted the need for new treatments that can overcome growth factor resistance [44]. Our finding of decreased cell surface co-receptors in a diseased state suggested that this could be an amenable target for increasing growth factor activity in disease states. We have recently shown that growth factor activity can be enhanced in healthy animals by co-delivering them with sdc-4 embedded in a liposomal carrier [67].

Here, we microencapsulated syndesomes in an alginate carrier and examined whether this treatment could overcome disease-induced resistance to growth factor stimulation. We subcutaneously implanted gels containing PBS, FGF-2, and FGF-2 with syndesomes in ob/ob mice after 15 weeks of high fat diet. The addition of syndesomes markedly enhanced vascularity (Figure 4.6A,B) as well as the vascularized layer thickness (Figure 4.7A,B). We observed similar alterations for the vascularized layer thickness for both WT and ob/ob mice. PECAM staining of the sections confirmed that the cellular layer around the gels was indeed vascular (Figure 4.9). We also performed Movat's Pentachrome Staining on the tissue sections that confirmed the cellular nature of the tissue surrounding the implant (Figure 4.8). Together these studies support that the delivery of the co-receptor proteins, which are reduced in the diseased tissue, can enhance the growth factor response and significantly overcome the growth factor resistance in this animal model of diabetes and obesity.

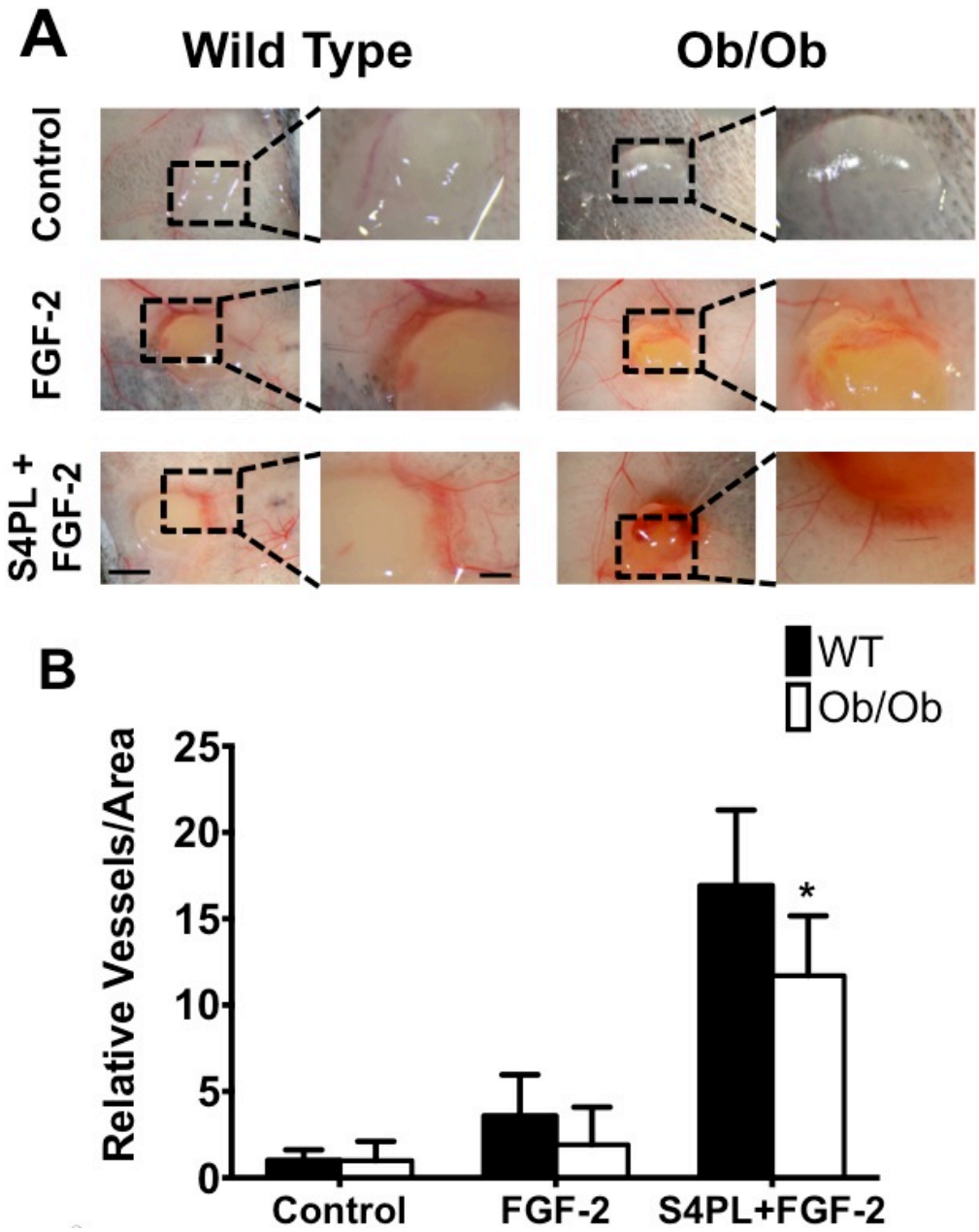

Figure 4.6 Alginate gels harvested after 7 days and macroscopically imaged (A). Vascularity around the gel was determined for the macroscopic images using Metamorph (B). Panel A - size bar = 3mm. Mag. size bar = 1mm. *Statistically different from WT group ($p < 0.05$). n=5. Adapted from [89].

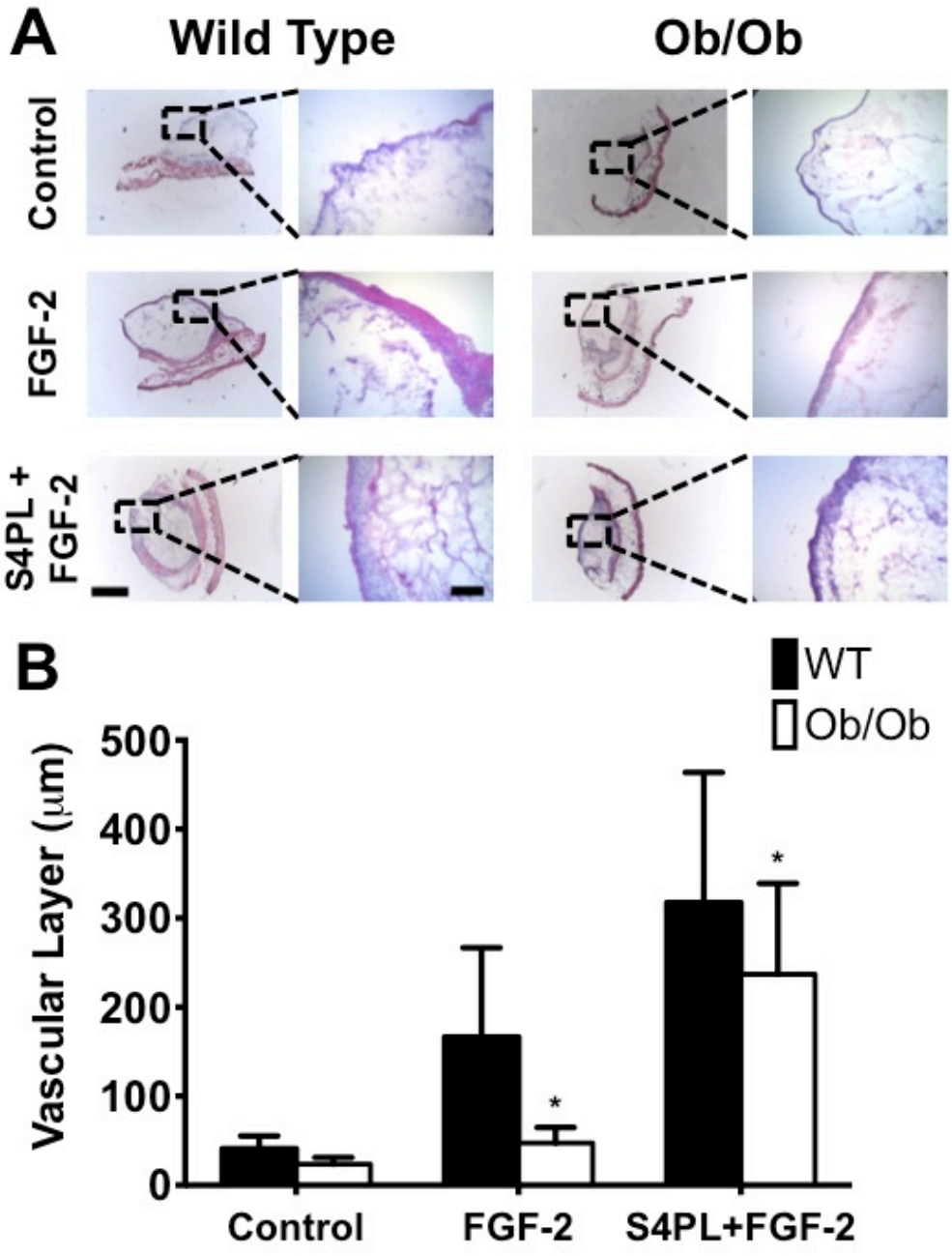

Figure 4.7 The alginate gels along with the skin, frozen, sectioned, and H&E stained (A). The thickness of the vascular layer was quantified by analyzing the H&E stained images on Metamorph (B). Panel A - size bar = 1mm. Mag. size bar = 250μm. *Statistically different from WT group ($p < 0.05$). n=5. Adapted from [89].

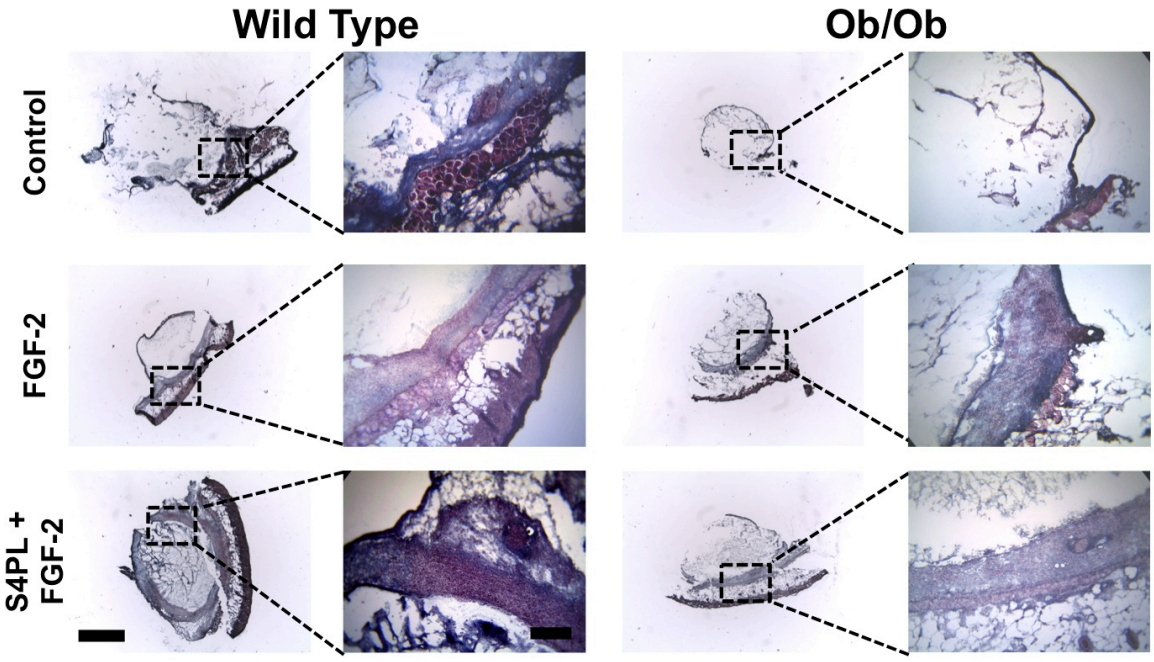

Figure 4.8 Movat's Pentachrome staining of the sections of alginate gels with PBS, FGF-2 and syndesomes with FGF-2 (S4PL+FGF-2). The gels were harvested after 7 days frozen, sectioned, and stained as shown here. Size bar = 1mm. Mag. size bar = 250μm. n=5. Adapted from [89].

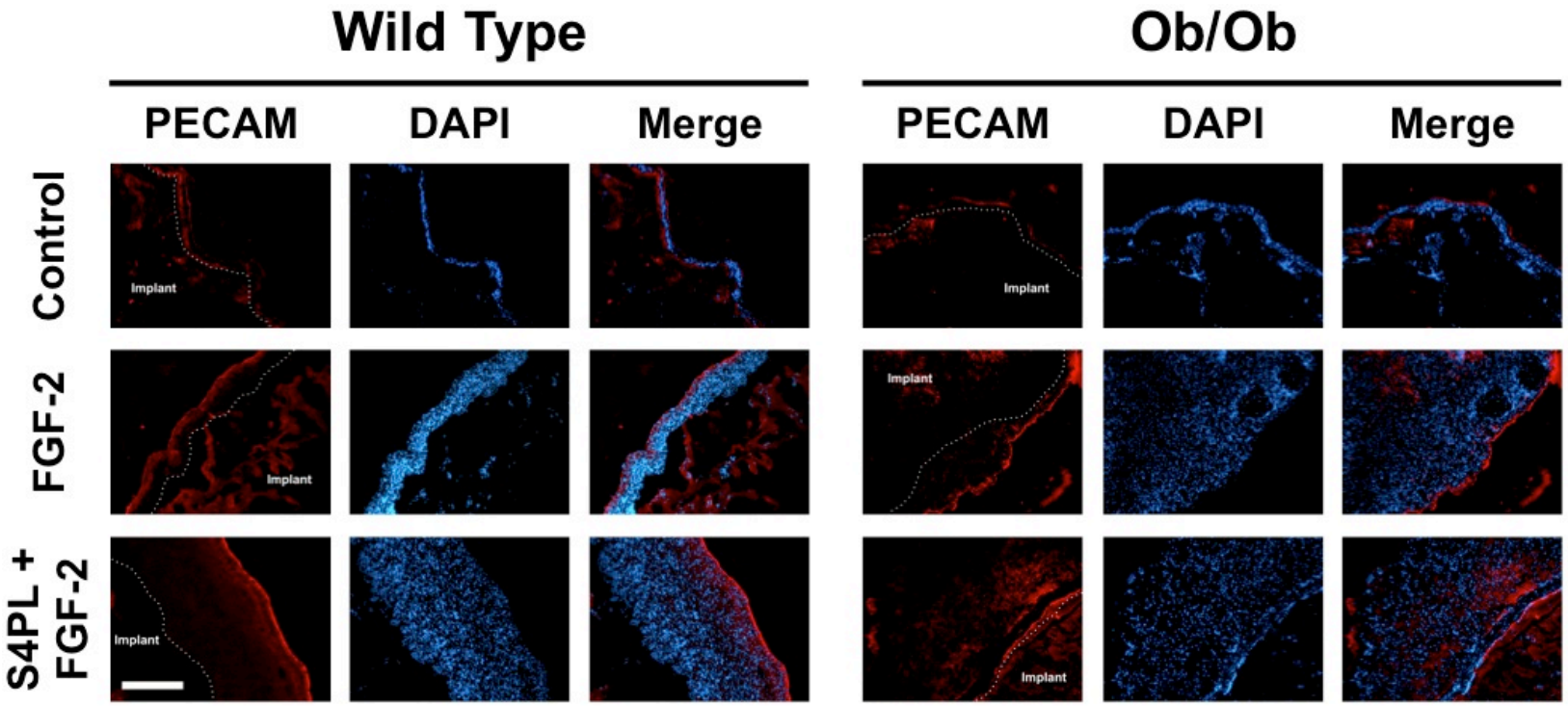

Figure 4.9 Sections immunostained with anti-PECAM antibody and imaged with an epifluorescence microscope. Size bar = 250μm. *Statistically different from ob/ob group ($p < 0.05$). n=5. Adapted from [89].

4.4 DISCUSSION

In our studies aimed at overcoming growth factor resistance, we focused our therapeutic strategy on restoring sdc-4 as a means for enhancing angiogenesis in the diseased state. Syndecan-4 is known to regulate FGFR-1 signaling and macropinocytosis [67, 107]. It also has pro-angiogenic activities through interactions with thrombospondin-1 [108] and regulates FGF-2 signaling [109]. Due to the continued challenges in applying exogenous gene delivery in humans [55], we developed a strategy to deliver co-receptors that are absent due to disease by using recombinant proteins embedded in a liposomal carrier [67]. Our major aim here was to test whether exogenously delivered growth factor co-receptors could overcome growth factor resistance that is caused by loss of co-receptors. In our studies, the syndesomes were highly effective in enhancing FGF-2 stimulation in mice with disease. Our findings suggest a unique approach for combating growth factor resistance at the level of co-receptor/receptor loss and illustrate an example of the efficacy of this strategy in an animal disease model. Liposomal co-receptor therapies may have the potential to treat many diseases in which the enhancement or reduction of signaling is caused by the loss of a co-receptor. Sdc-1 and nrp-1 (other co-receptors that were lost due to diseased state) would be appealing targets to explore for the development of additional therapeutics.

4.5 CONCLUSIONS

Briefly, we have shown that it is possible to identify deficiencies in growth factor signaling pathways in diseased tissues. We found that the diseased tissue is unable to make appropriate amount of protein in spite of higher gene expression levels and thus does not respond to the diseased state. Further, we have found that replenishing isolated components of the signaling cascade in an appropriate delivery system can markedly enhance *in vivo* response to growth factor treatments. These preliminary experiments demonstrate the feasibility and potential of this unique and powerful approach to increasing the efficacy of growth factor-based therapies in the clinical setting. However, much work remains in understanding and applying this approach to human disease.

Diabetes and associated peripheral diseases are a worldwide problem with no long-term solutions. To treat ischemia and non-healing foot ulcers, we aim to better understand the mechanisms acting in diseased patients and to develop a novel injectable gel for enhancing growth factor therapies. The basic findings and techniques developed in this thesis represent a paradigm shift in how growth factor signaling pathways are approached from a therapeutic perspective. While this work focuses on ischemia and vascular disease, growth factors are intimately involved in the mechanisms of many diseases including cancer growth and metastasis, wound healing and the immune response to infection. Thus, the innovative techniques we will develop will have a broad impact on the understanding and treatment of diverse disease states.

Chapter 5: Syndesomes Enhance Revascularization in Ischemic Muscle of Diseased and Diabetic Mouse

5.1 Introduction

Peripheral vascular disease (PVD) has serious clinical consequences for patients including atypical pain, intermittent claudication, foot ulcers, and ultimately, an increased risk for limb amputation and cardiovascular mortality [4]. The current clinical standard of care for PVD includes physical therapy, pharmacological interventions, endovascular stent placement and surgical bypass of stenosed arteries [9]. While these methods are used to treat the symptoms on a short-term basis, presently no durable, long-term treatment options exist in clinical use for patients with PVD. The diabetic population is particularly plagued by conditions caused by PVD, with high prevalence of foot ulcers and lacerations. Ankle-brachial index (ABI) screens have determined that the prevalence of PVD among diabetics is approximately 20-30% [110]. Although 50% of the patients are asymptomatic, their prognoses steadily worsens with time [4]. The 5-year mortality rate among patients with symptomatic PVD is about 20% [25]. Of those patients who develop critical limb ischemia, as many as 25% require amputation, increasing the mortality rate to 25% [26]. Type-2 diabetes has become a global epidemic afflicting about 347 million people and is responsible for the deaths of about 4.6 million people worldwide, according to the WHO. Since the risk of PVD is significantly increased in the presence of diabetes, it is essential to find viable treatment options for PVD. The ideal solution is to revascularize ischemic tissue and restore it to a healthy state of blood flow.

Several studies have examined the effectiveness of growth factors and associated genes, proteins, and cells for treating peripheral ischemia. The *TRAFFIC* trial, a phase I, randomized and double-blinded trial using delivery of bFGF-2, found no difference between placebo and double dose of treatments despite promising early studies [10, 11]. Similarly, a phase I/IIa trial for the delivery of hepatocyte growth factor plasmid found no significant benefit in comparison to placebo [14]. Clinical trials of implantation of bone marrow mononuclear cells have also shown no considerable improvement compared to present revascularization standards [110]. None of the existing studies have shown any statistically significant benefit over placebos.

The overarching goal of my thesis is to overcome the disease-induced growth factor resistance by delivering the missing growth factor co-receptors to revitalize the diseased tissue to a healthier phenotype. In the present chapter, we describe the experiments performed to test the syndesomal therapy to revascularize ischemic muscle in a diseased diabetic mouse model.

5.2 Materials and Methods

5.2.1 Animal Model

All animal experiments were performed with the approval of the Institutional Animal Care and Use Committee (IACUC) of University of Texas at Austin and in accordance with NIH guidelines "Guide for Care and Use of Laboratory Animals" for animal care. All the animal experiments were performed on a diabetic, obese and hyperlipidemic mouse model (ob/ob). They were fed for 15 weeks with a high-fat diet before being utilized for the surgeries. This was done to recapitulate the human diseased

condition more closely and simulate the physiological response of an obese diabetic person. The animals were sacrificed 14 days after the surgery and the tissues were used for histology and staining.

5.2.2 Implant Preparation

Spherical alginate beads encapsulating all the treatment groups were fabricated for the hind-limb ischemia surgery. Equal volumes of 4% sodium alginate (Sigma™) solution and 0.85% NaCl (Sigma™) solution were mixed and the syndesomes and/or growth factors were added to it. The solution was extruded through a syringe with an 18G needle into a 1.1% $CaCl_2$ solution and cross-linked for 1 hour at 4°C. About 3.6μg of FGF-2 and 0.34μg of syndecan-4 protein in the S4PL + FGF-2 group, and 3.6μg of FGF-2 in the FGF-2 group were encapsulated in the gels that were implanted in each mouse.

5.2.3 Hind Limb Ischemia Surgical Model

Mice were anaesthetized using 3% isoflurane gas. The left hind limb was shaved and surgically prepared with three swabs each of Betadine and 70% ethanol. A skin incision was made on the medial side of the thigh of the left hind limb, and the femoral artery was dissected free from the vessel bundle, without damaging the vein and nerve (Figure 5.1). The left femoral artery was then ligated with two sutures using 3-0 woven silk, just distal to the inguinal ligament. Alginate beads encapsulating syndesomes and/or FGF-2 were applied directly to the region surrounding the femoral artery (Figure 5.2). The wound was closed using resorbable sutures (5-0 vicryl). The animals were closely monitored and were administered with buprenorphine analgesic medication (0.1 mg/kg at 12-24 hour intervals) for two days following surgery. The animal's limb perfusion was

monitored daily using laser speckle imaging as described below. At day 14, mice were euthanized to harvest the gastrocnemius and quadriceps muscle of both ischemic and contralateral limb. Tissues were snap frozen in liquid N_2-chilled isopentane for further use.

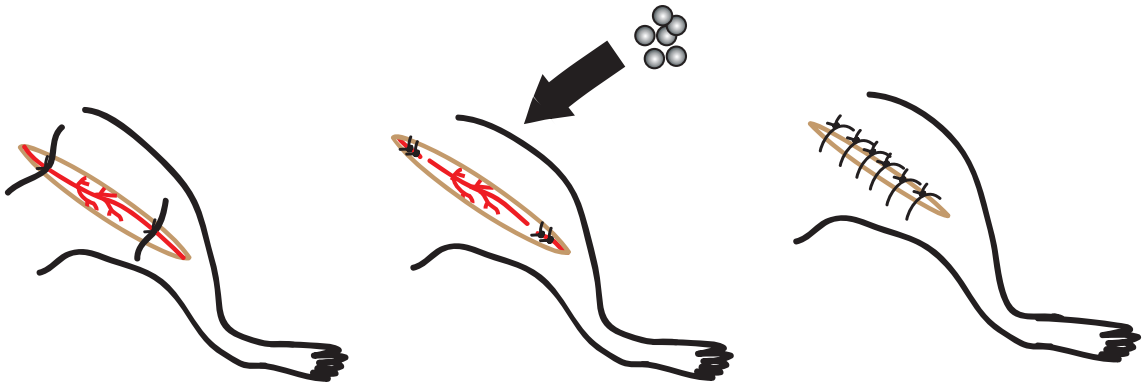

Figure 5.1 Schematic diagram showing left femoral artery ligation procedure to induce ischemia in the hind limbs of the mice. The alginate gels are implanted at the incision site and stitched with 5-0 sutures.

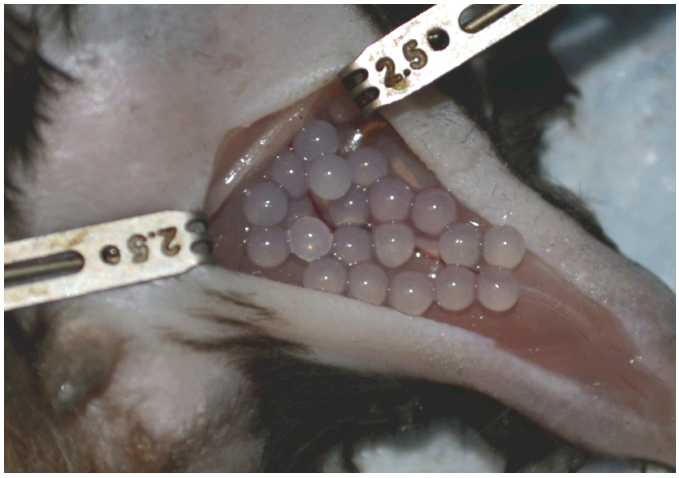

Figure 5.2 Macroscopic image of the left hind limb with ligated femoral artery and alginate gels in the incision site. The retractors keep the incision in place to facilitate the surgery.

5.2.4 Laser Speckle Contrast Imaging

The Laser Speckle Contrast Imager (LSCI) maps the tissue blood flow by the shift in laser light frequency due to the motion of blood [111] (Figure 5.3). This was used for serial noninvasive physiological evaluation of neovascularization by the animal's blood perfusion that was monitored at the time points. The blood perfusion in the ischemic limb (hind-limb ischemia surgery) was quantified relative of the contralateral control limb. The blood perfusions in the wounds (excisional wound surgery) were quantified relative to the wound with control gel implanted in the wound bed.

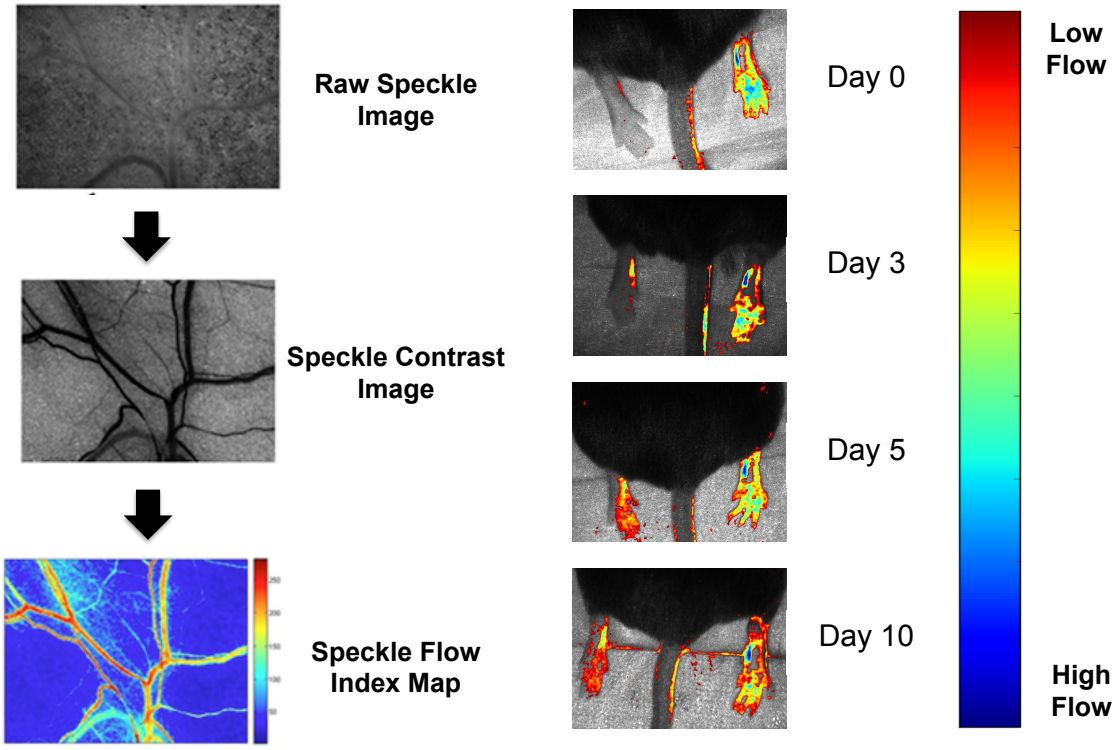

Figure 5.3 The raw speckle image converted into a speckle contrast image and then into a speckle heat map image showing relative blood flow (left). Non-invasive imaging of ischemic feet after the femoral ligation surgery showing blood perfusion in the feet relative to uninjured feet. The heat map bar shows the relative flow conditions for different colors (right).

5.2.5 Histology, Immunostaining, and Quantification

The muscle tissues were embedded in paraffin and 6μm sections were made using a microtome. H&E staining was performed for anatomical feature characterization, as described: the sections were de-paraffinized with two changes of xylene, 10 minutes each. They were re-hydrated in two changes of absolute alcohol for 5 minutes each, followed by 95% alcohol for 2 minutes and 70% alcohol for 2 minutes. The slides were then washed in 1X PBS for 5 minutes and placed on the slide warmer at 60°C for 1 hour. After a brief wash in distilled water, the sections are stained in Harris Hematoxylin solution for 8 minutes. This was followed by a 5-minute wash in running tap water to get rid of excess hematoxylin. Then the slides were put in differentiation buffer for 30 seconds and quickly washed under running tap water for 1 minute. This was followed by staining in Bluing reagent for 1 minute, a wash in running tap water for 5 minutes, a rinse in 95% alcohol, counterstain in Eosin solution for 1 minute, dehydration through 95% alcohol, two changes of absolute alcohol - 5 minutes each. Finally, the stains were cleared in two changes of xylene, 5 minutes each, and mounted with xylene-based mounting medium and cover glasses.

The slides were then Movat's stained to stain the various components in the tissue to probe more of the anatomical features. The sections were de-paraffinized and hydrated as described above. The slides were placed in a slide rack and mordanted with Bouin's fluid for 1 hour at 50°C. Traces of Picric acid were removed by washing in running water for 2 minutes. They were then stained in 1% Alcian Blue for 20 minutes and washed in distilled water by dipping 5 times in the bucket. Then the slides were placed in Alkaline alcohol for 10 minutes at 56°C. Slides were washed in running water for 2 minutes. Then they were stained in Orcein-Verheoff Hematoxylin solution for 15 minutes and washed in

distilled water twice by dipping and then running tap water rinses. This step is crucial since it stains for collagen and elastin. This was followed by Woodstain Scarlet-Acid Fuchsin stain for 2.5 minutes, 0.5% Acetic acid for 30 seconds, 5% Phosphotungstic acid for 7.5 minutes, 0.5 Acetic acid for 30 seconds, and ultimately, 3 ethanol washes of 1 minute each. The slides were then stained with Alcoholic Saffron for 8 minutes and 2 ethanol washes with three dips each. To clean the slides at the end, two 30-second dips in Xylene were used, and then mounted with cover glass and Cytoseal™ .

They were also immunostained using the Envision+ Dual Link Kit (Dako™) for M1 macrophage marker (CD86), M2 macrophage marker (CD163), and endothelial cell marker (von Willebrand factor). The slides were warmed for 10 minutes at 60°C on a slide warmer. Then they were de-paraffinized as described above. The next step in the protocol was vital and had to be carefully optimized for the fatty mouse tissues that were stained. The slide rack was placed in a bucket with Antigen Retrieval Solution (Dako) and placed in the microwave (1250W) for 2 minutes and 40 seconds. Then the bucket is placed in a water batch maintained at 80°C for 3 hours. This reduces the background staining significantly. The slides were cooled in solution for 20 minutes and washes in PBS twice for 5 minutes each. Then they were blocked in 20% normal fetal bovine serum in PBS for 45 minutes at room temperature. The slides were then washed two times for 5 minutes in PBS and a circle drawn around the section with a hydrophobic pen. The sections were peroxide blocked with dual enzyme block solution (Dako) and incubated for 30 minutes. It was followed by 3 washes in PBS for 5 minutes each. After that, the primary antibody in antibody diluent (Dako) was applied to the sections and incubated at 4°C for overnight. On the following day, the sections were washed in PBS thrice and then

the peroxidase labeled polymer (HRP) was added and incubated for 30 minutes at room temperature. Nine washes were done after that with PBS and waiting for 5 minutes every 3 washes. In the meantime, the DAB+ solution was prepared and added to the section. The incubation period was optimized according to the intensity of staining. After 3 washes in PBS, the slides were stained in Mayer's hematoxylin for 3 minutes. Finally they were washed in distilled water three times, mounted with crystal mount, and sealed with the cover glass and Cytoseal™ .

5.2.6 Statistical Analysis

The results were depicted as mean $\pm$ SEM. We used n=10 for hind limb ischemia surgery model. When comparing only two groups, Student's t-test was used. A two tailed probability with p-value, $p < 0.05$ was considered statistically significant and pairing was taken into consideration wherever necessary.

5.3 RESULTS

5.3.1 Syndesomes Restore Blood Perfusion in Ischemic Hind Limb of ob/ob Mice

We created hind limb ischemia in ob/ob mice through the complete ligation and subsequent removal of a portion of the femoral artery between the ties. This model creates ischemia in one of the limbs to simulate peripheral ischemia due to occlusive vascular disease. A major problem in diabetic patients is a lack of perfusion in the lower limb leading to poor healing outcomes [112]. We monitored the blood perfusion in the feet using laser speckle contrast imaging and found that by day 7, there were significant differences increased between the FGF-2 group and the syndesomes with FGF-2 group. The differences continued to increase with time and at day 14 the syndesome with FGF-2 group had about 86% recovery compared with about 50% recovery in the FGF-2 group (Figure 5.4). Thus, there was a steady increase in blood flow in the ischemic limbs relative to the contralateral limb. To confirm that the increase in perfusion was due to neovascularization in the treated tissue, we performed immunostaining for blood vessels (von Willebrand Factor). We observed a significant increase in the number of smaller vessels and larger vessels in both calf muscle and thigh muscles (Figure 5.5).

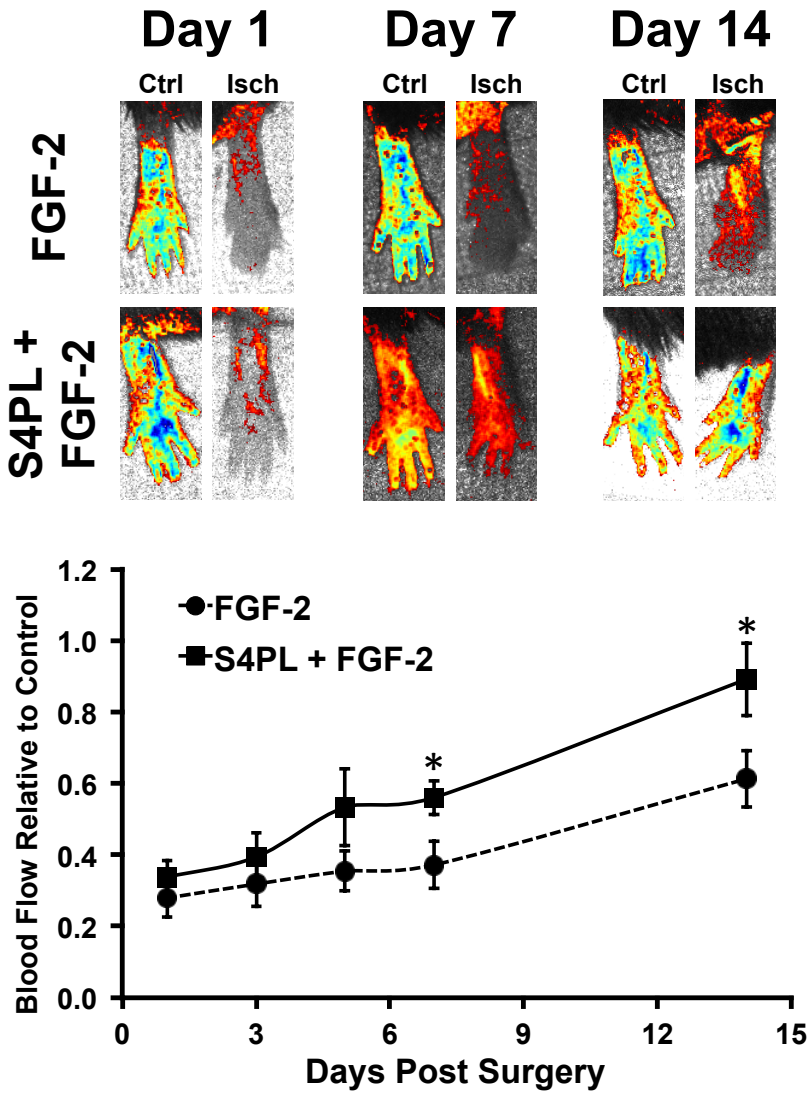

Figure 5.4 Syndesomes with FGF-2 significantly improve blood flow in the ischemic feet compared with FGF-2 alone. Upper panel shows laser speckle contrast images of the uninjured contralateral limb (Ctrl) and injured ischemic limb (Isch) over the course of time for both the treatments. Lower graph is the quantification of blood flow relative to the contralateral feet. *Statistically different from FGF-2 group ($p < 0.05$). n=10.

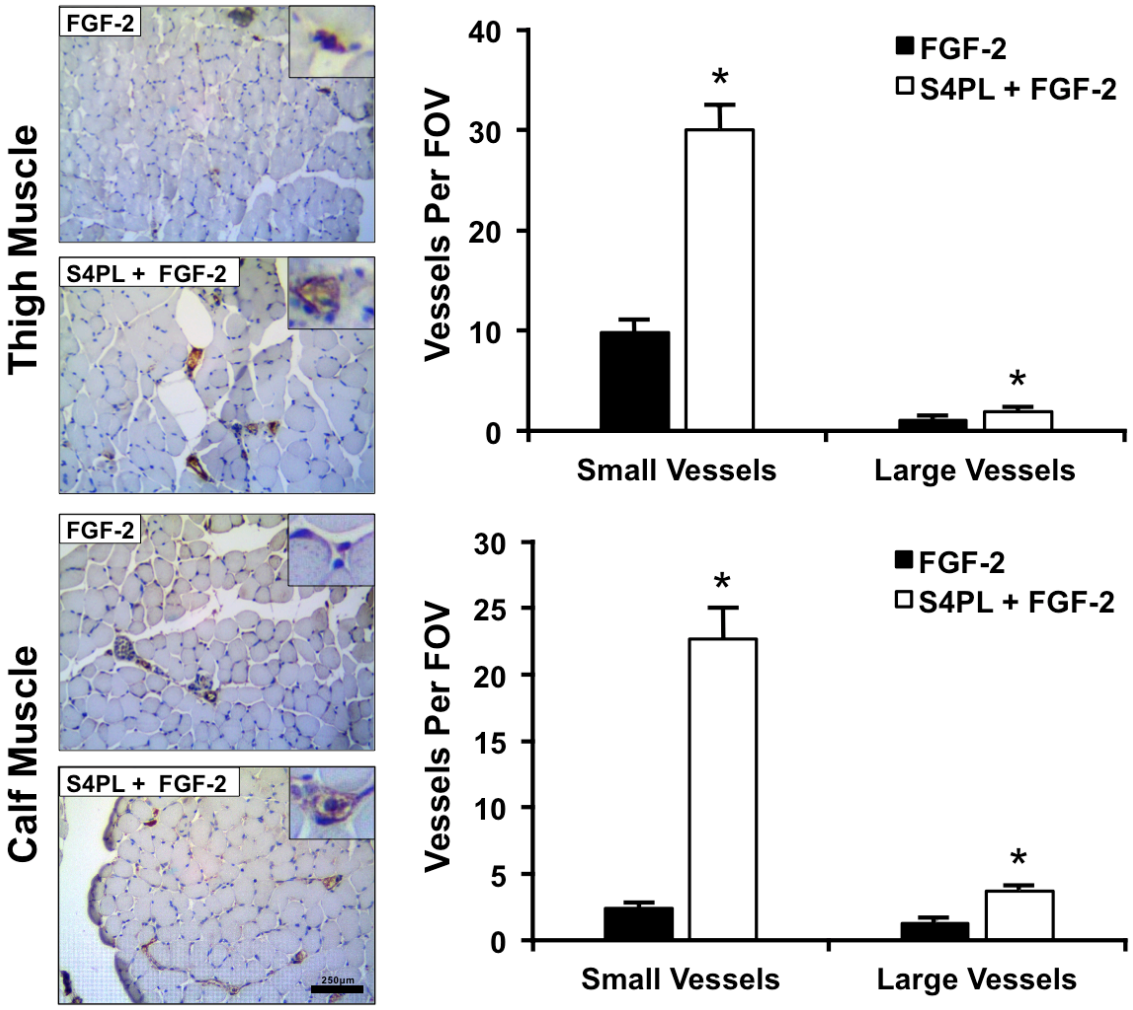

Figure 5.5 Syndesomes with FGF-2 dramatically enhance angiogenesis in both the quadriceps (thigh) and gastrocnemius (calf) muscles. The sections of the tissue were immunostained for the endothelial marker von Willebrand factor. Inset shows 3X-enlarged image with positive staining. Quantification of vessels shows dramatic up-regulation of vessels per field of view due to presence of syndesomes. Size bar is 250µm. Inset is 3X magnified. *Statistically different from FGF-2 group ($p < 0.05$). n=10.

5.3.2 Syndesomes Minimize Ischemic Changes in the Muscle fibers

Following femoral artery ligation, there can be loss/alterations of muscle fibers due to ischemia. We found in the H&E stains of the muscle sections that, mice treated with syndesomes and FGF-2 had significantly reduced number of muscle fibers exhibiting ischemic damage compared with the FGF-2 alone treatment group (Figure 5.6). The FGF-2 alone group had areas of gross focal and regional fiber necrosis, degeneration and loss of tissue structure. The loss in the muscle fibers was most likely due to ischemic and hypoxic condition that leads to degeneration of the fibers. This trend was observed in both calf and thigh muscles. We confirmed that the holes in the fibers were not freezing artifacts by comparing to the non-ischemic contralateral control limb samples harvested from the thigh and calf muscle. Another noticeable difference between the two groups was the migration of the nucleus to the center of the fiber. This is the first step for muscle repair [113] and was more predominant in the syndesome with FGF-2 group compared with the FGF-2 alone group.

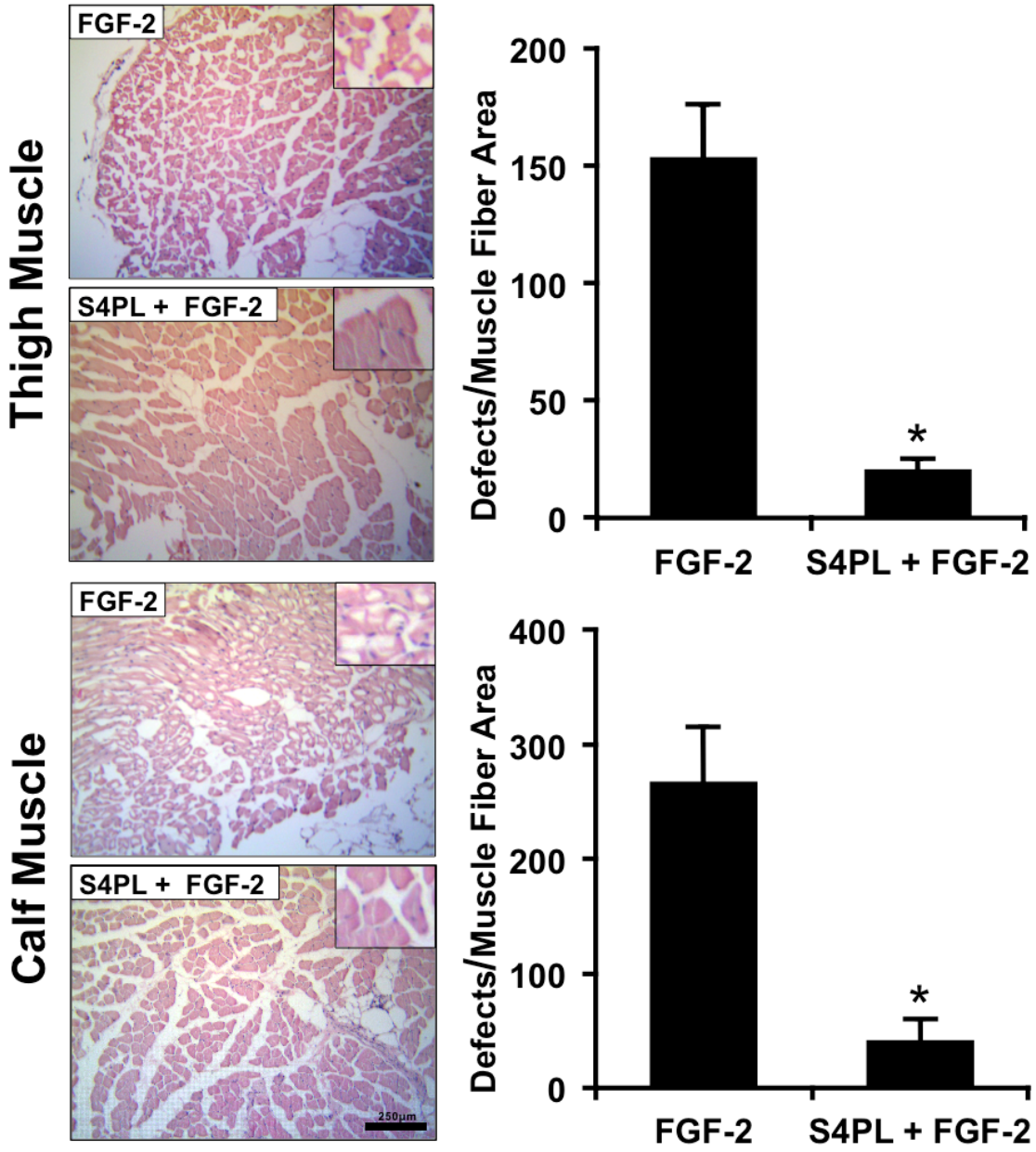

Figure 5.6 H&E stained images of thigh and calf muscle tissue at day 14 and quantification of the number of ischemic defects in the muscle fibers per unit area. Size bar is 250µm. Inset is 3X magnified. *Statistically different from FGF-2 group ($p < 0.05$). n=10.

5.3.3 Syndesomes Enhance Wound-Healing Macrophage Phenotype

We then examined whether syndesomes with FGF-2 alter the immunological response to ischemia when compared with FGF-2 treatment alone. The muscle tissue sections were immunostained for the inflammatory M1 macrophage marker (CD86). We quantified the ratio of positive staining to the total nucleus area. We found comparable M1 levels in calf and thigh muscle for both treatment groups (Figure 5.7). We also immunostained for alternatively activated M2 macrophages (CD163), which are considered to possess wound-healing characteristics. There was a significant increase in M2 positive cells in the cellular infiltrate surrounding both calf and thigh muscles in the S4PL+FGF-2 group compared with FGF-2 alone (Figure 5.8). Another major point to note here is that the sections were 6μm thick and so the stained images for M1 and M2 are from the same location. Keeping the background staining intensity same and superimposing the images, we found intense staining for M2 compared with M1 macrophages for the same cells. Hence the same cell is expressing more CD163 receptors compared with CD86 receptors. We think that over time, the macrophages would keep shifting towards the M2 phenotype to heal the wound effectively. It is now generally accepted that macrophages are inherently plastic in nature and that they switch between many phenotypes seamlessly [114]. Therefore, we can surmise that our therapy is probably driving the same macrophage cells towards a more wound-healing phenotype and away from inflammatory features.

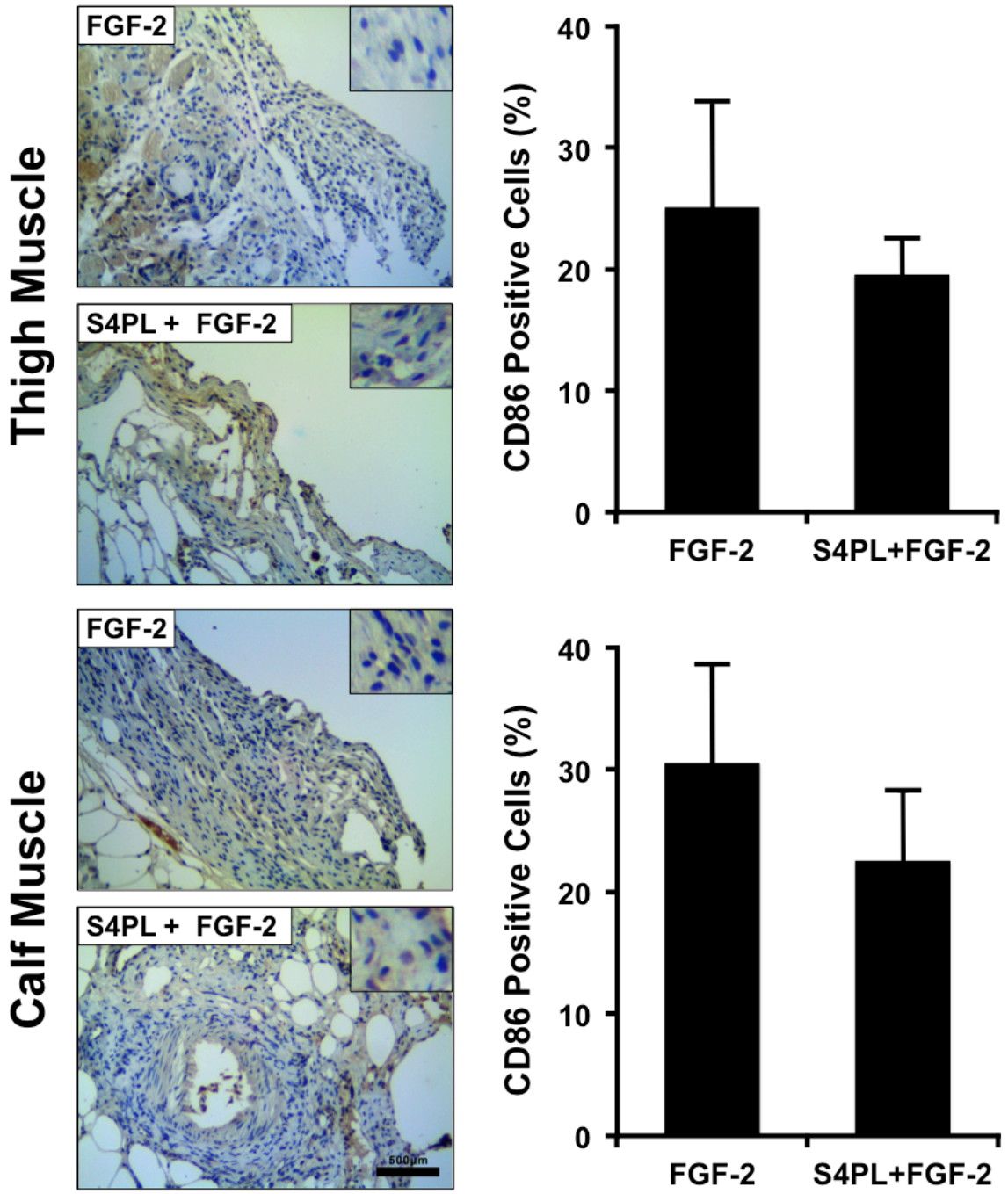

Figure 5.7 Muscle tissue from thigh and calf sectioned, and immunostained for inflammatory M1 macrophage marker (CD86) (left). Quantification of number of positive cells per unit nuclear (right). Size bar is 500µm. Inset is 3X magnified. n=10.

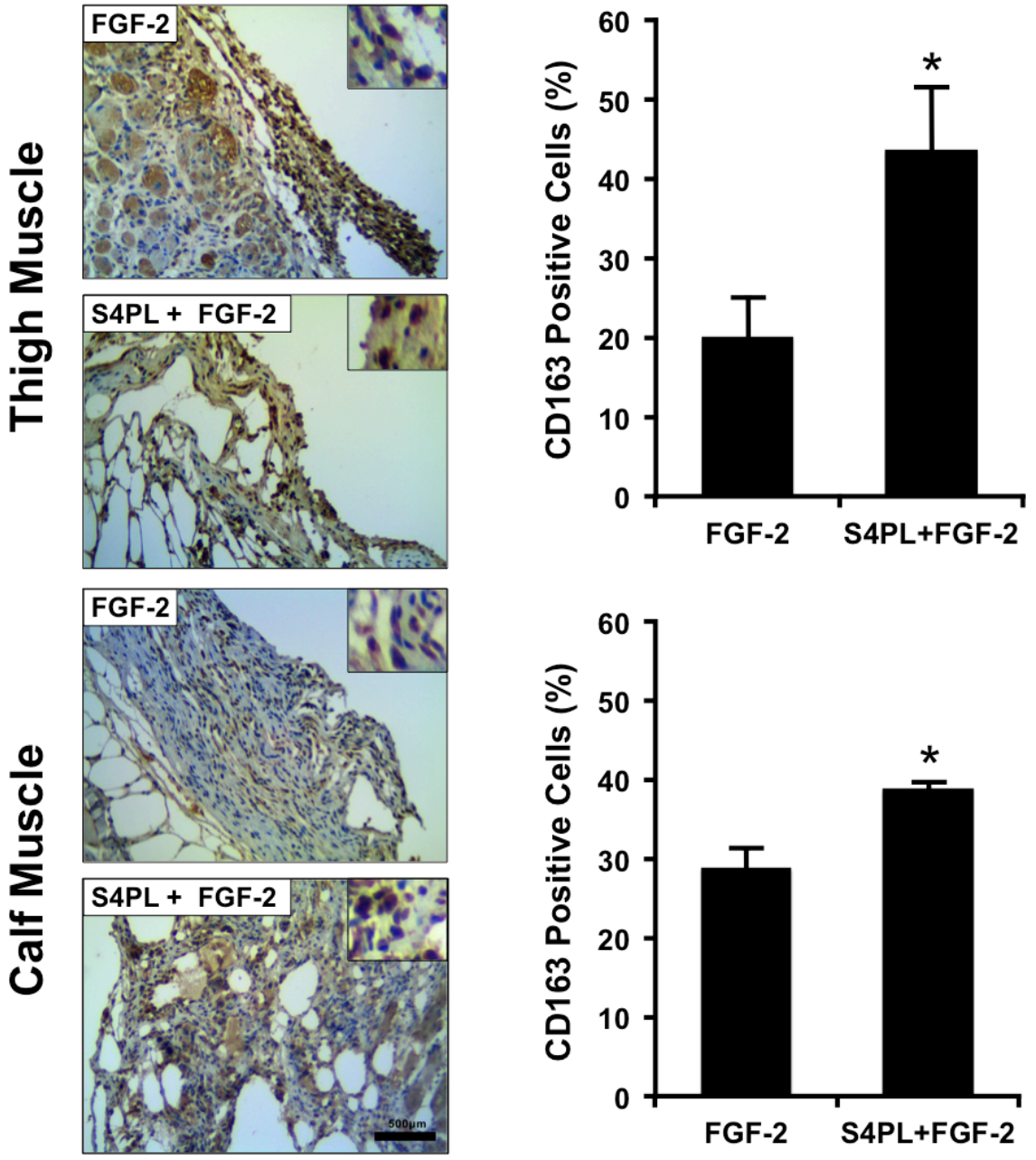

Figure 5.8 Sections from calf and thigh muscles stained for the alternatively activated M2 macrophage marker (CD163) (left). Quantification of positive staining (right). Size bar is 500µm. Inset is 3X magnified. *Statistically different from FGF-2 group ($p < 0.05$). n=10.

5.4 DISCUSSION

In this study, we demonstrated the efficacy of syndesome treatment for therapeutic angiogenesis in a clinically relevant diabetic hyperlipidemic mouse model. We believed that the resistance to growth factor therapy [89] is a significant obstacle to growth factor therapeutics and may underlie the equivocal or mild results that growth factor therapies have achieved in clinical trials in patients with complex disease in contrast to healthy animals. Thus, we hypothesize that the current approach of delivering only growth factors or growth promoting genes is fundamentally flawed in that it does not account for the alterations in tissue responsiveness to these factors due to metabolic disease.

Our overarching goal was to ensure the effectiveness of the therapy in a diseased environment, not just normal tissue. We found that ischemic limbs completely recovered within 14 days when treated with FGF-2 and syndesomes, compared with only partial recovery when treated with FGF-2 only. Histological analyses confirmed a significant increase in the number of blood vessels in both gastrocnemius and quadriceps muscles. Ischemic fibers in syndesome treatment group were also negligible. And most importantly, the therapy drives the macrophages towards an alternatively activated M2 phenotype.

5.5 CONCLUSIONS

Taken together, our studies support that co-delivery of syndecan-4 with FGF-2 significantly enhances revascularization in the ischemic hind limb in a clinically relevant diseased mouse model. Our studies demonstrate a significant increase in blood flow in the ischemic hind limb compared with the contralateral, which is due to enhanced therapeutic angiogenesis. There was also remarkable increase in alternatively activated M2 macrophage phenotype that favors wound healing in the tissue. This study is a notable first step towards finding efficient long-term solutions for patients suffering from myocardial or peripheral ischemia.

Chapter 6: Syndesomes Significantly Increase Cutaneous Wound Healing in a Diabetic ob/ob Mouse Model

6.1 Introduction

Type-2 diabetes is being called the "epidemic of our generation" and it is estimated by the World Health Organization that 347 million people suffer from diabetes mellitus worldwide [45, 46]. Diabetic neuropathy and microvascular angiopathy are common complications of diabetes and contribute to a 12-25% lifetime risk of developing chronic ulcers [51]. Specifically, diabetic foot ulcers are responsible for 25-50% of the total cost of diabetes treatment [52] and are the most common cause for limb amputations in the United States [53]. Diabetic ulcers are a complex clinical problem requiring a multifaceted treatment plan with standard therapeutic components including debridement of necrotic tissue, offloading, infection control, surgical revascularization, and limb elevation/compression [18, 19]. Unfortunately, these treatments routinely fail, leaving patients with chronic ulcers, and enhanced risk for limb amputation. Peripheral vascular disease (PVD) patients also suffer from non-healing wounds and ulcers due to reduced blood perfusion in lower extremities. PVD has a prevalence of 12-20% in the population 65 years and older in the US [6] and affected 202 million people worldwide in 2010 [1]. The increase in prevalence of strong risk factors like smoking, hypertension, obesity and metabolic syndrome indicate that the population affected by non-healing chronic ulcers will continue to grow in the future.

A number of advanced wound dressings have been used to attempt to heal these ulcers once standard care has failed. A host of wound dressing materials have been used to improve wound healing including natural biological materials such as honey [115] and chitosan [116] as well as modified materials such as silver-containing alginate dressings [117]. Bioactive dressings are an appealing strategy that has great potential to control and enhance wound healing. The most prevalent approaches to bioactive dressings can be broadly classified into the categories of local delivery of growth factors [118], delivery of therapeutic genes [119], or delivery of cells with the potential to enhance healing [120]. Of these three, only growth factors have been tested in large clinical trials perhaps due to the safety and logistical challenges for gene or stem cell therapy. Growth factor therapies have, for the most part, met with limited level of success and the majority of studies are small- to mid-sized clinical trials that often track only complete wound closure but not percent closure or time to closure, leaving the clinical recommendation for these therapies unclear. The only approved clinical growth factor treatment for chronic wounds is recombinant PDGF-BB (Becaplermin), and while approved by the FDA, it has received mixed success in clinical trials on chronic ulcers [121-123]. FGF-2 and EGF have either shown no improvement or shown only moderate benefits in small clinical trials [124-126]. Thus, while clinical trials have shown that growth factor therapies are safe and well tolerated by patients, there is a pronounced need to improve the efficacy of these treatments to maximize the benefit of these therapies and make them cost effective for our healthcare system.

The development of effective growth factor therapies would have a profound effect on the clinical treatment of diabetic patients with chronic ulcers and many other patient groups with difficult to heal wounds (e.g. pressure ulcers in the elderly, venous

ulcers, and infected wounds). Our proposed studies are focused on enhancing the effectiveness of FGF-2 and have a great potential to also be effective with other heparan-sulfate dependent growth factors including VEGF-A and HB-EGF. Thus, our work is poised to contribute to this field by developing new technology to enhance closure in healing-resistant wounds and has great potential for use in many other disorders that would benefit from effective growth factor therapies.

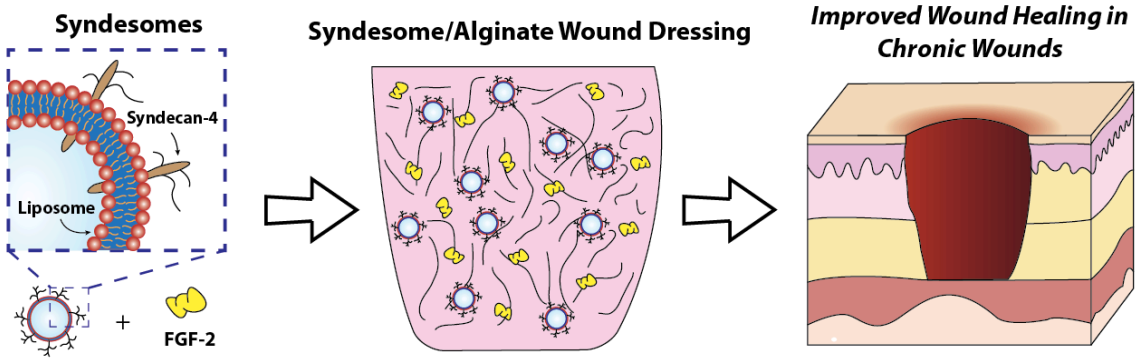

Figure 6.1 Overall goal of this chapter is to engineer alginate dressings that enhance wound healing in chronic wounds.

In the present chapter, we demonstrate the efficacy of syndesomal therapy in the context of full thickness wounds with silicone splints around them to simulate human-like wound healing, in a clinically pertinent diabetic and diseased mouse model (Figure 6.1).

6.2 Materials and Methods

6.2.1 Animal Model

All animal experiments were performed with the approval of the Institutional Animal Care and Use Committee (IACUC) of University of Texas at Austin and in

accordance with NIH guidelines “Guide for Care and Use of Laboratory Animals” for animal care. All the animal experiments were performed on a diabetic, obese, and hyperlipidemic mouse model (ob/ob). They were fed for 15 weeks with a high-fat diet before being utilized for the surgeries. This was done to recapitulate the human diseased condition more closely and simulate the physiological response of an obese diabetic person. The animals were sacrificed 2, 5, or 14 days after the surgery and the tissues were used for histology, staining, flow cytometry, and other analyses.

6.2.2 Implant preparation

Alginate gels were fabricated as 6.5mm-diameter disks for the excisional wound surgery. Equal volumes of 4% sodium alginate (Sigma™) solution and 0.85% NaCl (Sigma™) solution were mixed and the syndesomes and/or growth factors were added to it. A custom-made high throughput mold was used to make the exact shape so that it fits the wounds (Figure 6.2). The gels were then cross-linked in 1.1% $CaCl_2$ for 1 hour at 4°C. 5µg of FGF-2 and/or 0.5µg of syndecan-4 protein were encapsulated in the gel, according to the sample (control, FGF-2, S4PL, or S4PL+FGF-2) in each disk implanted.

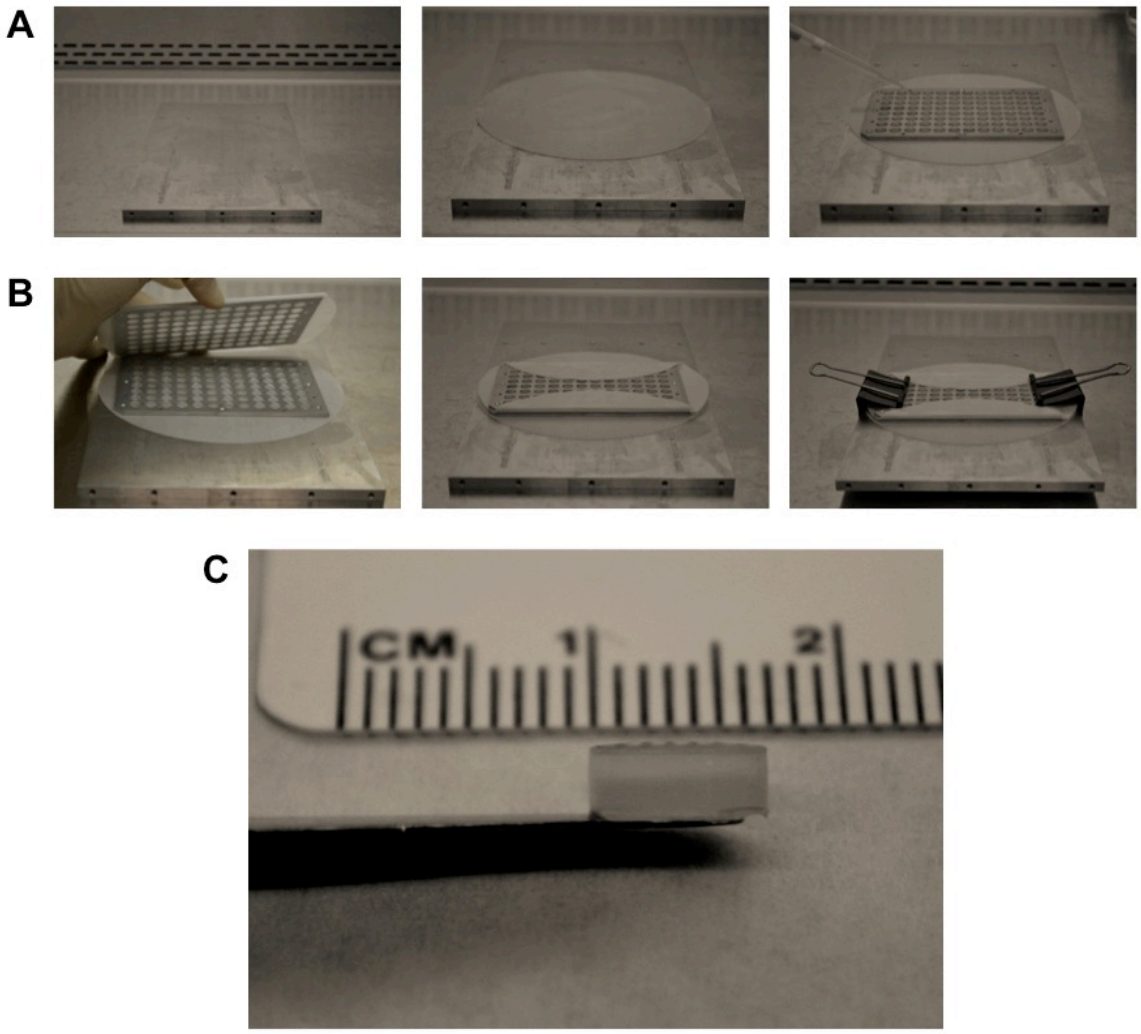

Figure 6.2 Custom made high throughput mold for alginate disk fabrication for implantation in the mouse excisional wound model. (A) The sterile metal piece was placed in the biosafety cabinet and a filter paper soaked with 1.1% $CaCl_2$ was placed on it. The metal mold was put on top of the filter paper. The 4% alginate solution was added to the wells drop-wise and then covered with another mold wrapped in a wet filter paper. (B) More $CaCl_2$ solution was added to the setup and clamped on both sides to keep it in place. The entire setup was moved to the cold room to keep the gels at 4°C. (C) After 1 hour of incubation we have the cross-linked alginate disks that are 6.5mm in diameter and fits the wound perfectly.

6.2.3 Excisional Splinted Wound Healing Model

The methods followed in the experiments were based on the protocol outlined in the paper by Wang *et.al* [127] and shown in the Figure 6.3 and 6.4. A sterile 5mm biopsy punch was used to outline a pattern of four wounds, two on either side of the midline on the dorsum of the mouse. A toroidal-shaped splint was fashioned from a 0.5mm thick silicone sheet and was placed so that the wound was centered within the splint. 6-0 nylon sutures and instant glue were used to fix the splint to the skin and to ensure position and no wound contraction. Alginate gel disks of 5mm-diameter encapsulating syndesomes and/or FGF-2 were then applied directly to the region of the open wound. Tegaderm was used to cover all the wounds. Macroscopic images of wounds were taken on day 0, 7, and 14; which were later used for wound closure quantification. The animals were euthanized at day 14 and the wound was biopsied with a 10mm biopsy punch. The tissues were snap frozen in liquid N_2-chilled isopentane and used for further analysis.

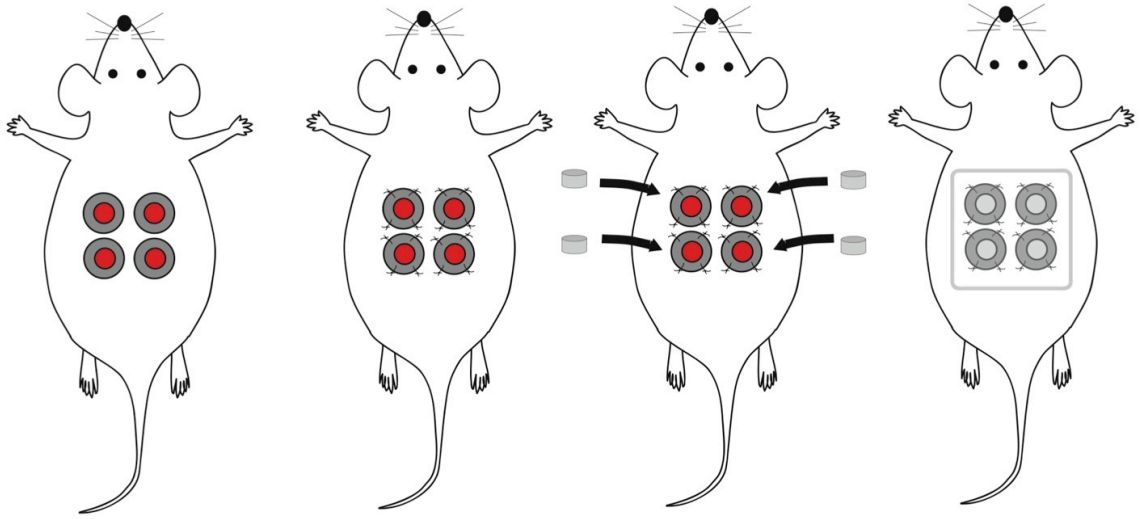

Figure 6.3 Schematic diagram showing the splinted excisional wound model procedure in ob/ob mice.

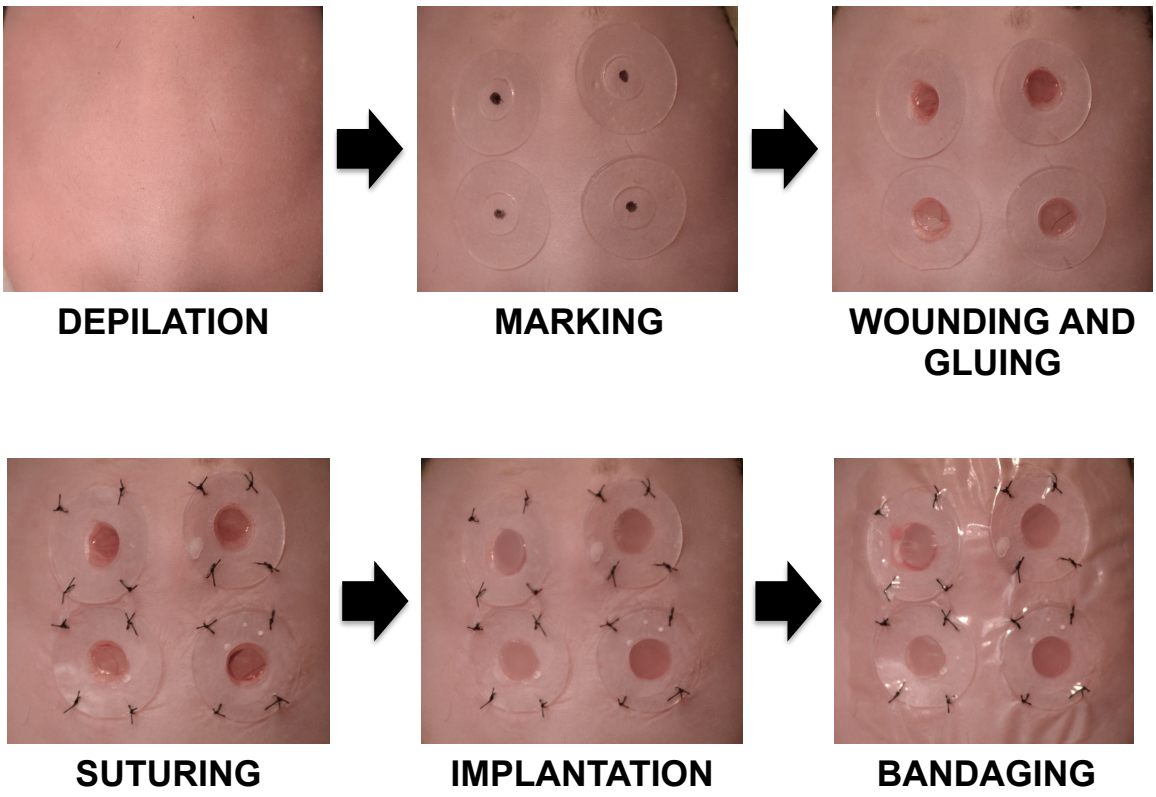

Figure 6.4 The steps followed for the excisional wound model surgery. The dorsal surface of the ob/ob mouse is depilated. Full thickness wounds are made on the dorsal surface, a silicone splint is glued around the wound to prevent contraction and the splint is stitched to keep the splints in place. The alginate gel is finally implanted in the open wound and covered with a transparent wound dressing Tegaderm.

6.2.4 Flow Cytometry

The wounds (day 2 and 5) were excised out using a 10mm sterile biopsy punch and cut from the center into two disc shaped pieces. Half of the tissue was used for cryosectioning and histology. The other half was digested [128] in an enzyme cocktail and used for flow cytometry experiments. The single cell suspension derived from the

wound tissue was maintained at 10^6 cells/ml in the FACS staining buffer (BD Biosciences). The samples were blocked with 1μg/ml (final concentration) of Rat IgG2b that blocks the Fc receptor (BD Biosciences) for 30 minutes on ice. The cells were then stained with all the following antibodies for 30 minutes on ice: anti-mouse F4/80 PE-Cy7 (eBiosciences), anti-human CD206 FITC (BD Biosciences) and anti-mouse CD86 Biotin Ig (BD Biosciences). Two washes were performed with FACS staining buffer. The PerCP streptavidin antibody was used to stain the samples for another 30 minutes on ice. The samples were finally washed twice with the FACS staining buffer. The samples were fixed with 500μl of Cytofix buffer (BD Biosciences) and resuspended in 1ml buffer and stored at 4°C. All the samples were run together on the BD LSRFortessa™ machine and the data were later analyzed using the FlowJo analysis software.

6.2.5 Histology and Staining

The wound tissues were embedded in paraffin and 6μm sections were made using a microtome. The sections were de-paraffinized with two changes of xylene, 10 minutes each. They were re-hydrated in two changes of absolute alcohol, 5 minutes each, followed by 95% alcohol for 2 minutes and 70% alcohol for 2 minutes. The slides were then washed in 1X PBS for 5 minutes and placed on the slide warmer at 60°C for 1 hour. After a brief wash in distilled water, the sections are stained in Harris Hematoxylin solution for 8 minutes. This was followed by a 5-minute wash in running tap water to get rid of excess hematoxylin. Then the slides were put in differentiation buffer for 30 seconds and quickly washed under running tap water for 1 minute. This is followed by staining in Bluing reagent for 1 minute, a wash in running tap water for 5 minutes, a rinse in 95% alcohol, counterstain in Eosin solution for 1 minute, dehydration through 95%

alcohol, two changes of absolute alcohol, for 5 minutes each. Finally, the stains are cleared in two changes of xylene, 5 minutes each, and mounted with xylene-based mounting medium and cover glasses.

The slides were Movat's stained to stain the various components in tissue to probe the anatomical features. The sections were de-paraffinized and hydrated as described above. The slides were placed in a slide rack and mordanted with Bouin's fluid for 1 hour at 50°C. Traces of Picric acid were removed by washing in running water for 2 minutes. They were then stained in 1% Alcian Blue for 20 minutes and washed in distilled water by dipping 5 times in the bucket. Then the slides were placed in Alkaline alcohol for 10 minutes at 56°C. Slides were washed in running water for 2 minutes. Then they were stained in Orcein-Verheoff Hematoxylin solution for 15 minutes and washed in distilled water twice by dipping, and then running tap water rinses. This step is crucial since it stains for collagen and elastin. This was followed by staining in Woodstain Scarlet-Acid Fuchsin stain for 2.5 minutes, 0.5% Acetic acid for 30 seconds, 5% Phosphotungstic acid for 7.5 minutes, 0.5 Acetic acid for 30 seconds and ultimately 3 ethanol washes of 1 minute each. The slides were then stained with Alcoholic Saffron for 8 minutes and 2 ethanol washes with three dips each. To clean the slides at the end, two 30-second dips in Xylene were used and then mounted with cover glass and Cytoseal™ .

They were also immunostained using the Envision+ Dual Link Kit (Dako™) for epidermal keratinocyte marker (cytokeratin), M1 macrophage marker (CD86), M2 macrophage marker (CD163) and endothelial cell marker (von Willebrand factor). The slides were warmed for 10 minutes at 60°C on a slide warmer. Then they were de-paraffinized as described above. The next step in the protocol was vital and had to be carefully optimized for the fatty mouse tissues that were stained. The slide rack was

placed in a bucket with Antigen Retrieval Solution (Dako) and placed in the microwave (1250W) for 2 minutes and 40 seconds. Then the bucket is placed in a water batch maintained at 80°C for 3 hours. This reduces the background staining significantly. The slides were cooled in solution for 20 minutes and washed in PBS twice for 5 minutes each. Then they were blocked in 20% normal fetal bovine serum in PBS for 45 minutes at room temperature. The slides were then washed two times for 5 minutes in PBS and a circle drawn around the section with a hydrophobic pen. The sections were peroxide blocked with dual enzyme block solution (Dako) and incubated for 30 minutes. It was followed by 3 washes in PBS for 5 minutes each. After that, the primary antibody in antibody diluent (Dako) was applied to the sections and incubated at 4°C for overnight. On the following day, the sections were washed in PBS thrice and then the peroxidase labeled polymer (HRP) was added, and incubated for 30 minutes at room temperature. Nine washes were done after that with PBS, waiting for 5 minutes every 3 washes. In the meantime, the DAB+ solution was prepared and added to the section. The incubation period was optimized according to the staining intensity obtained. After 3 washes in PBS, the slides were stained in Mayer's hematoxylin for 3 minutes. Finally they were washed in distilled water three times, mounted with crystal mount, and sealed with the cover glass and Cytoseal™ .

6.2.6 Statistical Analysis

All the results were shown as mean $\pm$ SEM. We used n=8 for the excisional wound healing model. When comparing only two groups, Student's t-test was used. A two tailed probability with p-value $p < 0.05$ was considered statistically significant and pairing taken into consideration wherever necessary.

6.3 RESULTS

6.3.1 Syndesomes improve wound closure of full thickness wounds

We tested the effectiveness of our therapy for diabetic wound healing in an ob/ob mouse model. These mice develop diabetes, obesity, and have reduced wound closure [91]. We created alginate wound dressings that matched the geometry of the wounds using a custom-designed mold (Figure 6.2). The integrity of the liposomes in the alginate dressing was confirmed using transmission electron microscopy following thin sectioning (Figure 4.3). To examine whether syndesomes could enhance wound healing we created full thickness wounds of 5mm in diameter on the backs of these mice and attached a silicone splint around the wound using glue and sutures to prevent contraction. This was important because mice and other rodents have a layer of muscle underneath the skin that provides for increased wound contraction after cutaneous injury, which is absent in human wound healing. After 7 days, the wounds were photographed macroscopically and imaged with laser speckle contrast imager for blood perfusion. The gels were then replaced with a new gel with the same treatment and the mice were allowed to heal for another 7 days. A macroscopic analysis of wound closure revealed a two-fold decrease in wound size after 14 days with the syndesome with FGF-2 treatment in comparison to FGF-2 alone (Figure 6.5, 6.6, 6.7). Histological, morphometric analysis, and staining for cytokeratin revealed enhanced re-epithelization in the syndesome with FGF-2 group (Figure 6.8, 6.9, 6.10).

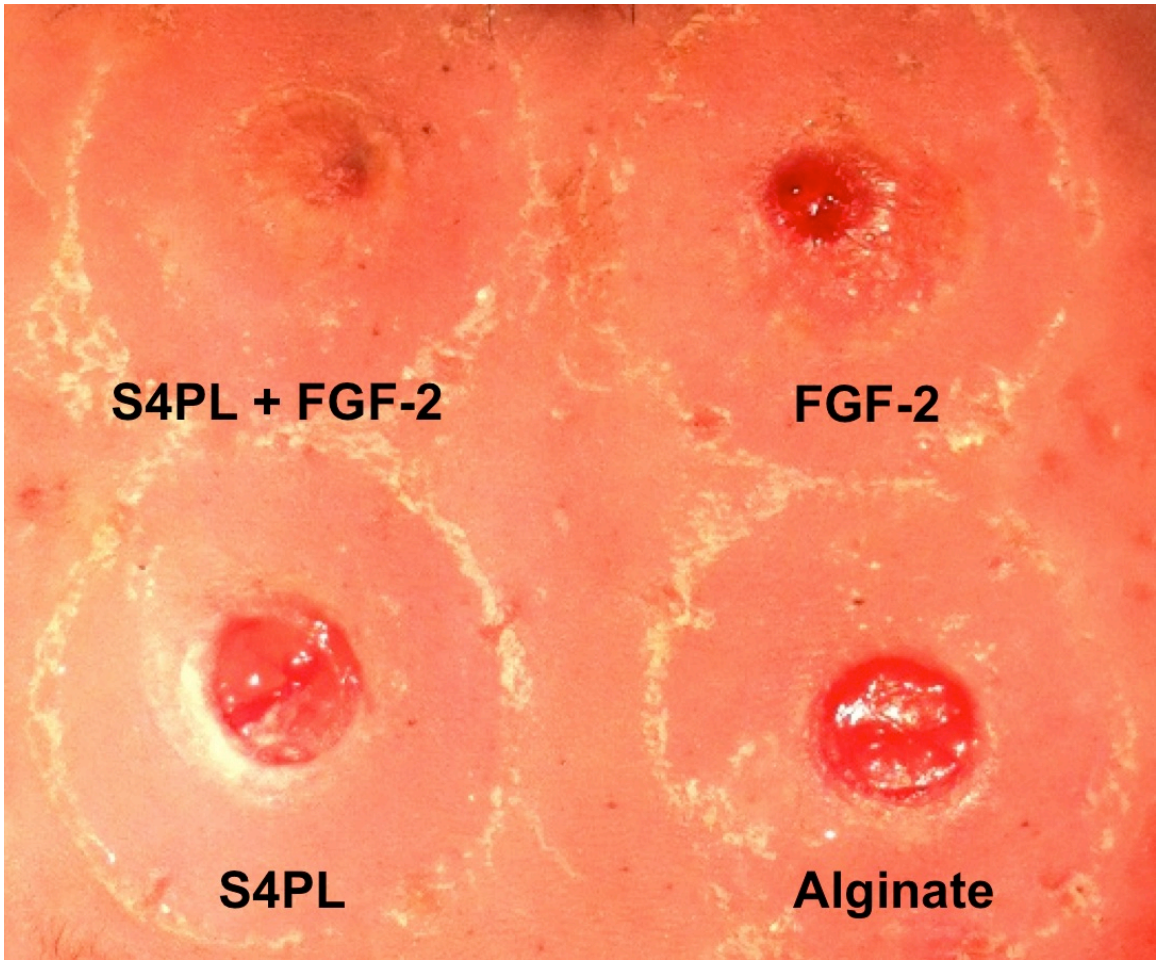

Figure 6.5 Macroscopic en-face image of the entire dorsal surface of the mouse at day 14 with the alginate gels removed and wounds cleaned.

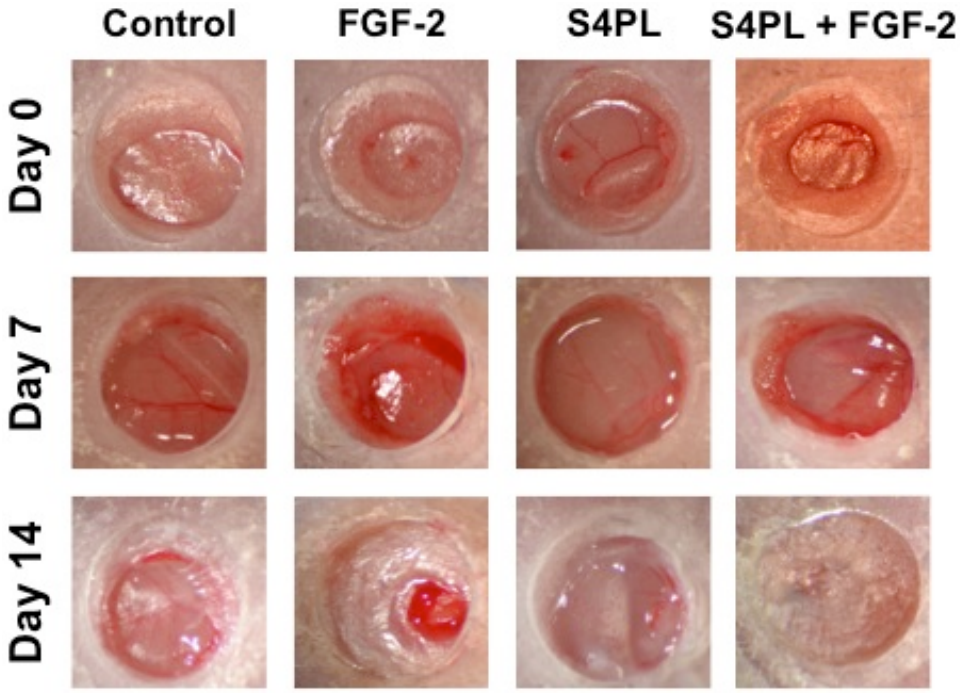

Figure 6.6 Wound closure panel. Macroscopic images of the wounds with the silicone splints around them at days 0, 7, and 14.

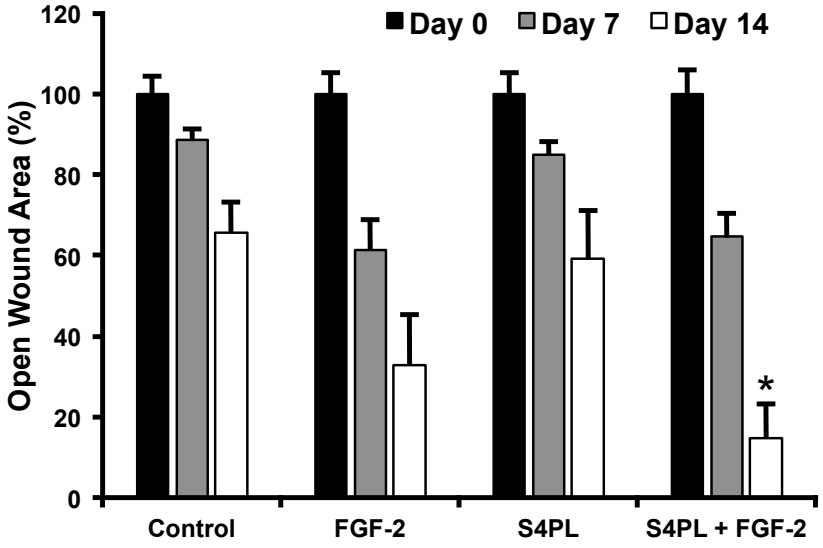

Figure 6.7 Quantification of wound closure area for the 4 treatment groups at days 0, 7, and 14. *Statistically different from all the groups ($p < 0.05$). n=8.

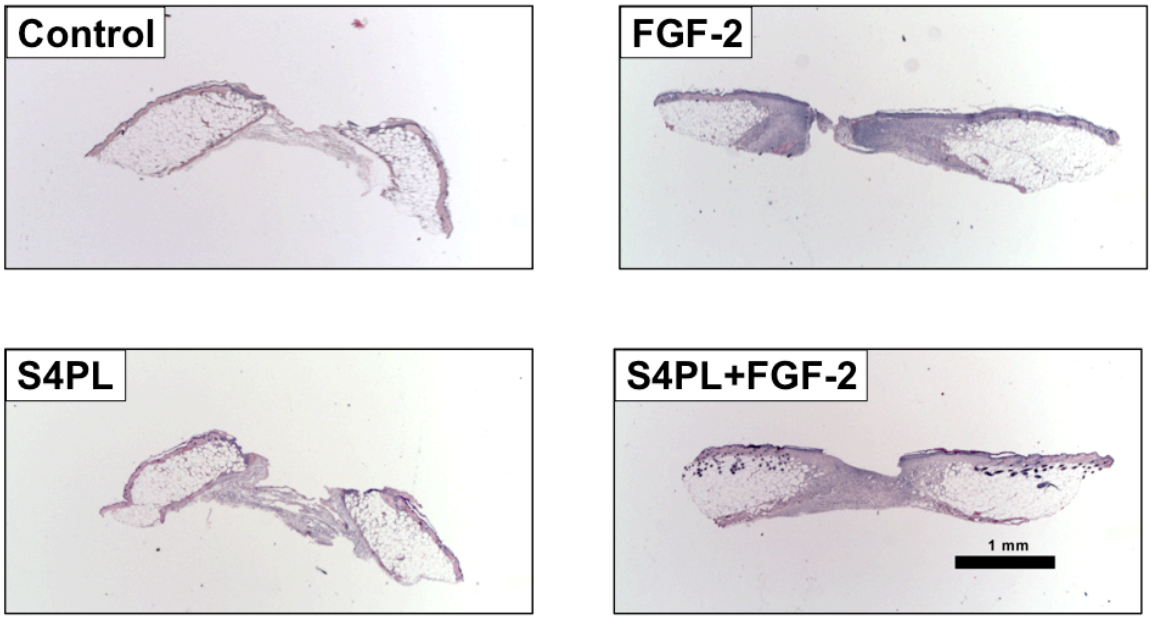

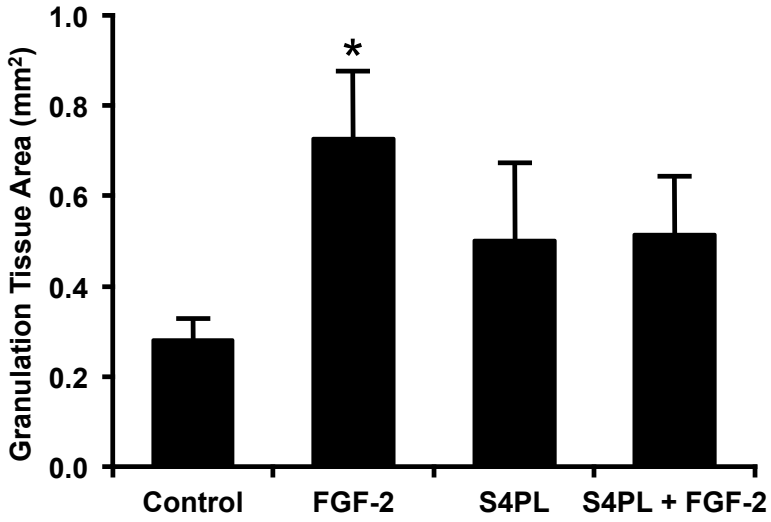

Figure 6.8 Hematoxylin & Eosin stained wound sections at day 14 for control, FGF-2, and syndesomes with FGF-2 treated groups. Quantification of granulation tissue area (mm^2) in the wound sections. Size bar is 1mm. *Statistically different from all other groups ($p < 0.05$). n=8.

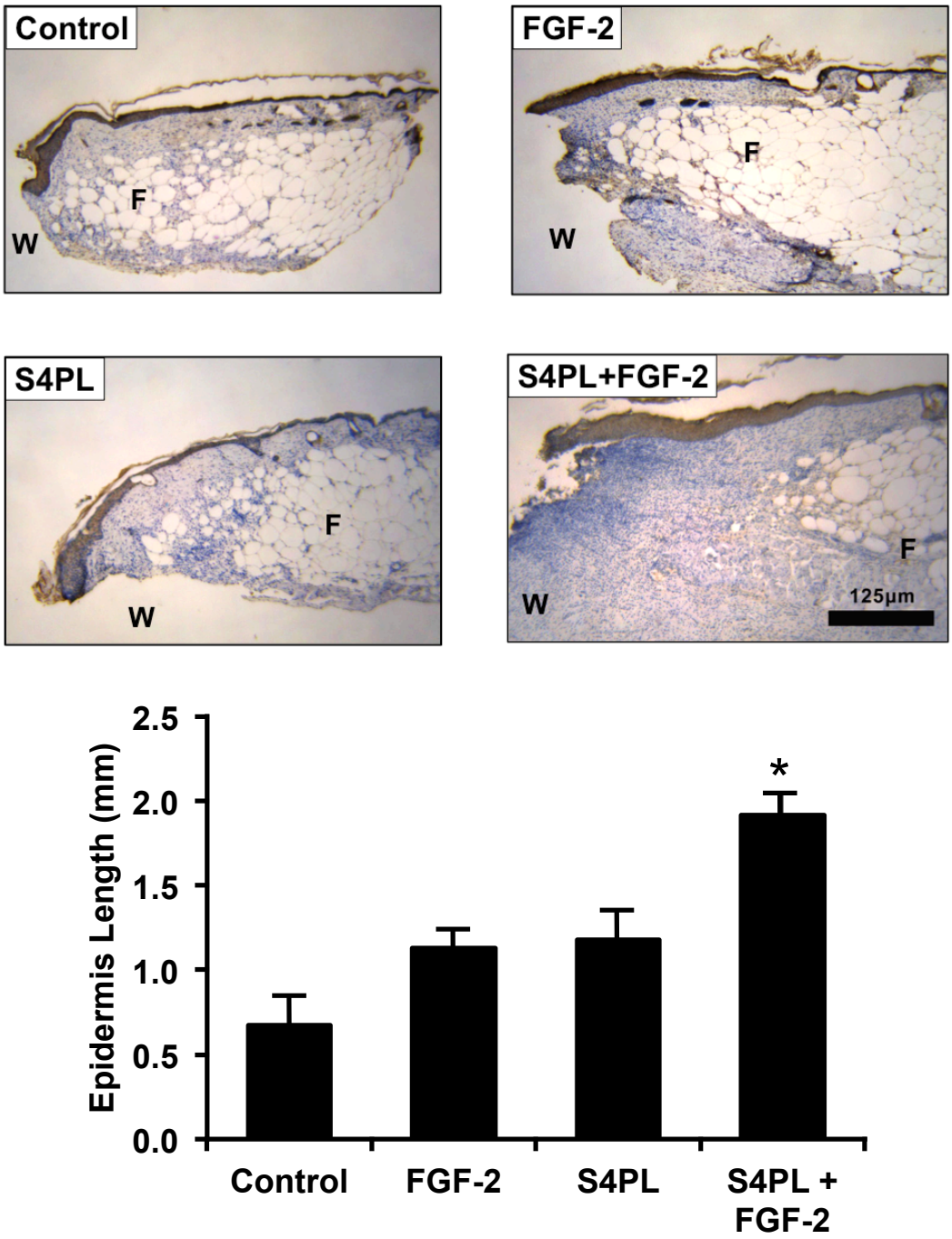

Figure 6.9 Images of the wound micro-sections immunostained with the cytokeratin antibody staining for epidermal layer containing keratin. Quantification of the epidermal regrowth beyond the fat defect in the skin. Size bar is 125µm. *Statistically different from all other groups ($p < 0.05$). n=8.

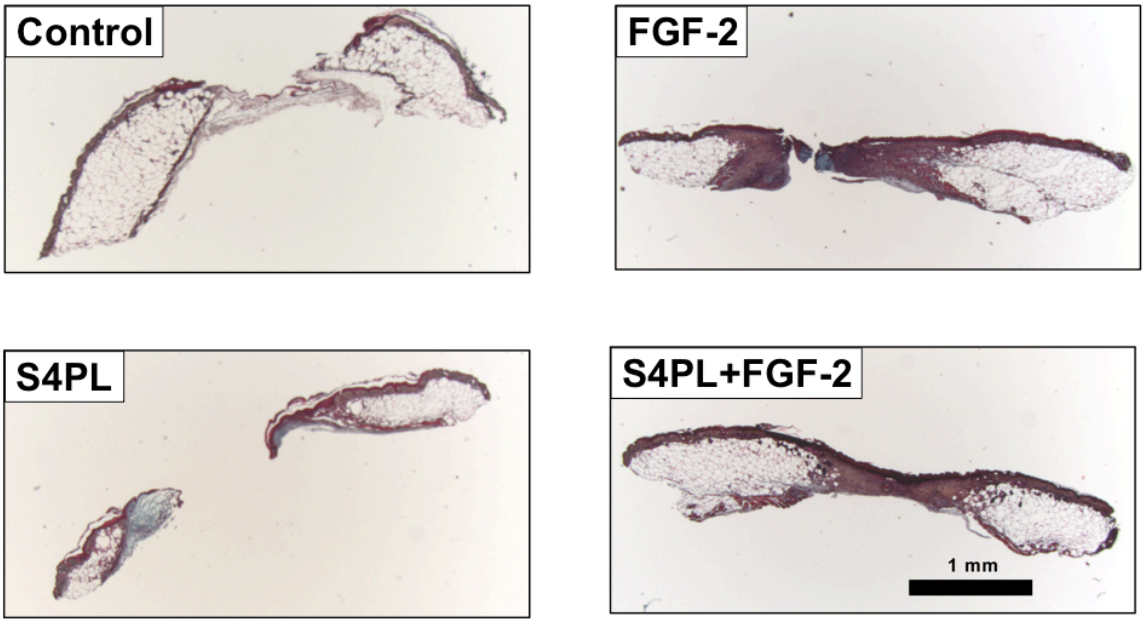

Figure 6.10 Movat's pentachrome stained images of the wound tissue sections at day 14. Size bar is 1mm.

6.3.2 Syndesomes Increase Blood Flow into the Wound Through Revascularization

We found that there was a significant increase of blood perfusion at day 7 in the syndesomes with FGF-2 compared with other groups (Figure 6.11). By day 14, we had difficult imaging through the healed wound surface since the wound was almost healed for the syndesome group but not for the control group. The control wound showed maximum blood perfusion at day 14 compared to all other groups because it was the least healed among all the groups. Hence we only show results up to day 7 here. We suspected that it was because of new vessels forming in the wound like we saw in the hind limb ischemia experiment. Histological immunostaining for blood vessels (vWF) showed increased numbers of vessels in the wound bed (Figure 6.12). The granulation tissue

around the wound was more in FGF-2 group compared with all other groups, but was normal in the syndesome groups. We probed deeper into the immunological cascade related to the wound healing response.

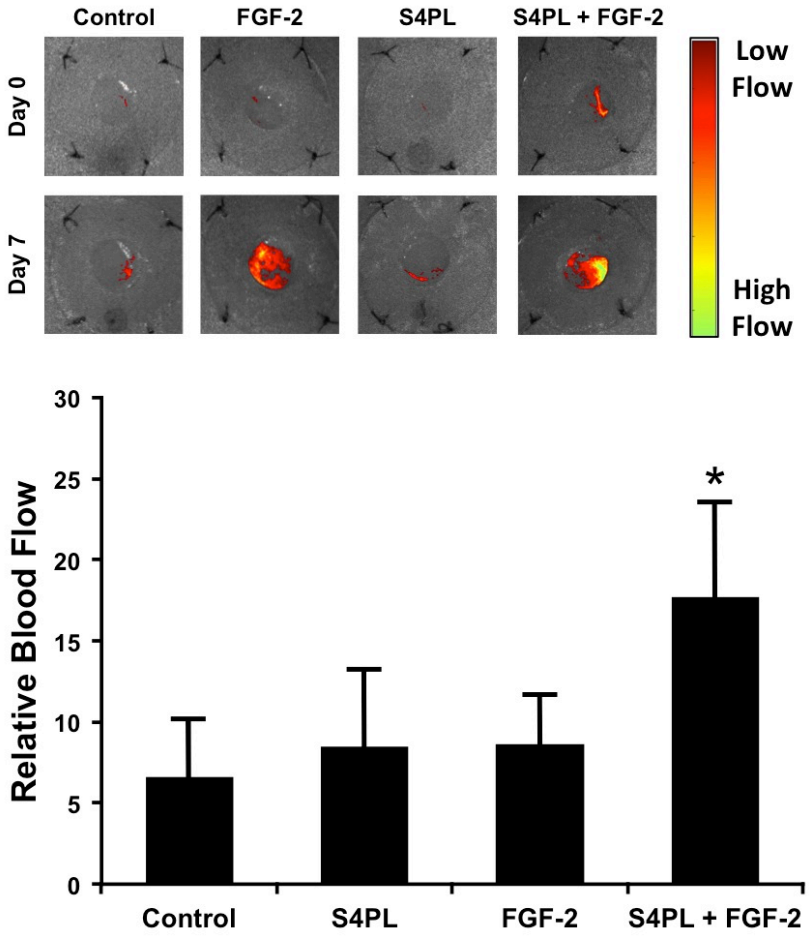

Figure 6.11 Panel of laser speckle contrast images of all the wounds at days 0 and 7. The color bar on the right shows relative blood perfusion (upper). Quantification of relative blood flow in the wound compared with day 0 (lower). *Statistically different from FGF-2 group ($p < 0.05$). n=8.

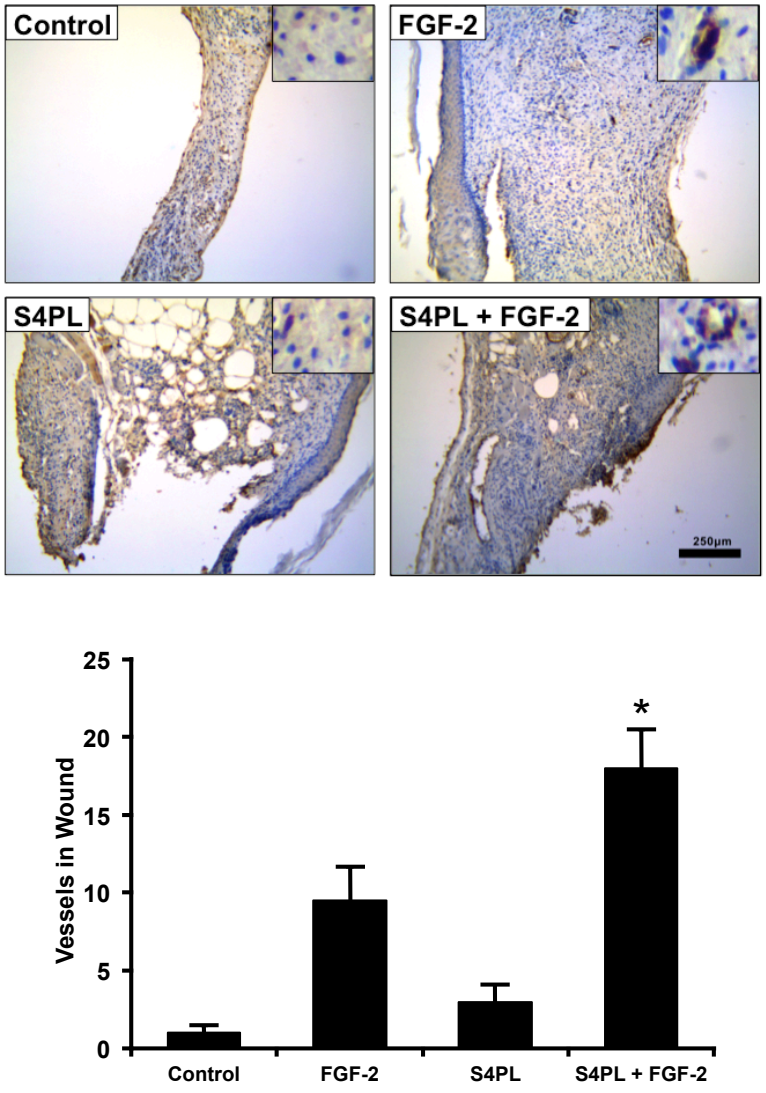

Figure 6.12 Immunostained images of the wound micro-sections stained for the endothelial cell marker von Willebrand factor. Quantification of the number of vessels in the wound bed in the immunostained images. Size bar is 250µm. Inset is 3X magnified. *Statistically different from all other groups ($p < 0.05$). n=8.

6.3.3 Syndesomes Modulate Immune Response to Pro-Wound Healing Phenotype

Wound healing is a complex physiological process that has many players involved in it, especially the immune cells like macrophages [129]. The notion of distinct

macrophage phenotypes has been changing in the recent years and now macrophage characters are believed to be particularly plastic [114]. The wound tissue was biopsied, fixed and embedded in paraffin for micron thick sections. Immunostaining for M1 macrophage marker (CD86) demonstrated significantly reduced expression for M1 markers in the syndesome with FGF-2 (S4PL+FGF-2) and the syndesome alone groups, compared with FGF-2 alone (Figure 6.13). Thus, syndecan-4 protein is likely modulating the inflammatory response. The quantification was performed by calculating the ratio of the number of DAB positive cells to the total number of cells represented by their blue nucleus. Staining for the M2 macrophage marker (CD163) revealed significant up-regulation of M2 phenotype in both S4PL and S4PL+FGF-2 groups compared to FGF-2 alone (Figure 6.14). If we superimpose the CD86 and CD163 images on each other, we observe the distinct differences in all the treatment groups. To understand the temporal changes in the immune response to the therapy, we performed flow cytometry on the wound cells at days 2 and 6. The events were gated to have cells and then gated to sort out the macrophages (Figure 6.15). We noticed that there was a significant reduction from day 2 to 6, in the number of macrophage cells when treated with the syndesomes and FGF-2. The CD86 intensity remained constant for all the groups while the CD206 intensity was higher in the syndesome with FGF-2 group, which means increase in the wound healing phenotype by day 6 (Figure 6.16). In conclusion, the syndesome therapy is driving the macrophages from the inflammatory to the wound healing phenotype, which is probably one of the reasons why we see enhanced wound healing in this treatment group.

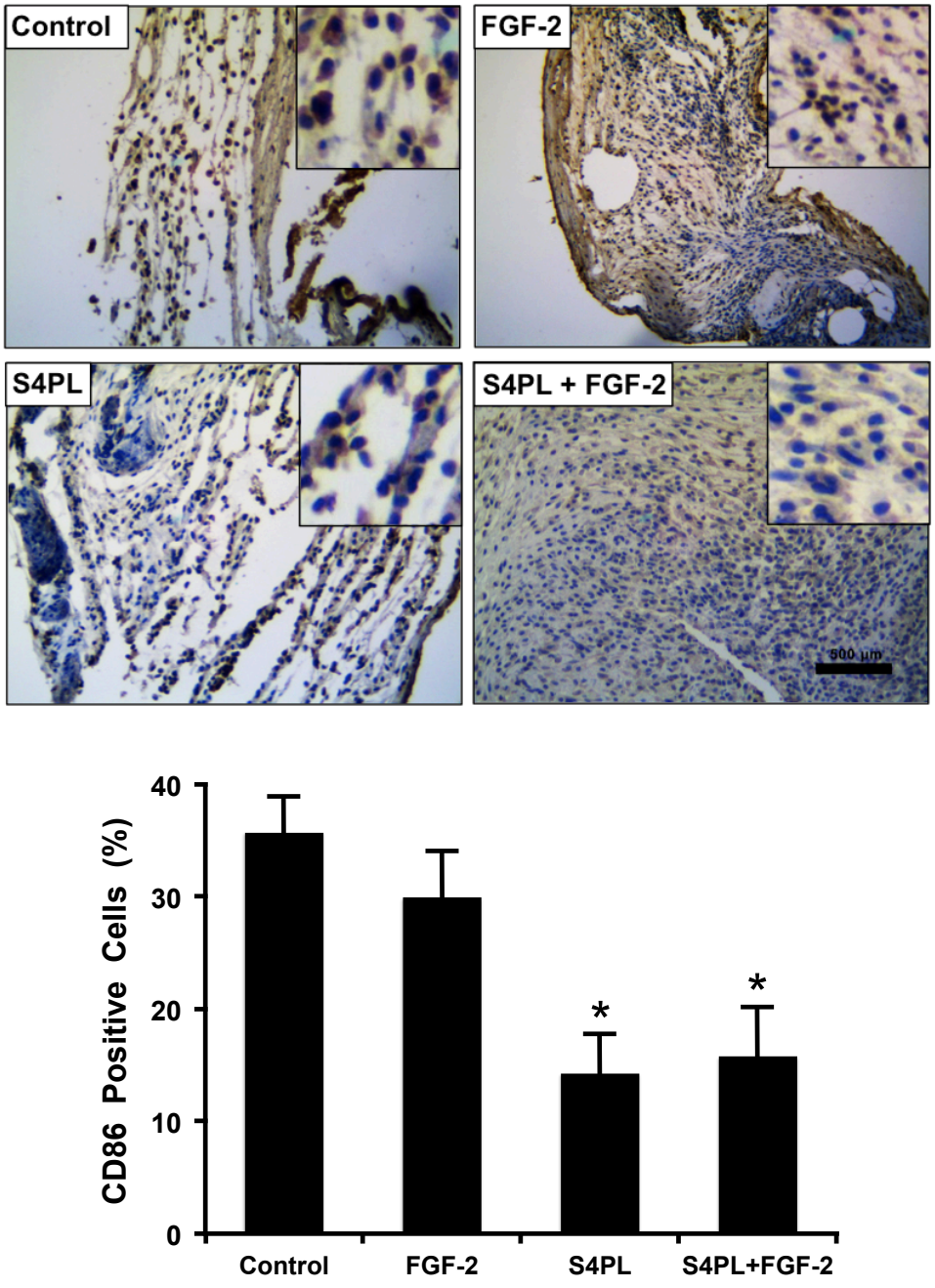

Figure 6.13 M1 macrophage marker (CD86) immunostained images of the wound sections at day 14 (upper). Quantification of the ratio of the positively stained cells with the nuclear area (lower). Size bar is 500µm. Inset is 3X magnified. *Statistically different from FGF-2 group ($p < 0.05$). n=8.

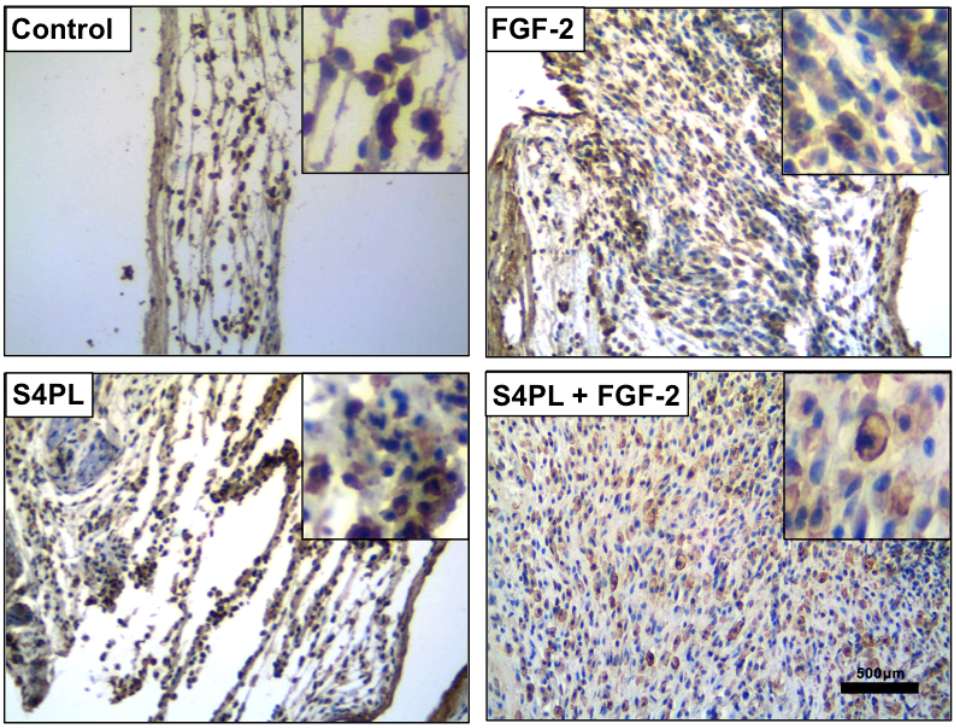

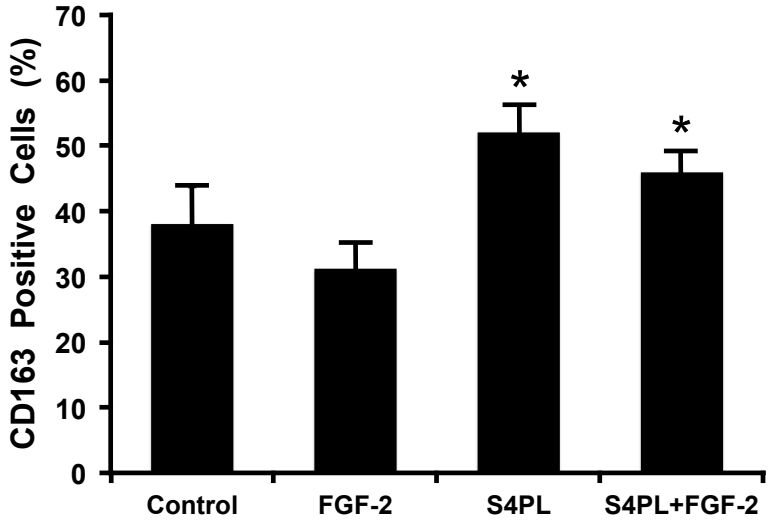

Figure 6.14 Wound micro-sections immunostained with CD163 antibody which is a marker for alternatively activated M2 macrophages at day 14 (upper). Quantification of the ratio of the positively stained cells with the nuclear area (lower). Size bar is 500µm. Inset is 3X magnified. *Statistically different from FGF-2 group ($p < 0.05$). n=8.

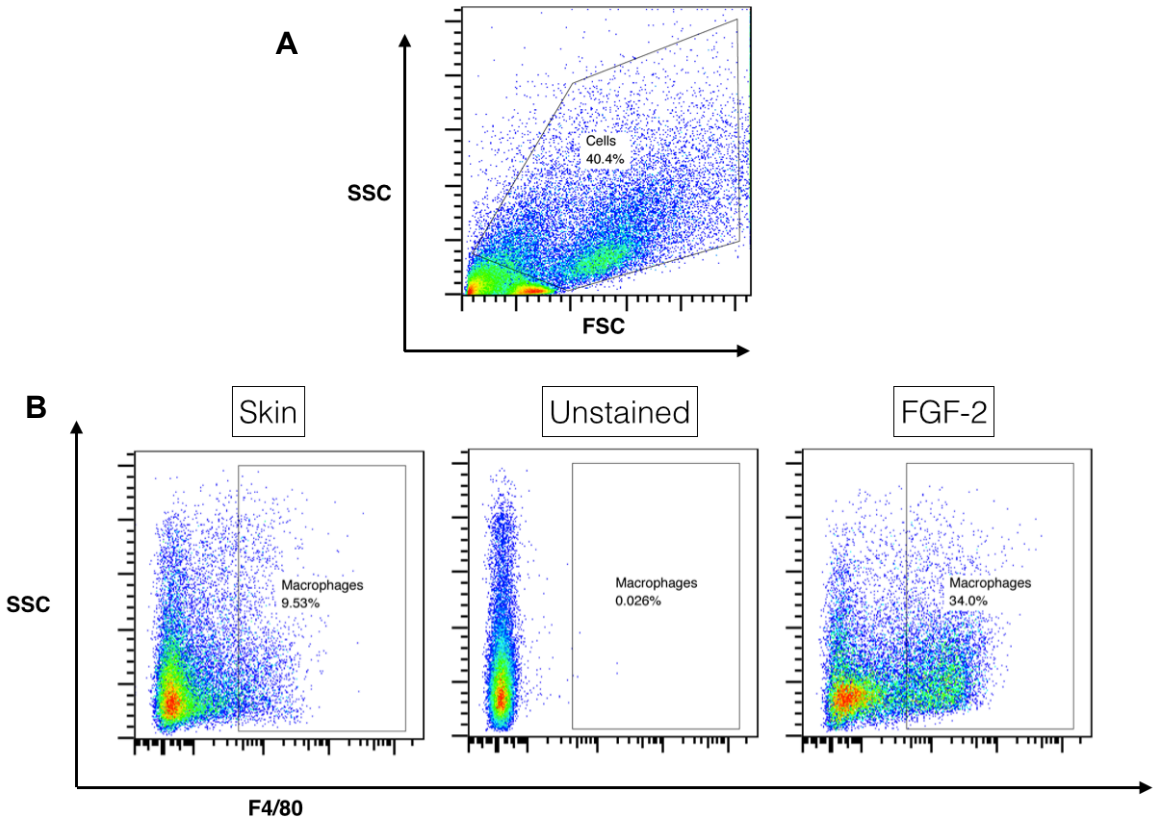

Figure 6.15 Flow cytometry on wound cells. (**A**) Primary gate named "Cells" on the entire population of wound cells by looking at the side scatter (SSC) versus forward scatter (FSC) plot. (**B**) Plot of side scatter (SSC) versus the fluorescent intensity of F4/80 in the gated populations of stained skin, unstained skin and FGF-2 treated wound. The secondary gate named "Macrophages" was defined such that the unstained skin doesn't have events and the stained skin has less than 10% cells inside the gated population. The fluorescent intensities of all the markers were evaluated for this secondary gated population in the next figure.

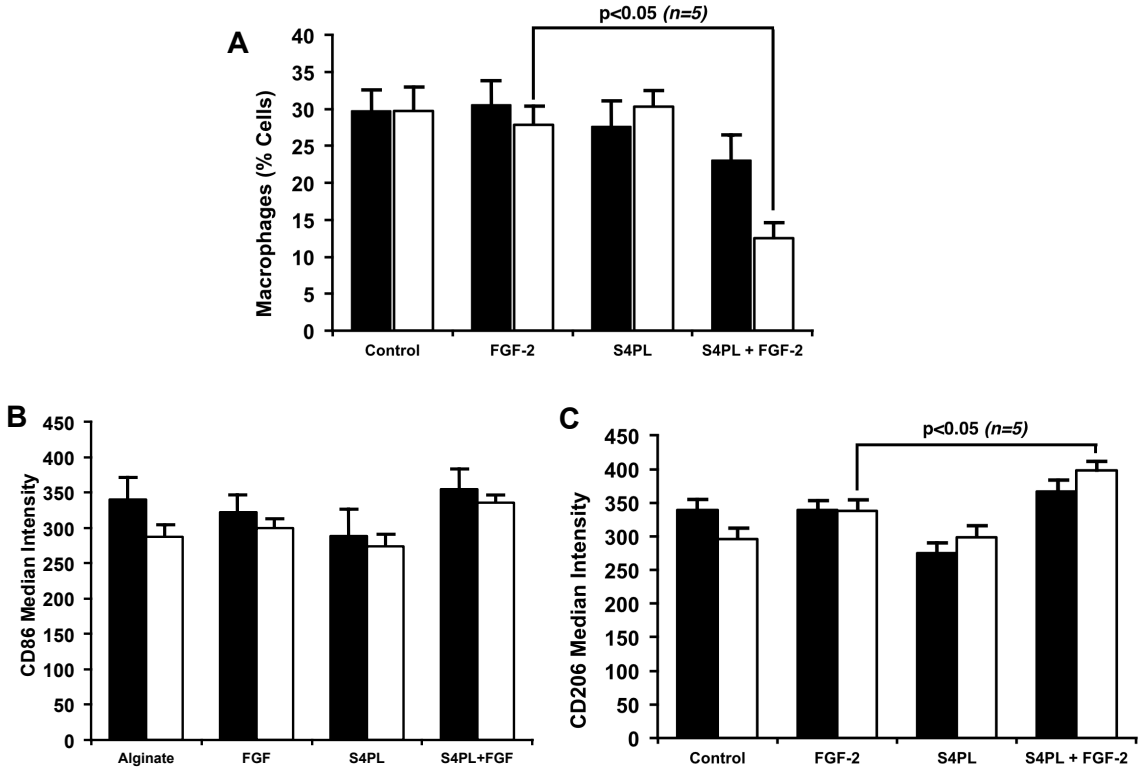

Figure 6.16 Plots of % cells and median fluorescent intensities. Black bars represent day 2 and white bars represent day 6. (**A**) Graph shows % cells that are macrophages. (**B**) Graph shows median fluorescent intensity of PerCP CD86 of all the groups. (**C**) CD206 median fluorescent intensity of the treatment groups.

6.4 DISCUSSION

This study is a major step in understanding how clinically common diseases, such as diabetes, metabolic syndrome and hyperlipidemia alter the response to growth factor therapy and in developing new therapeutic options effective in inducing neo-vascularization of ischemic tissues in disease states. However, we acknowledge that there is a need to optimize the therapy targeting all the major growth factors.

Previous studies support a role for syndecan-4 in wound healing and have found that syndecan-4 gene expression promotes fibroblast migration and regulates integrin

signaling and small GTPases during wound healing [77, 86]. Syndecan-4 also enhances keratinocyte migration [81] and is necessary for migration of fibroblasts in 3D gels [87]. In addition, syndecan-4 is induced in the skin following wounding in both mice and neonatal humans [88]. Finally, mice with knockout of syndecan-4 have delayed wound healing and angiogenesis [75]. Our previous studies have shown that syndesomes improve the signaling response to FGF-2, particularly the proliferation, migration and nuclear localization of FGF-2 in endothelial cells [67]. In addition, we found that syndesomes improved the angiogenic response to FGF-2 in diabetic mice in a subcutaneous implantation model [89].

Here we have taken our previous studies a step further towards clinical translation. We have shown that the syndesome therapy is effective in healing full thickness wounds that are splinted to simulate the human healing behavior. Briefly, syndesomes enhance wound closure significantly more than any other treatment group by day 14. Although we have limited insight about the temporal progression of the healing process, it seems that the majority of the wound heals between days 7 and 14. Histology and immunostaining with cytokeratin confirmed that syndesomes up-regulate the re-epithelialization beyond the initial wound margin. Like we observed in the last chapter, syndesomes improve the revascularization in the wound compared to other treatment groups. Since blood perfusion to the wound is imperative for healing [130-132], we think that syndesome-mediated angiogenesis assists in the wound healing process as well. Finally, and most notably, we observed immune modulation of macrophages from a pro-inflammatory M1 phenotype to an anti-inflammatory M2 phenotype, by the syndesomes, which was absent in the other treatment groups. This finding is phenomenal because inflammation is always accompanied with growth factor treatments [133, 134].

Therefore, we envisage that this technology of co-delivering the co-receptors along with growth factors might be an effective solution to increasing the efficacy of growth factor therapy in a clinical setting.

6.5 CONCLUSIONS

The convincing results in ischemic tissue described in the last chapter spurred us to try the therapy in a wound healing experiment. Briefly, in this chapter we have shown the effectiveness of the syndesome therapeutics in a clinically relevant diseased ob/ob mouse model and an excisional-splinted wound model, which simulates the human wound healing process. Syndesomes enhanced cutaneous wound closure and re-epithelialization in comparison with all the other groups. They also significantly increased the number of vessels in the wound bed aiding in the wound healing process. Remarkably, syndesomes caused immune modulation of macrophages towards an anti-inflammatory phenotype without any adverse immune response. Thus, we are hopeful that this novel co-delivery system will be helpful to treat patients with wounds with underlying ischemic conditions.

Chapter 7: Conclusions and Future Work

7.1 Conclusions

The broad goal of this thesis was to understand the reasons behind the failure of clinical trials with growth factor therapy. We hypothesized that the reason for this therapeutic failure must lie in the target tissue characteristics. In animal models, ischemia is typically induced in a healthy animal by surgically ligating an artery either in the peripheral muscle or coronary artery; and wounds are fashioned on healthy animals, mostly without splints allowing them to shrink by contraction, which is absent in humans. Consequently, the wound or ischemia develops acutely in an animal that is otherwise healthy. In human clinical use, the patient has developed ischemia or chronic wounds most often through a long-term disease process. Thus, by the time patients have developed clinical recognizable symptoms, they have had the disease for an extended period of time and the considerable compensatory mechanisms of the human body have been overwhelmed. These compensatory mechanisms could include the induction of the very angiogenic factors that we are attempting to use as therapeutic inducers of blood vessel growth. Accordingly, the presence of long-term disease likely implies the presence of innate mechanisms to defeat growth factor therapy without modification.

This thesis describes a novel and innovative line of investigation to enhance the growth factor-based treatment of the disease. Rather than focusing on exploring new growth factors, cell types, or combinations of these, we proposed a two-pronged approach to the problem: *(1) identify the "broken links" in the known growth factor pathways in clinical patient samples and animal models of disease (2) co-treat diseased*

tissues with novel therapeutics that repair revascularization signaling pathways to allow growth factor therapies to be efficacious in diseased condition.

This work, to the best of our knowledge, is the first in-depth functional analysis of why diseased tissues are resistant to growth factor signaling and how the functional ability to a healthy state can be restored under these conditions. Throughout the study, we have used the ob/ob mouse model, which is a leptin-deficient mouse with clinically relevant characteristics including obesity, hypercholesterolemia, pre-diabetes, hyperglycemia, and insulin resistance. To the best of our understanding, this is the best model to simulate the diseased condition in human patients with diabetes and other vascular complications. Our studies show significant loss of the co-receptors due to presence of disease in the ob/ob mouse model compared to healthy mice, leading to immense resistance to growth factor-based angiogenesis (Chapter 3). We decided to focus on one of the most important growth factors, FGF-2 and studied one out of the two co-receptors (sdc-1 and sdc-4). Co-delivery of the missing co-receptor protein with the growth factor was able to overcome some of the resistance (Chapter 4). To match the response of the normal healthy mouse, we might have to deliver all the missing co-receptors with the associated growth factors. However, this was a first proof-of-concept experiment that confirmed our hypothesis. To test the effectiveness of the therapy in a pertinent model, we decided to use hind limb ischemia and an excisional wound model with diseased ob/ob mice. The syndesomes not only enhanced revascularization in the ischemic limbs (Chapter 5) but also improved the wound closure and re-epithelialization of wounds (Chapter 6) while showing minimal adverse inflammatory response.

On a global level, the basic findings and techniques developed in this thesis represent a paradigm shift in how growth factor signaling pathways are approached from

a therapeutic perspective. While this work focuses on ischemia and vascular disease, growth factors are intimately involved in the mechanisms of many diseases including cancer growth and metastasis, wound healing, and the immune response to infection. Thus, the innovative techniques we will develop will have a broad impact on the understanding and treatment of diverse disease states.

7.2 FUTURE WORK

7.2.1 Large Animal Studies

With the conclusive results that we have described in this thesis in the mouse model, we would like to test our therapy in a large animal model so that we can quickly translate into the clinic. We have forged collaboration with Bridge PTS (Preclinical Testing Services) in San Antonio and we will be starting the studies on a porcine model soon. Various porcine models of both type-1 and type-2 diabetes have been reported in the literature [135]. The most widely used model uses Yucatan minipigs with multiple low dosage injections of streptozotocin or alloxan to induce diabetes before the start of the study, and simultaneously feeding the animal with a high fat diet to induce metabolic syndrome [135, 136]. We will have an n=5 and will continue the study up to 4 weeks to assess the temporal response to the treatment groups. The wound closure rate will be evaluated using the macroscopic dimensions of the wound over the course of the study. Revascularization will be monitored with the laser speckle contrast imager that shows relative blood perfusion and hyper spectral spatial frequency domain imager to observe the tissue oxygenation and health.

7.2.2 Intra-cellular Trafficking Studies

We would also like to investigate the subcellular mechanism of syndesome uptake and action. FGF-2 will be tagged with Alexa Fluor 647 succinimidyl ester for 1 hour at room temperature as previously shown in the lab [67]. The HEK293Ta cells will be transfected with fluorescent Rab5 [137], Rab7 [137], and Rab11 [138] proteins. The five different compositions of syndesomes will be delivered to endothelial cells *in vitro* and tracked over a period of two days using a confocal microscope. We will also use adult human dermal fibroblasts from healthy and diabetic sources to tease out differences in subcellular trafficking. This will give us insight into how the syndesomes alter growth factor trafficking at the subcellular level and locations of various cytosolic components during the response to growth factor therapy.

References

[1] F. G. Fowkes, D. Rudan, I. Rudan, V. Aboyans, J. O. Denenberg, M. M. McDermott*, et al.*, "Comparison of global estimates of prevalence and risk factors for peripheral artery disease in 2000 and 2010: a systematic review and analysis," *Lancet,* vol. 382, pp. 1329-40, Oct 19 2013.

[2] M. A. Allison, E. Ho, J. O. Denenberg, R. D. Langer, A. B. Newman, R. R. Fabsitz*, et al.*, "Ethnic-specific prevalence of peripheral arterial disease in the United States," *Am J Prev Med,* vol. 32, pp. 328-33, Apr 2007.

[3] A. T. Hirsch, M. H. Criqui, D. Treat-Jacobson, J. G. Regensteiner, M. A. Creager, J. W. Olin*, et al.*, "Peripheral arterial disease detection, awareness, and treatment in primary care," *JAMA,* vol. 286, pp. 1317-24, Sep 19 2001.

[4] J. F. Lau, M. D. Weinberg, and J. W. Olin, "Peripheral artery disease. Part 1: clinical evaluation and noninvasive diagnosis," *Nat Rev Cardiol,* vol. 8, pp. 405-18, Jul 2011.

[5] W. T. Meijer, A. W. Hoes, D. Rutgers, M. L. Bots, A. Hofman, and D. E. Grobbee, "Peripheral arterial disease in the elderly: The Rotterdam Study," *Arterioscler Thromb Vasc Biol,* vol. 18, pp. 185-92, Feb 1998.

[6] E. Selvin, K. Wattanakit, M. W. Steffes, J. Coresh, and A. R. Sharrett, "HbA1c and peripheral arterial disease in diabetes: the Atherosclerosis Risk in Communities study," *Diabetes Care,* vol. 29, pp. 877-82, Apr 2006.

[7] A. American Diabetes, "Economic costs of diabetes in the U.S. in 2012," *Diabetes Care,* vol. 36, pp. 1033-46, Apr 2013.

[8] K. Futrega, M. King, W. B. Lott, and M. R. Doran, "Treating the whole not the hole: necessary coupling of technologies for diabetic foot ulcer treatment," *Trends Mol Med,* vol. 20, pp. 137-42, Mar 2014.

[9] M. D. Weinberg, J. F. Lau, K. Rosenfield, and J. W. Olin, "Peripheral artery disease. Part 2: medical and endovascular treatment," *Nat Rev Cardiol,* vol. 8, pp. 429-41, Aug 2011.

[10] R. J. Lederman, F. O. Mendelsohn, R. D. Anderson, J. F. Saucedo, A. N. Tenaglia, J. B. Hermiller*, et al.*, "Therapeutic angiogenesis with recombinant fibroblast growth factor-2 for intermittent claudication (the TRAFFIC study): a randomised trial," *Lancet,* vol. 359, pp. 2053-8, Jun 15 2002.

[11] D. F. Lazarous, E. F. Unger, S. E. Epstein, A. Stine, J. L. Arevalo, E. Y. Chew*, et al.*, "Basic fibroblast growth factor in patients with intermittent claudication: results of a phase I trial," *J Am Coll Cardiol,* vol. 36, pp. 1239-44, Oct 2000.

[12] N. van Royen, S. H. Schirmer, B. Atasever, C. Y. Behrens, D. Ubbink, E. E. Buschmann*, et al.*, "START Trial: a pilot study on STimulation of ARTeriogenesis using subcutaneous application of granulocyte-macrophage

colony-stimulating factor as a new treatment for peripheral vascular disease," *Circulation,* vol. 112, pp. 1040-6, Aug 16 2005.

[13] S. Nikol, I. Baumgartner, E. Van Belle, C. Diehm, A. Visona, M. C. Capogrossi*, et al.*, "Therapeutic angiogenesis with intramuscular NV1FGF improves amputation-free survival in patients with critical limb ischemia," *Mol Ther,* vol. 16, pp. 972-8, May 2008.

[14] R. Morishita, H. Makino, M. Aoki, N. Hashiya, K. Yamasaki, J. Azuma*, et al.*, "Phase I/IIa clinical trial of therapeutic angiogenesis using hepatocyte growth factor gene transfer to treat critical limb ischemia," *Arterioscler Thromb Vasc Biol,* vol. 31, pp. 713-20, Mar 2011.

[15] Y. H. Kusumanto, V. van Weel, N. H. Mulder, A. J. Smit, J. J. van den Dungen, J. M. Hooymans*, et al.*, "Treatment with intramuscular vascular endothelial growth factor gene compared with placebo for patients with diabetes mellitus and critical limb ischemia: a double-blind randomized trial," *Hum Gene Ther,* vol. 17, pp. 683-91, Jun 2006.

[16] H. Shigematsu, K. Yasuda, T. Iwai, T. Sasajima, S. Ishimaru, Y. Ohashi*, et al.*, "Randomized, double-blind, placebo-controlled clinical trial of hepatocyte growth factor plasmid for critical limb ischemia," *Gene Ther,* vol. 17, pp. 1152-61, Sep 2010.

[17] S. Matoba, T. Tatsumi, T. Murohara, T. Imaizumi, Y. Katsuda, M. Ito*, et al.*, "Long-term clinical outcome after intramuscular implantation of bone marrow mononuclear cells (Therapeutic Angiogenesis by Cell Transplantation [TACT] trial) in patients with chronic limb ischemia," *Am Heart J,* vol. 156, pp. 1010-8, Nov 2008.

[18] K. Alexiadou and J. Doupis, "Management of diabetic foot ulcers," *Diabetes Ther,* vol. 3, p. 4, Nov 2012.

[19] E. A. Ayello, "What does the wound say? Why determining etiology is essential for appropriate wound care," *Adv Skin Wound Care,* vol. 18, pp. 98-109; quiz 110-1, Mar 2005.

[20] N. W. Shammas, "Epidemiology, classification, and modifiable risk factors of peripheral arterial disease," *Vasc Health Risk Manag,* vol. 3, pp. 229-34, 2007.

[21] R. L. Pande and M. A. Creager, "Socioeconomic Inequality and Peripheral Artery Disease Prevalence in US Adults," *Circ Cardiovasc Qual Outcomes,* Jul 1 2014.

[22] E. Marrett, M. DiBonaventura, and Q. Zhang, "Burden of peripheral arterial disease in Europe and the United States: a patient survey," *Health Qual Life Outcomes,* vol. 11, p. 175, 2013.

[23] J. D. Hooi, A. D. Kester, H. E. Stoffers, M. M. Overdijk, J. W. van Ree, and J. A. Knottnerus, "Incidence of and risk factors for asymptomatic peripheral arterial occlusive disease: a longitudinal study," *Am J Epidemiol,* vol. 153, pp. 666-72, Apr 1 2001.

[24] R. L. Pande, T. S. Perlstein, J. A. Beckman, and M. A. Creager, "Secondary prevention and mortality in peripheral artery disease: National Health and

Nutrition Examination Study, 1999 to 2004," *Circulation,* vol. 124, pp. 17-23, Jul 5 2011.

[25] J. I. Weitz, J. Byrne, G. P. Clagett, M. E. Farkouh, J. M. Porter, D. L. Sackett*, et al.*, "Diagnosis and treatment of chronic arterial insufficiency of the lower extremities: a critical review," *Circulation,* vol. 94, pp. 3026-49, Dec 1 1996.

[26] A. M. O'Hare, D. V. Glidden, C. S. Fox, and C. Y. Hsu, "High prevalence of peripheral arterial disease in persons with renal insufficiency: results from the National Health and Nutrition Examination Survey 1999-2000," *Circulation,* vol. 109, pp. 320-3, Jan 27 2004.

[27] N. Fiotti, C. Giansante, E. Ponte, C. Delbello, S. Calabrese, T. Zacchi*, et al.*, "Atherosclerosis and inflammation. Patterns of cytokine regulation in patients with peripheral arterial disease," *Atherosclerosis,* vol. 145, pp. 51-60, Jul 1999.

[28] M. C. Kleinegris, H. ten Cate, and A. J. ten Cate-Hoek, "D-dimer as a marker for cardiovascular and arterial thrombotic events in patients with peripheral arterial disease. A systematic review," *Thromb Haemost,* vol. 110, pp. 233-43, Aug 2013.

[29] P. W. Stather, N. Sylvius, J. B. Wild, E. Choke, R. D. Sayers, and M. J. Bown, "Differential microRNA expression profiles in peripheral arterial disease," *Circ Cardiovasc Genet,* vol. 6, pp. 490-7, Oct 2013.

[30] M. R. Stacy, Y. Yu da, M. W. Maxfield, I. M. Jaba, B. P. Jozwik, Z. W. Zhuang*, et al.*, "Multimodality imaging approach for serial assessment of regional changes in lower extremity arteriogenesis and tissue perfusion in a porcine model of peripheral arterial disease," *Circ Cardiovasc Imaging,* vol. 7, pp. 92-9, Jan 2014.

[31] T. W. Rooke, A. T. Hirsch, S. Misra, A. N. Sidawy, J. A. Beckman, L. K. Findeiss*, et al.*, "2011 ACCF/AHA Focused Update of the Guideline for the Management of Patients With Peripheral Artery Disease (updating the 2005 guideline): a report of the American College of Cardiology Foundation/American Heart Association Task Force on Practice Guidelines," *J Am Coll Cardiol,* vol. 58, pp. 2020-45, Nov 1 2011.

[32] V. S. Kudagi and C. J. White, "Endovascular stents: a review of their use in peripheral arterial disease," *Am J Cardiovasc Drugs,* vol. 13, pp. 199-212, Jun 2013.

[33] L. Norgren, W. R. Hiatt, J. A. Dormandy, M. R. Nehler, K. A. Harris, and F. G. Fowkes, "Inter-Society Consensus for the Management of Peripheral Arterial Disease (TASC II)," *J Vasc Surg,* vol. 45 Suppl S, pp. S5-67, Jan 2007.

[34] D. Tirziu and M. Simons, "Angiogenesis in the human heart: gene and cell therapy," *Angiogenesis,* vol. 8, pp. 241-51, 2005.

[35] M. Simons, B. H. Annex, R. J. Laham, N. Kleiman, T. Henry, H. Dauerman*, et al.*, "Pharmacological treatment of coronary artery disease with recombinant fibroblast growth factor-2: double-blind, randomized, controlled clinical trial," *Circulation,* vol. 105, pp. 788-93, Feb 19 2002.

[36] T. D. Henry, B. H. Annex, G. R. McKendall, M. A. Azrin, J. J. Lopez, F. J. Giordano*, et al.*, "The VIVA trial: Vascular endothelial growth factor in Ischemia for Vascular Angiogenesis," *Circulation,* vol. 107, pp. 1359-65, Mar 18 2003.

[37] R. J. Lederman, A. N. Tenaglia, R. D. Anderson, J. B. Hermiller, K. Rocha-Singh, F. O. Mendelsohn*, et al.*, "Design of the therapeutic angiogenesis with recombinant fibroblast growth factor-2 for intermittent claudication (TRAFFIC) trial," *Am J Cardiol,* vol. 88, pp. 192-5, A6-7, Jul 15 2001.

[38] J. E. Udelson, V. Dilsizian, R. J. Laham, N. Chronos, J. Vansant, M. Blais*, et al.*, "Therapeutic angiogenesis with recombinant fibroblast growth factor-2 improves stress and rest myocardial perfusion abnormalities in patients with severe symptomatic chronic coronary artery disease," *Circulation,* vol. 102, pp. 1605-10, Oct 3 2000.

[39] S. Rajagopalan, E. R. Mohler, 3rd, R. J. Lederman, F. O. Mendelsohn, J. F. Saucedo, C. K. Goldman*, et al.*, "Regional angiogenesis with vascular endothelial growth factor in peripheral arterial disease: a phase II randomized, double-blind, controlled study of adenoviral delivery of vascular endothelial growth factor 121 in patients with disabling intermittent claudication," *Circulation,* vol. 108, pp. 1933-8, Oct 21 2003.

[40] C. L. Grines, M. W. Watkins, G. Helmer, W. Penny, J. Brinker, J. D. Marmur*, et al.*, "Angiogenic Gene Therapy (AGENT) trial in patients with stable angina pectoris," *Circulation,* vol. 105, pp. 1291-7, Mar 19 2002.

[41] A. J. Comerota, R. C. Throm, K. A. Miller, T. Henry, N. Chronos, J. Laird*, et al.*, "Naked plasmid DNA encoding fibroblast growth factor type 1 for the treatment of end-stage unreconstructible lower extremity ischemia: preliminary results of a phase I trial," *J Vasc Surg,* vol. 35, pp. 930-6, May 2002.

[42] J. Belch, W. R. Hiatt, I. Baumgartner, I. V. Driver, S. Nikol, L. Norgren*, et al.*, "Effect of fibroblast growth factor NV1FGF on amputation and death: a randomised placebo-controlled trial of gene therapy in critical limb ischaemia," *Lancet,* vol. 377, pp. 1929-37, Jun 4 2011.

[43] M. A. Creager, J. W. Olin, J. J. Belch, G. L. Moneta, T. D. Henry, S. Rajagopalan*, et al.*, "Effect of hypoxia-inducible factor-1alpha gene therapy on walking performance in patients with intermittent claudication," *Circulation,* vol. 124, pp. 1765-73, Oct 18 2011.

[44] B. H. Annex, "Therapeutic angiogenesis for critical limb ischaemia," *Nat Rev Cardiol,* vol. 10, pp. 387-96, May 14 2013.

[45] K. Futrega, M. King, W. B. Lott, and M. R. Doran, "Treating the whole not the hole: necessary coupling of technologies for diabetic foot ulcer treatment," *Trends Mol Med,* Jan 30 2014.

[46] "Economic costs of diabetes in the U.S. in 2012," *Diabetes Care,* vol. 36, pp. 1033-46, Apr 2013.

[47] A. American Diabetes, "Diagnosis and classification of diabetes mellitus," *Diabetes Care,* vol. 37 Suppl 1, pp. S81-90, Jan 2014.

[48] C. C. Cowie, K. F. Rust, D. D. Byrd-Holt, E. W. Gregg, E. S. Ford, L. S. Geiss, *et al.*, "Prevalence of diabetes and high risk for diabetes using A1C criteria in the U.S. population in 1988-2006," *Diabetes Care,* vol. 33, pp. 562-8, Mar 2010.

[49] C. C. Cowie, K. F. Rust, E. S. Ford, M. S. Eberhardt, D. D. Byrd-Holt, C. Li, *et al.*, "Full accounting of diabetes and pre-diabetes in the U.S. population in 1988-1994 and 2005-2006," *Diabetes Care,* vol. 32, pp. 287-94, Feb 2009.

[50] W. H. Herman and R. M. Cohen, "Racial and ethnic differences in the relationship between HbA1c and blood glucose: implications for the diagnosis of diabetes," *J Clin Endocrinol Metab,* vol. 97, pp. 1067-72, Apr 2012.

[51] N. Singh, D. G. Armstrong, and B. A. Lipsky, "Preventing foot ulcers in patients with diabetes," *JAMA,* vol. 293, pp. 217-28, Jan 12 2005.

[52] D. G. Armstrong, V. A. Kanda, L. A. Lavery, W. Marston, J. L. Mills, Sr., and A. J. Boulton, "Mind the gap: disparity between research funding and costs of care for diabetic foot ulcers," *Diabetes Care,* vol. 36, pp. 1815-7, Jul 2013.

[53] J. Larsson, C. D. Agardh, J. Apelqvist, and A. Stenstrom, "Long-term prognosis after healed amputation in patients with diabetes," *Clin Orthop Relat Res,* pp. 149-58, May 1998.

[54] R. H. Adams and K. Alitalo, "Molecular regulation of angiogenesis and lymphangiogenesis," *Nat Rev Mol Cell Biol,* vol. 8, pp. 464-78, Jun 2007.

[55] D. M. Ornitz, "FGFs, heparan sulfate and FGFRs: complex interactions essential for development," *Bioessays,* vol. 22, pp. 108-12, Feb 2000.

[56] N. Ferrara, H. P. Gerber, and J. LeCouter, "The biology of VEGF and its receptors," *Nat Med,* vol. 9, pp. 669-76, Jun 2003.

[57] C. Pellet-Many, P. Frankel, H. Jia, and I. Zachary, "Neuropilins: structure, function and role in disease," *Biochem J,* vol. 411, pp. 211-26, Apr 15 2008.

[58] E. Chen, S. Hermanson, and S. C. Ekker, "Syndecan-2 is essential for angiogenic sprouting during zebrafish development," *Blood,* vol. 103, pp. 1710-9, Mar 1 2004.

[59] E. J. Battegay, J. Rupp, L. Iruela-Arispe, E. H. Sage, and M. Pech, "PDGF-BB modulates endothelial proliferation and angiogenesis in vitro via PDGF beta-receptors," *J Cell Biol,* vol. 125, pp. 917-28, May 1994.

[60] C. H. Heldin and B. Westermark, "Mechanism of action and in vivo role of platelet-derived growth factor," *Physiol Rev,* vol. 79, pp. 1283-316, Oct 1999.

[61] S. G. Ball, C. Bayley, C. A. Shuttleworth, and C. M. Kielty, "Neuropilin-1 regulates platelet-derived growth factor receptor signalling in mesenchymal stem cells," *Biochem J,* vol. 427, pp. 29-40, Apr 1 2010.

[62] C. Pellet-Many, P. Frankel, I. M. Evans, B. Herzog, M. Junemann-Ramirez, and I. C. Zachary, "Neuropilin-1 mediates PDGF stimulation of vascular smooth muscle cell migration and signalling via p130Cas," *Biochem J,* vol. 435, pp. 609-18, May 1 2011.

[63] J. Kim, J. H. Lee, H. S. Park, J. Hwang, I. O. Han, Y. S. Bae, *et al.*, "Syndecan-4 regulates platelet-derived growth factor-mediated MAP kinase activation by

altering intracellular reactive oxygen species," *FEBS Lett,* vol. 582, pp. 2725-30, Aug 6 2008.

[64] N. Fukai, R. D. Kenagy, L. Chen, L. Gao, G. Daum, and A. W. Clowes, "Syndecan-1: an inhibitor of arterial smooth muscle cell growth and intimal hyperplasia," *Arterioscler Thromb Vasc Biol,* vol. 29, pp. 1356-62, Sep 2009.

[65] R. Cao, E. Brakenhielm, X. Li, K. Pietras, J. Widenfalk, A. Ostman*, et al.*, "Angiogenesis stimulated by PDGF-CC, a novel member in the PDGF family, involves activation of PDGFR-alphaalpha and -alphabeta receptors," *FASEB J,* vol. 16, pp. 1575-83, Oct 2002.

[66] J. Moriya, X. Wu, J. Zavala-Solorio, J. Ross, X. H. Liang, and N. Ferrara, "PDGF-C promotes revascularization in ischemic limbs of diabetic mice," *J Vasc Surg,* Jul 13 2013.

[67] E. Jang, H. Albadawi, M. T. Watkins, E. R. Edelman, and A. B. Baker, "Syndecan-4 proteoliposomes enhance fibroblast growth factor-2 (FGF-2)-induced proliferation, migration, and neovascularization of ischemic muscle," *Proc Natl Acad Sci U S A,* vol. 109, pp. 1679-84, Jan 31 2012.

[68] J. R. Couchman and C. A. Pataki, "An introduction to proteoglycans and their localization," *J Histochem Cytochem,* vol. 60, pp. 885-97, Dec 2012.

[69] S. Tumova, A. Woods, and J. R. Couchman, "Heparan sulfate proteoglycans on the cell surface: versatile coordinators of cellular functions," *Int J Biochem Cell Biol,* vol. 32, pp. 269-88, Mar 2000.

[70] C. C. Chua, N. Rahimi, K. Forsten-Williams, and M. A. Nugent, "Heparan sulfate proteoglycans function as receptors for fibroblast growth factor-2 activation of extracellular signal-regulated kinases 1 and 2," *Circ Res,* vol. 94, pp. 316-23, Feb 20 2004.

[71] J. L. Dreyfuss, C. V. Regatieri, T. R. Jarrouge, R. P. Cavalheiro, L. O. Sampaio, and H. B. Nader, "Heparan sulfate proteoglycans: structure, protein interactions and cell signaling," *An Acad Bras Cienc,* vol. 81, pp. 409-29, Sep 2009.

[72] S. Sarrazin, W. C. Lamanna, and J. D. Esko, "Heparan sulfate proteoglycans," *Cold Spring Harb Perspect Biol,* vol. 3, Jul 2011.

[73] M. Bernfield, R. Kokenyesi, M. Kato, M. T. Hinkes, J. Spring, R. L. Gallo*, et al.*, "Biology of the syndecans: a family of transmembrane heparan sulfate proteoglycans," *Annu Rev Cell Biol,* vol. 8, pp. 365-93, 1992.

[74] C. C. Lopes, C. P. Dietrich, and H. B. Nader, "Specific structural features of syndecans and heparan sulfate chains are needed for cell signaling," *Braz J Med Biol Res,* vol. 39, pp. 157-67, Feb 2006.

[75] F. Echtermeyer, M. Streit, S. Wilcox-Adelman, S. Saoncella, F. Denhez, M. Detmar*, et al.*, "Delayed wound repair and impaired angiogenesis in mice lacking syndecan-4," *J Clin Invest,* vol. 107, pp. R9-R14, Jan 2001.

[76] C. Y. Fears and A. Woods, "The role of syndecans in disease and wound healing," *Matrix Biol,* vol. 25, pp. 443-56, Sep 2006.

[77] M. D. Bass, R. C. Williamson, R. D. Nunan, J. D. Humphries, A. Byron, M. R. Morgan*, et al.*, "A syndecan-4 hair trigger initiates wound healing through caveolin- and RhoG-regulated integrin endocytosis," *Dev Cell,* vol. 21, pp. 681-93, Oct 18 2011.

[78] S. Brule, N. Charnaux, A. Sutton, D. Ledoux, T. Chaigneau, L. Saffar*, et al.*, "The shedding of syndecan-4 and syndecan-1 from HeLa cells and human primary macrophages is accelerated by SDF-1/CXCL12 and mediated by the matrix metalloproteinase-9," *Glycobiology,* vol. 16, pp. 488-501, Jun 2006.

[79] P. L. Voyvodic, D. Min, R. Liu, E. Williams, V. Chitalia, A. K. Dunn*, et al.*, "Loss of syndecan-1 induces a pro-inflammatory phenotype in endothelial cells with a dysregulated response to atheroprotective flow," *J Biol Chem,* vol. 289, pp. 9547-59, Apr 4 2014.

[80] A. Purushothaman, T. Uyama, F. Kobayashi, S. Yamada, K. Sugahara, A. C. Rapraeger*, et al.*, "Heparanase-enhanced shedding of syndecan-1 by myeloma cells promotes endothelial invasion and angiogenesis," *Blood,* vol. 115, pp. 2449-57, Mar 25 2010.

[81] E. Araki, Y. Momota, T. Togo, M. Tanioka, K. Hozumi, M. Nomizu*, et al.*, "Clustering of syndecan-4 and integrin beta1 by laminin alpha 3 chain-derived peptide promotes keratinocyte migration," *Mol Biol Cell,* vol. 20, pp. 3012-24, Jul 2009.

[82] J. C. Rodriguez-Manzaneque, D. Carpizo, C. Plaza-Calonge Mdel, A. X. Torres-Collado, S. N. Thai, M. Simons*, et al.*, "Cleavage of syndecan-4 by ADAMTS1 provokes defects in adhesion," *Int J Biochem Cell Biol,* vol. 41, pp. 800-10, Apr 2009.

[83] O. Reizes, S. C. Benoit, and D. J. Clegg, "The role of syndecans in the regulation of body weight and synaptic plasticity," *Int J Biochem Cell Biol,* vol. 40, pp. 28-45, 2008.

[84] T. Kojima, A. Takagi, M. Maeda, T. Segawa, A. Shimizu, K. Yamamoto*, et al.*, "Plasma levels of syndecan-4 (ryudocan) are elevated in patients with acute myocardial infarction," *Thromb Haemost,* vol. 85, pp. 793-9, May 2001.

[85] T. Manon-Jensen, H. A. Multhaupt, and J. R. Couchman, "Mapping of matrix metalloproteinase cleavage sites on syndecan-1 and syndecan-4 ectodomains," *FEBS J,* vol. 280, pp. 2320-31, May 2013.

[86] R. Brooks, R. Williamson, and M. Bass, "Syndecan-4 independently regulates multiple small GTPases to promote fibroblast migration during wound healing," *Small GTPases,* vol. 3, pp. 73-9, Apr-Jun 2012.

[87] F. Lin, X. D. Ren, G. Doris, and R. A. Clark, "Three-dimensional migration of human adult dermal fibroblasts from collagen lattices into fibrin/fibronectin gels requires syndecan-4 proteoglycan," *J Invest Dermatol,* vol. 124, pp. 906-13, May 2005.

[88] R. Gallo, C. Kim, R. Kokenyesi, N. S. Adzick, and M. Bernfield, "Syndecans-1 and -4 are induced during wound repair of neonatal but not fetal skin," *J Invest Dermatol,* vol. 107, pp. 676-83, Nov 1996.

[89] S. Das, G. Singh, and A. B. Baker, "Overcoming disease-induced growth factor resistance in therapeutic angiogenesis using recombinant co-receptors delivered by a liposomal system," *Biomaterials,* vol. 35, pp. 196-205, Jan 2014.

[90] V. T. Samuel and G. I. Shulman, "Mechanisms for insulin resistance: common threads and missing links," *Cell,* vol. 148, pp. 852-71, Mar 2 2012.

[91] O. Seitz, C. Schurmann, N. Hermes, E. Muller, J. Pfeilschifter, S. Frank*, et al.*, "Wound healing in mice with high-fat diet- or ob gene-induced diabetes-obesity syndromes: a comparative study," *Exp Diabetes Res,* vol. 2010, p. 476969, 2010.

[92] O. Bouhidel, S. Pons, R. Souktani, R. Zini, A. Berdeaux, and B. Ghaleh, "Myocardial ischemic postconditioning against ischemia-reperfusion is impaired in ob/ob mice," *Am J Physiol Heart Circ Physiol,* vol. 295, pp. H1580-6, Oct 2008.

[93] C. Emanueli, A. Caporali, N. Krankel, B. Cristofaro, S. Van Linthout, and P. Madeddu, "Type-2 diabetic Lepr(db/db) mice show a defective microvascular phenotype under basal conditions and an impaired response to angiogenesis gene therapy in the setting of limb ischemia," *Front Biosci,* vol. 12, pp. 2003-12, 2007.

[94] S. Schiekofer, G. Galasso, K. Sato, B. J. Kraus, and K. Walsh, "Impaired revascularization in a mouse model of type 2 diabetes is associated with dysregulation of a complex angiogenic-regulatory network," *Arterioscler Thromb Vasc Biol,* vol. 25, pp. 1603-9, Aug 2005.

[95] P. Lindstrom, "The physiology of obese-hyperglycemic mice [ob/ob mice]," *ScientificWorldJournal,* vol. 7, pp. 666-85, 2007.

[96] A. H. Fischer, K. A. Jacobson, J. Rose, and R. Zeller, "Hematoxylin and eosin staining of tissue and cell sections," *CSH Protoc,* vol. 2008, p. pdb prot4986, 2008.

[97] W. Garvey, A. Fathi, F. Bigelow, B. Carpenter, and C. Jimenez, "Improved Movat pentachrome stain," *Stain Technol,* vol. 61, pp. 60-2, Jan 1986.

[98] N. Ilan, M. Elkin, and I. Vlodavsky, "Regulation, function and clinical significance of heparanase in cancer metastasis and angiogenesis," *Int J Biochem Cell Biol,* vol. 38, pp. 2018-39, 2006.

[99] E. Adeghate, "Molecular and cellular basis of the aetiology and management of diabetic cardiomyopathy: a short review," *Mol Cell Biochem,* vol. 261, pp. 187-91, Jun 2004.

[100] M. R. Skilton, J. P. Chin-Dusting, A. M. Dart, L. Brazionis, O. Lantieri, K. O'Dea*, et al.*, "Metabolic health, obesity and 9-year incidence of peripheral arterial disease: the D.E.S.I.R. study," *Atherosclerosis,* vol. 216, pp. 471-6, Jun 2011.

[101] G. Chen, D. Wang, R. Vikramadithyan, H. Yagyu, U. Saxena, S. Pillarisetti*, et al.*, "Inflammatory cytokines and fatty acids regulate endothelial cell heparanase expression," *Biochemistry,* vol. 43, pp. 4971-7, May 4 2004.
[102] A. B. Baker, A. Groothuis, M. Jonas, D. S. Ettenson, T. Shazly, E. Zcharia*, et al.*, "Heparanase alters arterial structure, mechanics, and repair following endovascular stenting in mice," *Circ Res,* vol. 104, pp. 380-7, Feb 13 2009.
[103] A. B. Baker, W. J. Gibson, V. B. Kolachalama, M. Golomb, L. Indolfi, C. Spruell*, et al.*, "Heparanase regulates thrombosis in vascular injury and stent-induced flow disturbance," *J Am Coll Cardiol,* vol. 59, pp. 1551-60, Apr 24 2012.
[104] A. B. Baker, Y. S. Chatzizisis, R. Beigel, M. Jonas, B. V. Stone, A. U. Coskun*, et al.*, "Regulation of heparanase expression in coronary artery disease in diabetic, hyperlipidemic swine," *Atherosclerosis,* vol. 213, pp. 436-42, Dec 2010.
[105] E. Tkachenko, J. M. Rhodes, and M. Simons, "Syndecans: new kids on the signaling block," *Circ Res,* vol. 96, pp. 488-500, Mar 18 2005.
[106] A. N. Alexopoulou, H. A. Multhaupt, and J. R. Couchman, "Syndecans in wound healing, inflammation and vascular biology," *Int J Biochem Cell Biol,* vol. 39, pp. 505-28, 2007.
[107] A. Elfenbein, A. Lanahan, T. X. Zhou, A. Yamasaki, E. Tkachenko, M. Matsuda*, et al.*, "Syndecan 4 regulates FGFR1 signaling in endothelial cells by directing macropinocytosis," *Sci Signal,* vol. 5, p. ra36, May 8 2012.
[108] S. S. Nunes, M. A. Outeiro-Bernstein, L. Juliano, F. Vardiero, H. B. Nader, A. Woods*, et al.*, "Syndecan-4 contributes to endothelial tubulogenesis through interactions with two motifs inside the pro-angiogenic N-terminal domain of thrombospondin-1," *J Cell Physiol,* vol. 214, pp. 828-37, Mar 2008.
[109] Y. Zhang, J. Li, C. Partovian, F. W. Sellke, and M. Simons, "Syndecan-4 modulates basic fibroblast growth factor 2 signaling in vivo," *Am J Physiol Heart Circ Physiol,* vol. 284, pp. H2078-82, Jun 2003.
[110] S. P. Marso and W. R. Hiatt, "Peripheral arterial disease in patients with diabetes," *J Am Coll Cardiol,* vol. 47, pp. 921-9, Mar 7 2006.
[111] A. B. Parthasarathy, W. J. Tom, A. Gopal, X. Zhang, and A. K. Dunn, "Robust flow measurement with multi-exposure speckle imaging," *Opt Express,* vol. 16, pp. 1975-89, Feb 4 2008.
[112] B. Bruhn-Olszewska, A. Korzon-Burakowska, M. Gabig-Ciminska, P. Olszewski, A. Wegrzyn, and J. Jakobkiewicz-Banecka, "Molecular factors involved in the development of diabetic foot syndrome," *Acta Biochim Pol,* vol. 59, pp. 507-13, 2012.
[113] E. S. Folker and M. K. Baylies, "Nuclear positioning in muscle development and disease," *Front Physiol,* vol. 4, p. 363, 2013.
[114] D. M. Mosser and J. P. Edwards, "Exploring the full spectrum of macrophage activation," *Nat Rev Immunol,* vol. 8, pp. 958-69, Dec 2008.
[115] J. Majtan, "Honey: An immunomodulator in wound healing," *Wound Repair Regen,* vol. 22, pp. 187-92, Mar 2014.

[116] T. Dai, M. Tanaka, Y. Y. Huang, and M. R. Hamblin, "Chitosan preparations for wounds and burns: antimicrobial and wound-healing effects," *Expert Rev Anti Infect Ther,* vol. 9, pp. 857-79, Jul 2011.
[117] H. Beele, F. Meuleneire, M. Nahuys, and S. L. Percival, "A prospective randomised open label study to evaluate the potential of a new silver alginate/carboxymethylcellulose antimicrobial wound dressing to promote wound healing," *Int Wound J,* vol. 7, pp. 262-70, Aug 2010.
[118] R. Goldman, "Growth factors and chronic wound healing: past, present, and future," *Adv Skin Wound Care,* vol. 17, pp. 24-35, Jan-Feb 2004.
[119] L. K. Branski, C. T. Pereira, D. N. Herndon, and M. G. Jeschke, "Gene therapy in wound healing: present status and future directions," *Gene Ther,* vol. 14, pp. 1-10, Jan 2007.
[120] P. Zahorec, J. Koller, L. Danisovic, and M. Bohac, "Mesenchymal stem cells for chronic wounds therapy," *Cell Tissue Bank,* Mar 21 2014.
[121] B. Buchberger, M. Follmann, D. Freyer, H. Huppertz, A. Ehm, and J. Wasem, "The evidence for the use of growth factors and active skin substitutes for the treatment of non-infected diabetic foot ulcers (DFU): a health technology assessment (HTA)," *Exp Clin Endocrinol Diabetes,* vol. 119, pp. 472-9, Sep 2011.
[122] N. Papanas and E. Maltezos, "Becaplermin gel in the treatment of diabetic neuropathic foot ulcers," *Clin Interv Aging,* vol. 3, pp. 233-40, 2008.
[123] R. C. Fang and R. D. Galiano, "A review of becaplermin gel in the treatment of diabetic neuropathic foot ulcers," *Biologics,* vol. 2, pp. 1-12, Mar 2008.
[124] J. L. Richard, C. Parer-Richard, J. P. Daures, S. Clouet, D. Vannereau, J. Bringer, *et al.*, "Effect of topical basic fibroblast growth factor on the healing of chronic diabetic neuropathic ulcer of the foot. A pilot, randomized, double-blind, placebo-controlled study," *Diabetes Care,* vol. 18, pp. 64-9, Jan 1995.
[125] J. I. Fernandez-Montequin, B. Y. Betancourt, G. Leyva-Gonzalez, E. L. Mola, K. Galan-Naranjo, M. Ramirez-Navas, *et al.*, "Intralesional administration of epidermal growth factor-based formulation (Heberprot-P) in chronic diabetic foot ulcer: treatment up to complete wound closure," *Int Wound J,* vol. 6, pp. 67-72, Feb 2009.
[126] J. B. Acosta, W. Savigne, C. Valdez, N. Franco, J. S. Alba, A. del Rio, *et al.*, "Epidermal growth factor intralesional infiltrations can prevent amputation in patients with advanced diabetic foot wounds," *Int Wound J,* vol. 3, pp. 232-9, Sep 2006.
[127] X. Wang, J. Ge, E. E. Tredget, and Y. Wu, "The mouse excisional wound splinting model, including applications for stem cell transplantation," *Nat Protoc,* vol. 8, pp. 302-9, Feb 2013.
[128] A. L. Brubaker, D. F. Schneider, J. L. Palmer, D. E. Faunce, and E. J. Kovacs, "An improved cell isolation method for flow cytometric and functional analyses

of cutaneous wound leukocytes," *Journal of Immunological Methods,* vol. 373, pp. 161-166, Oct 28 2011.
[129] S. K. Brancato and J. E. Albina, "Wound macrophages as key regulators of repair: origin, phenotype, and function," *Am J Pathol,* vol. 178, pp. 19-25, Jan 2011.
[130] D. R. Knighton, I. A. Silver, and T. K. Hunt, "Regulation of wound-healing angiogenesis-effect of oxygen gradients and inspired oxygen concentration," *Surgery,* vol. 90, pp. 262-70, Aug 1981.
[131] S. Guo and L. A. Dipietro, "Factors affecting wound healing," *J Dent Res,* vol. 89, pp. 219-29, Mar 2010.
[132] F. B. LaVan and T. K. Hunt, "Oxygen and wound healing," *Clin Plast Surg,* vol. 17, pp. 463-72, Jul 1990.
[133] G. Andres, D. Leali, S. Mitola, D. Coltrini, M. Camozzi, M. Corsini*, et al.*, "A pro-inflammatory signature mediates FGF2-induced angiogenesis," *J Cell Mol Med,* vol. 13, pp. 2083-108, Aug 2009.
[134] M. Presta, G. Andres, D. Leali, P. Dell'Era, and R. Ronca, "Inflammatory cells and chemokines sustain FGF2-induced angiogenesis," *Eur Cytokine Netw,* vol. 20, pp. 39-50, Jun 2009.
[135] D. A. Bellinger, E. P. Merricks, and T. C. Nichols, "Swine models of type 2 diabetes mellitus: insulin resistance, glucose tolerance, and cardiovascular complications," *ILAR J,* vol. 47, pp. 243-58, 2006.
[136] M. Zhang, X. Y. Lv, J. Li, Z. G. Xu, and L. Chen, "The characterization of high-fat diet and multiple low-dose streptozotocin induced type 2 diabetes rat model," *Exp Diabetes Res,* vol. 2008, p. 704045, 2008.
[137] A. Vonderheit and A. Helenius, "Rab7 associates with early endosomes to mediate sorting and transport of Semliki forest virus to late endosomes," *PLoS Biol,* vol. 3, p. e233, Jul 2005.
[138] A. Choudhury, M. Dominguez, V. Puri, D. K. Sharma, K. Narita, C. L. Wheatley*, et al.*, "Rab proteins mediate Golgi transport of caveola-internalized glycosphingolipids and correct lipid trafficking in Niemann-Pick C cells," *J Clin Invest,* vol. 109, pp. 1541-50, Jun 2002.

Vita

Subhamoy Das was born and brought up in Rourkela, a small steel township in northern Odisha. He graduated from high school in 2005 with a focus on science including biology. After studying Electronics and Instrumentation engineering for a year at National Institute of Technology, Rourkela, Subhamoy moved to Indian Institute of Technology, Kharagpur for his undergraduate education. He majored in Biotechnology and Biochemical Engineering working with Dr. Tapas Kumar Maiti for the senior thesis research project. During the summer of 2009, Subhamoy visited Dr. Jasper Rine's laboratory at the University of California, Berkeley. This internship experience acted as a catalyst for his keener interest in research that led him to pursue graduate education in USA. Subhamoy graduated from IIT Kharagpur in 2010 with his Bachelor of Technology (Honors) degree and started graduate school in the Department of Biomedical Engineering at the University of Texas, Austin. He worked towards his Ph.D. degree under the supervision of Dr. Aaron Baker in the Laboratory for Cardiovascular Bioengineering and Therapeutics. They worked together and published regularly in renowned journals. The focus area of Subhamoy's research during his Ph.D. was to study diseased animal and human tissues to understand the mechanisms due to which growth factor therapy is relatively ineffective in human clinical trials and subsequently engineering sustained release hydrogels to deliver the therapy in a localized region.

Permanent email: subhamoy.das@utexas.edu

This dissertation was typed by the author.